

**NON-INVASIVE ESTIMATION OF SOIL HYDRAULIC PARAMETERS IN BOREAL
PODZOLIC SOILS USING GROUND-PENETRATING RADAR AND
HYDROLOGICAL MODELS**

By

© **Juwonlo Dahunsi**

A thesis submitted to the School of Graduate Studies in partial fulfillment of the requirements for
the degree of

Master of Science

In

Boreal Ecosystems and Agricultural Sciences

School of Science and the Environment

Grenfell Campus

Memorial University of Newfoundland

November 2024

Corner Brook, Newfoundland and Labrador, Canada

**Non-Invasive Estimation of Soil Hydraulic Parameters in Boreal Podzolic Soils Using
Ground-Penetrating Radar and Hydrological Models**

By

Juwonlo Dahunsi

A thesis submitted to the School of Graduate Studies

In partial fulfillment of the requirements for the degree of

Master of Science

In

Boreal Ecosystems and Agricultural Sciences

Approved:

School of Graduate Studies

Supervisor (Dr. Lakshman Galagedara)

Date

Co-Supervisor

Dr. Mumtaz Cheema

Committee Member

Dr. Mano Krishnapillai

Abstract

Obtaining information on soil hydraulic parameters (SHPs), including their spatiotemporal variation, is fundamental to understanding flow and transport processes in the vadose zone. This research examined the potential of coupling time-lapse ground-penetrating radar direct ground wave (GPR-DGW) information with hydrological models for non-invasive estimation of SHPs in a boreal podzolic soil using two experimental studies. The first research study focused on estimating soil water content (SWC) variation in podzolic soil using GPR-DGW and predicting field-saturated hydraulic conductivity (K_{fs}) by integrating the estimated SWC variations into the Green-Ampt (GA) model. The second study investigated the potential of integrating SWC variation derived from GPR-DGW in the Hydrus-1D model for obtaining Mualem-van Genuchten (M-vG) parameters and simulating soil water dynamics. Both studies involved short-term Beerkan infiltration experiments monitored using a surface GPR system of 500 MHz center frequency, collecting time-lapsed traces every 5 s. The first study revealed that GPR-DGW can successfully provide continuous, reliable SWC variation data during a short-term infiltration, which proved useful in obtaining probable K_{fs} values from the GA model. The second study also found that reliable M-vG parameters can be obtained through the inversion of SWC variations from GPR-DGW in the Hydrus-1D model. In addition, good correlations were observed between measured SWC variation and those simulated using the inverted M-vG parameters. Overall, this research demonstrates a significant advancement in using GPR as a reliable and robust technique for large-scale SHPs prediction in boreal podzolic soils, with the possibility of extending to other soil types in future research.

General Summary

The province of Newfoundland and Labrador faces significant challenges in agriculture and land conservation efforts due to the low water retention capacity and rapid drainage of its podzolic soil, among other factors. These soil conditions limit the efficiency of both irrigation and natural water retention in the landscape. Sustainable management of these soils requires a better understanding of soil hydraulic parameters (SHPs), especially their variation in both spatial and temporal scales. This study assessed the potential of estimating SHPs by integrating ground-penetrating radar (GPR) information with hydrological models as an alternative to current invasive and point-scale methods. The research studies involved short-term infiltration experiments monitored by GPR. Findings from this study showed that reliable SHPs can be obtained by integrating soil water content variations estimated from GPR as parameters in hydrological models. This study demonstrates the potential of using GPR for large-scale, non-invasive estimation of SHPs in boreal podzolic soils, which can be useful for precision agriculture and efficient soil water management to enhance crop yield and productivity in boreal climate.

Acknowledgments

I am grateful to the source of strength and wisdom for the capacity to start and complete this work.

I would like to thank my supervisor, Dr. Lakshman Galagedara, for his invaluable guidance and support throughout this study and my master's program. Beyond soil hydrology, I have learned valuable life lessons through his mentorship. I am equally grateful to my co-advisor and committee members, Dr. Mumtaz Cheema and Dr. Mano Krishnapillai, for their feedback and suggestions that improved the quality of this work.

I gratefully acknowledge the financial support provided by the Natural Sciences and Engineering Research Council of Canada (Discovery Grant: RGPIN-2019-04614), Industry, Energy and Innovation of the Government of Newfoundland and Labrador (IET Grant: 5404-1962-102), and the School of Graduate Studies, Memorial University of Newfoundland (MUN), that made this work possible. Special thanks to the Department of Fisheries, Forestry, and Agriculture, Government of Newfoundland and Labrador, for providing and clearing the research field for this work.

I am very thankful to PhD Candidate, Sashini Pathirana, for her support during my field and laboratory work, data processing, and for proofreading my manuscripts. I am grateful to members of the Soil Hydrology and Agrophysics research group and my colleagues in the Boreal Ecosystems and Agricultural Sciences (BEAS) program, Grenfell Campus-Memorial University of Newfoundland, for all their valuable suggestions and support. Finally, I would like to thank my family and friends for their support and encouragement, especially during the challenging times of completing this thesis.

Juwonlo Dahunsi (*MUN #202194385*)

Table of Contents

Abstract.....	iii
General Summary.....	iv
Acknowledgments.....	v
Table of Contents.....	vi
List of Tables.....	x
List of Figures.....	xi
List of Abbreviations.....	xiii
CHAPTER ONE.....	1
1.1. Background and Rationale for the Study.....	1
1.2. Thesis Objectives and Hypotheses.....	5
1.3. Thesis Organization.....	6
1.4. References.....	8
Co-authorship Statement for Review Paper.....	15
CHAPTER TWO.....	16
Advances in Ground Penetrating Radar Application for Estimating Soil Hydraulic Parameters: A Mini-Review.....	16
Abstract.....	16
2.1. Introduction.....	17
2.2. Ground Penetrating Radar Principles and Methods.....	20

2.3. Surface GPR For Soil Hydraulic Parameters Estimation.....	22
2.4. Borehole GPR For Soil Hydraulic Parameters Estimation.....	24
2.5. Off-ground GPR for Soil Hydraulic Parameters Estimation.....	27
2.6. Discussion.....	31
2.7. Conclusions and Future Outlook.....	33
2.8. Acknowledgements.....	35
2.9. References.....	36
Co-authorship Statement for Study One.....	48
CHAPTER THREE.....	50
Estimating Soil Hydraulic Conductivity from Time-lapsed Ground-penetrating Radar Data in Podzolic Soils using the Green-Ampt Model.....	50
Abstract.....	50
3.1. Introduction.....	51
3.2. Methodology.....	55
3.2.1. Study area.....	55
3.2.2. Field data collection.....	56
3.2.3. GPR data processing.....	59
3.2.4. Estimating wetting front depth.....	60
3.2.5. Estimation of saturated hydraulic conductivity using the Green-Ampt model.....	61
3.2.6. Statistical analysis.....	62
3.3. Results and Discussion.....	63

3.3.1. Monitoring of soil water content variation during infiltration.....	63
3.3.2. Estimating wetting front depth using the relationship between soil water content monitored by moisture probes and ground-penetrating radar.....	67
3.3.3. Estimating field-saturated hydraulic conductivity using SWC variations and wetting front depth in the Green-Ampt model.....	69
3.3.4. Soil water content variations at the two locations.....	71
3.3.5. Estimating field-saturated hydraulic conductivity using SWC variations from both locations.....	72
3.4. Conclusions.....	75
3.5. Acknowledgements.....	76
3.6. References.....	77
Appendices.....	87
Co-authorship Statement for Study Two.....	92
CHAPTER FOUR.....	93
Using Hydrus-1D Modeling to Predict Soil Hydraulic Parameters of Podzolic Soils from Time- lapsed Ground-penetrating Radar Data.....	93
Abstract.....	93
4.1. Introduction.....	94
4.2. Methodology.....	97
4.2.1. Experimental set-up.....	97
4.2.2. Hydrus-1D modeling.....	100
4.2.3. Model evaluation.....	103

4.3. Results and Discussion.....	104
4.3.1. Soil water content variation (inverse modeling for calibration).....	104
4.3.2. Inverted soil hydraulic parameters.....	106
4.3.3. Soil water content variation (forward modeling for validation).....	109
4.4. Conclusions.....	112
4.5. Acknowledgments.....	114
4.6. References.....	115
CHAPTER FIVE.....	122
5.1. General Discussion and Conclusions.....	122
5.2. Limitations of this Study.....	124
5.3. Recommendations.....	125
References and Bibliography.....	126

List of Tables

Table 2.1 Comparison of surface, borehole, and off-ground ground penetrating radar (GPR) potentials for soil hydraulic characterization showing advantages and limitations of each technique.....	30
Table 4.1 Inverted hydraulic parameters from the field and laboratory experiments compared to other methods.....	107
Table 4.2 RMSE and NSE values for the validation of the simulated results.....	111

List of Figures

Figure 2.1 Flowchart of coupled inversion of ground penetrating radar (GPR) travel times (blue pathway) and coupled full-waveform inversion (CFWI) (green pathway) (Adapted from Yu et al. 2021 and 2022). SCE-UA = Shuffled Complex Evolution-University of Arizona.....	27
Figure 2.2 Network visualization map illustrating the primary areas of ground-penetrating radar (GPR) applications in studying water-related issues in the last 20 years (2004 -2023).....	29
Figure 3.1 Experimental set-up for the Beeken infiltration experiment and data collection using 500 MHz ground-penetrating radar (GPR) transducers. a) side view and b) top-down.....	59
Figure 3.2 Variation in average soil water content (SWC, v/v) monitored by soil moisture probes (SMPs) at 5 cm, 10 cm, 15 cm, and 20 cm depths.....	65
Figure 3.3 Comparison of average soil water content (SWC, v/v) variation estimated and monitored by ground-penetrating radar (GPR) and soil moisture probes (SMPs), respectively....	66
Figure 3.4 Ground-penetrating radar (GPR) radargrams obtained during one of the infiltration experiments at Location 1.....	66
Figure 3.5 Site-specific calibrated relationships between soil moisture probes soil water content (SMPs-SWC, v/v) and average ground-penetrating radar dielectric constant (GPR- K_r) at different depths: a) 5 cm, b) 10 cm, c) 15 cm, and d) 20 cm.....	68
Figure 3.6 Comparison of field-saturated hydraulic conductivity (K_{fs}) estimates derived from using the Green-Ampt (GA) model for ground-penetrating radar soil water content (GPR-SWC, v/v), and soil moisture probes soil water content (SMPs-SWC, v/v), with Saxton and Rawls (2006) estimates and traditional GA parameters as benchmarks.....	70

Figure 3.7 Correlation between average dielectric constant (K_r) obtained at Locations 1 and 2	71
Figure 3.8 Comparison of average ground-penetrating radar soil water content (GPR-SWC, v/v) variations at Locations 1 and 2 with infiltration time.....	72
Figure 3.9 Comparison of field-saturated hydraulic conductivity (K_{fs}) estimates derived from ground-penetrating radar soil water content variations (GPR-SWC, v/v), BEST-Intercept, BEST- Steady, and Guelph permeameter (GP), with Saxton and Rawls (2006) estimates and traditional Green-Ampt (GA)- K_s parameters as benchmarks.....	74
Fig. 3.10: Calibration of Soil Moisture Probes (SMPs) for measuring soil water content. GM- Gravimetric Method; SMPs – Soil Moisture Probes.....	91
Figure 4.1 Data collection set-up for the Beerkan infiltration experiment monitored by ground- penetrating radar (GPR).....	99
Figure 4.2 Flow chart presenting the integration of ground-penetrating radar-monitored infiltration experiment and Hydrus-1D simulation. The shaded rectangles represent key results in the workflow that are later presented and discussed in this paper. GPR- ground-penetrating radar.....	102
Figure 4.3 Measured and simulated soil water content (SWC) variation for the calibration using the first a) field and b) laboratory experiments versus time. RMSE - root mean square errors (cm^3/cm^3); NSE - Nash-Sutcliffe modeling efficiency.....	105
Figure 4.4 Scatter plots of simulated soil water content (SWC) variation using calibrated hydraulic parameters versus measured SWC variation from ground-penetrating radar for a) field and b)	

laboratory experiments. The solid lines correspond to the 1:1 line, and the dashed lines correspond to the linear regression lines.....110

List of Abbreviations

1D - One-dimensional

2D - Two-dimensional

3D - Three-dimensional

BEST - Beerkan estimation of soil transfer

CH - Constant head

CMP - Common midpoint

DGW - Direct ground wave

DR - Direct ring

EM - Electromagnetic

EMI - Electromagnetic induction

ERT - Electrical resistivity tomography

ES-MDA - Ensemble smoother with multiple data assimilation

FO - Fixed offset

F(t) - Cumulative infiltration

FWI - Full waveform inversion

GA - Green-Ampt

GM - Gravimetric method

GP - Guelph permeameter

GPR – Ground-penetrating radar

IA - Inverse auger

$K(\theta)$ - Unsaturated hydraulic conductivity

K_{fs} - Field-saturated hydraulic conductivity

K_r – Dielectric constant

K_s - Saturated hydraulic conductivity

L - Wetted depth

Max - Maximum

MHz - MegaHertz

MOG - Multi-offset gathering

M-vG - Mualem-van Genuchten

NSE - Nash-Sutcliffe efficiency

OM – Organic matter

PSD – Particle size distribution

PTF - Peto-transfer functions

RMSE - Root mean square error

RFS - Rainfall simulator

SIR - Sequential importance resampling

SHPs - Soil hydraulic parameters

SMPs - Soil moisture probes

SR - Single-ring

SWC - Soil water content

T - Time

TDR - Time domain reflectometry

TI - Tension infiltrometer

VRP - Vertical radar profiling

v/v - Volumetric

WARR - Wide-angle reflection and refraction

ZOP - Zero-offset profiling

CHAPTER ONE

1.1. Background and Rationale for the Study

The province of Newfoundland and Labrador is predominantly characterized by podzolic soils, which are typically sandy, stony, and shallow (Sanborn et al., 2011). These soil conditions pose challenges to soil water management and agricultural productivity due to low water retention capacity, rapid drainage, and high susceptibility of the soils to erosion. To ensure effective and sustainable land and water resources management, accurate subsurface characterization and information on relevant soil properties, especially mapping their spatiotemporal variation, are needed. Soil hydraulic parameters (SHPs) serve as key indicators of soil quality, crucial for the sustainable management of land and water resources (Singh et al., 2023). They play a significant role in managing water flow and contaminant transport processes (Vereecken et al., 2007; Rezaei et al., 2016).

Saturated hydraulic conductivity (K_s) and soil water retention parameters are vital SHPs that enhance irrigation planning, erosion control, plant water uptake, land remediation, and hydrological modeling (Fernández-Gálvez et al., 2019; Indoria et al., 2020; Castellini et al., 2021). Various mathematical models have been developed to represent these SHPs, including the Mualem-van Genuchten (M-vG) function, which integrates soil water retention parameters (residual water content - θ_r , saturated water content - θ_s , and shape parameters - α and n) introduced by van Genuchten (1980) with Mualem's (1976) pore-size distribution model for K_s (Schaap and van Genuchten, 2006).

Current methods for directly measuring SHPs are time-consuming, labor-intensive, and often involve processes that disturb the soil, which can lead to degradation (Zou et al., 2023).

Additionally, these methods are limited in their capacity to continuously capture the spatiotemporal variability of soil properties (Huang and Shao, 2019).

Geophysical techniques offer a promising alternative for subsurface characterization, allowing for the assessment of spatio-temporal variation of soil properties over larger areas with minimal or no disturbance (Corwin and Lesch, 2003). Commonly used techniques to assess soil spatio-temporal variation include Electromagnetic Induction (EMI), Electrical Resistivity Tomography (ERT), and Ground-penetrating radar (GPR) (Allred et al., 2010; Binley et al., 2015; Bitella et al., 2015; Lombardi et al., 2022).

These techniques operate based on different principles. EMI involves transmitting low-frequency electromagnetic waves (1-100 kHz) into the ground and measuring the soil's response to the induced electromagnetic field through electrical conductivity and magnetic permeability (Doolittle and Brevik, 2014). ERT sends a direct current (DC) through electrodes into the soil and measures the resulting potential differences (Yasir et al., 2019). GPR, on the other hand, determines the dielectric constant (K_r) and electrical conductivity (σ) of the soil by analyzing the travel time and amplitude of high-frequency electromagnetic waves (10 - 3600 MHz) as they propagate through the soil (Weiler et al., 1994; Pathirana et al., 2023).

GPR has particularly gained popularity in soil hydrological studies due to the direct relationship of K_r to soil water content (SWC) (Topp et al., 1980). The large contrast between the K_r of water (80) and all other soil constituents (air \sim 1; solid phase: 3 \sim 10) makes GPR relevant for estimating SWC (Liu et al., 2019). Hence, GPR has been widely used in SWC estimation for over two decades (Chanzy et al., 1996; Galagedara et al., 2003; Lunt et al., 2005; Mangel et al., 2012; Pathirana et al., 2024). A detailed overview of GPR's operating principle is provided in Dahunsi et al. (2023).

GPR emits electromagnetic waves through a transmitter antenna, which are detected by a receiver antenna (Zajícová and Chuman, 2019). The waves received and interpreted by the receiver antenna are in three main forms: air wave, direct ground wave (DGW), and reflected wave (Galagedara et al., 2003). The DGW is a direct wave that propagates directly from the transmitter to the receiver just beneath the soil surface (Huisman et al., 2001) and is, therefore, useful in assessing shallow soil properties (Huisman et al., 2003).

Although GPR cannot directly measure SHPs, its sensitivity to fluid distribution makes it a valuable tool in this area (Kowalsky et al., 2005; Zhang et al., 2022). By combining GPR data from infiltration experiments with hydrological models, several studies have successfully estimated SHPs using different approaches (Kowalsky et al., 2005; Scholer et al., 2012; Yu et al., 2022; Zou et al., 2023).

Notably, many of these approaches have used GPR to monitor infiltration or irrigation processes over time. However, the development of simpler methods, such as the Beerkan Estimation of Soil Transfer (BEST) parameter method, offers a more cost-effective and rapid approach for conducting infiltration experiments in both field and laboratory conditions (Lassabatère et al., 2006). This procedure allows for straightforward infiltration tests using a simple ring, with a small amount of water added at intervals over a short period (Angulo-Jaramillo et al., 2019; Fernández-Gálvez et al., 2019).

Hydrological models are used to simulate water flow based on input data and can be classified into empirical, conceptual, and physically-based models (Willems, 2000; Jajarmizadeh et al., 2012). Physically-based model, which simulates water movement using fundamental physics laws, offers a more detailed representation of hydrological processes compared to empirical and conceptual

models (Willems, 2000). Among these, the Green-Ampt (GA) and Hydrus-1D models are widely used for simulating soil water flow (Green and Ampt, 1911; Šimůnek et al., 1998).

The GA model is a semi-analytical approach that applies the principle of mass conservation and Darcy's law to describe one-dimensional vertical flow through a uniform soil column (Mohammadzadeh-Habili and Heidarpour, 2015). Known for its simplicity, the GA model requires fewer parameters than other infiltration models (Li et al., 2022). It is particularly effective for coarse-textured soils exhibiting sharply defined wetting fronts (Baiamonte, 2019), making it well-suited for simulating water flow in podzolic soils.

Hydrus-1D, on the other hand, is a more comprehensive physically-based model that uses computational methods to simulate one-dimensional water, heat, and solute movement in variably saturated soils (Šimůnek et al., 1998). It solves the Richards equation and is applicable across a wider range of boundary conditions, soil types, and properties (Šimůnek et al., 2008). More details about the GA and Hydrus-1D models are provided in Chapters 3 and 4 of this thesis, respectively.

The integration of GPR data into hydrological models for estimating SHPs, especially in boreal podzolic soils, remains underexplored. In addition, the application of GPR-DGW for capturing near-surface soil water dynamics has not been investigated. While some studies have used Hydrus-1D with GPR-derived SWC (GPR-SWC) variation for SHP estimation, to the best of this study's knowledge, limited or no studies have examined the use of the GA model in this context. Most existing studies focus on long-term infiltration experiments, with little or no emphasis given to more economical methods like the Beerkan infiltration procedure.

1.2. Thesis Objectives and Hypotheses

This thesis explored the potential for estimating SHPs in boreal podzolic soils by combining hydrological models with SWC variations derived from time-lapse GPR-DGW measurements during short-duration Beerkan infiltration experiments.

The study had two main objectives, each with sub-objectives:

1. Evaluate the potential for using GPR-DGW in estimating SWC variation and predicting field-saturated hydraulic conductivity (K_{fs}) by integrating the estimated SWC variation into the GA model:
 - I. To explore the potential of GPR-DGW to capture SWC variation during a limited-duration infiltration experiment.
 - II. To estimate field saturated hydraulic conductivity (K_{fs}) by using the SWC variation estimated from GPR time-lapse data in the GA model and assess the accuracy of the estimates.
2. Investigate the use of GPR-DGW data and the Hydrus-D model for obtaining M-vG parameters and simulating soil water dynamics in boreal podzolic soils:
 - I. To obtain M-vG parameters through the Hydrus-1D inverse modeling of SWC variation obtained from GPR-DGW.
 - II. To validate and evaluate the potential for simulating soil water movement based on the inverted M-vG parameters.

This study hypothesized that GPR-DGW could accurately monitor SWC variation during a short-term Beerkan infiltration procedure in boreal podzolic soils. Furthermore, it was hypothesized that these variations, when used as inputs in the GA and Hydrus-1D models, could provide reliable estimates of SHPs, including the Mualem-van Genuchten (M-vG) parameters.

Overall, this study aims to contribute to ongoing efforts to develop efficient methods for large-scale characterization of SHPs, offering valuable insights for precision agriculture and the sustainable management of land and water resources.

1.3. Thesis Organization

This thesis is structured in a manuscript style and divided into five chapters. The thesis consists of an introduction chapter, a review chapter, two study chapters, and a final chapter for general discussion and conclusion.

Chapter One: “*Introduction.*” This chapter provides the background and rationale for the study, problem statement, objectives, and hypotheses of the thesis.

Chapter Two: “*Advances in Ground Penetrating Radar Application for Estimating Soil Hydraulic Properties: A Mini Review.*” This chapter reviews recent studies and advances in applying GPR to study soil water dynamics and SHPs estimation. This chapter has been submitted, accepted, and published in the Canadian Biosystems Engineering (CBE) Journal.¹

Chapter Three: “*Estimating Soil Hydraulic Conductivity from Time-lapsed Ground-penetrating Radar Data in Podzolic Soils using the Green-Ampt Model.*” This chapter evaluates the potential for monitoring SWC changes using GPR time-lapse data and estimating K_{fs} by employing the GA

¹ Dahunsi, J., Pathirana, S., Cheema, M., Krishnapillai, M., Galagedara, L., 2023. Advances in Ground Penetrating Radar application for estimating soil hydraulic properties: A mini-review. Canadian Biosystems Engineering/Le génie des biosystèmes au Canada 65, 1.17–1.27. <https://doi.org/10.7451/CBE.2023.65.1.17>.

model. The study was conducted on the field at two locations in a podzolic soil site in western Newfoundland, Canada. This chapter has been submitted for publication in the “Journal of Hydrology” and a revision has been requested based on reviewers’ feedback.²

Chapter Four: “*Using Hydrus-1D Modeling to Predict Soil Hydraulic Parameters of Podzolic Soils from Time-Lapsed Ground-Penetrating Radar Data.*” This chapter assesses the integration of GPR time-lapse data with Hydrus-1D modeling to calibrate, validate, and evaluate M-vG parameters and simulate soil water dynamics in podzolic soils using GPR-DGW data. The study utilized field and laboratory infiltration experiments conducted using the Beerkan method. This chapter will be submitted to the “Geoderma Regional Journal” for publication.

Chapter Five: “*General Discussion, Conclusions, Limitations, and Recommendations.*” This chapter presents a general discussion, conclusion and limitations of the study and suggests recommendations for future research.

² Dahunsi, J., Pathirana, S., Cheema, M., Krishnapillai, M., Galagedara, L., 2024. Estimating soil hydraulic conductivity from time-lapse ground-penetrating radar data in Podzolic soils using the Green-Ampt model. Journal of Hydrology–HYDROL62404 (revision requested).

1.4. References

- Allred, B.J., Freeland, R.S., Farahani, H.J., Collins, M.E., 2010. Agricultural geophysics: Past, present, and future. 23rd EEGS Symposium on the Application of Geophysics to Engineering and Environmental Problems, cp-175. <https://doi.org/10.4133/1.3445432>.
- Angulo-Jaramillo, R., Bagarello, V., Di Prima, S., Gosset, A., Iovino, M., Lassabatere, L., 2019. Beerkan Estimation of Soil Transfer parameters (BEST) across soils and scales. *Journal of Hydrology* 576, 239–261. <https://doi.org/10.1016/j.jhydrol.2019.06.007>.
- Baiamonte, G., 2019. SCS curve number and Green-Ampt infiltration models. *Journal of Hydrologic Engineering* 24(10), 04019034. [https://doi.org/10.1061/\(ASCE\)HE.1943-5584.0001838](https://doi.org/10.1061/(ASCE)HE.1943-5584.0001838).
- Binley, A., Hubbard, S.S., Huisman, J.A., Revil, A., Robinson, D.A., Singha, K., Slater, L.D., 2015. The emergence of hydrogeophysics for improved understanding of subsurface processes over multiple scales. *Water Resources Research* 51(6), 3837–3866. <https://doi.org/10.1002/2015WR017016>.
- Bitella, G., Rossi, R., Loperte, A., Satriani, A., Lapenna, V., Perniola, M., Amato, M., 2015. Geophysical techniques for plant, soil, and root research related to sustainability. In: *The sustainability of agro-food and natural resource systems in the Mediterranean Basin*, Springer International Publishing, Cham, pp. 353–372.
- Castellini, M., Di Prima, S., Moret-Fernández, D., Lassabatere, L., 2021. Rapid and accurate measurement methods for determining soil hydraulic properties: A review. *Journal of Hydrology and Hydromechanics* 69(2), 121–139. <https://doi.org/10.2478/johh-2021-0002>.

- Chanzy, A., Tarussov, A., Bonn, F., Judge, A., 1996. Soil water content determination using a digital ground-penetrating radar. *Soil Science Society of America Journal* 60(5), 1318–1326. <https://doi.org/10.2136/sssaj1996.03615995006000050005x>.
- Corwin, D.L., Lesch, S.M., 2003. Application of soil electrical conductivity to precision agriculture: Theory, principles, and guidelines. *Agronomy Journal* 95(3), 455–471. <https://doi.org/10.2134/agronj2003.4550>.
- Dahunsi, J., Pathirana, S., Cheema, M., Krishnapillai, M., Galagedara, L., 2023. Advances in Ground Penetrating Radar application for estimating soil hydraulic properties: A mini-review. *Canadian Biosystems Engineering/Le génie des biosystèmes au Canada* 65, 1.17–1.27. <https://doi.org/10.7451/CBE.2023.65.1.17>.
- Doolittle, J.A., Brevik, E.C., 2014. The use of electromagnetic induction techniques in soils studies. *Geoderma* 223, 33–45. <https://doi.org/10.1016/j.geoderma.2014.01.027>.
- Fernández-Gálvez, J., Pollacco, J.A.P., Lassabatere, L., Angulo-Jaramillo, R., Carrick, S., 2019. A general Beerkan Estimation of Soil Transfer parameters method predicting hydraulic parameters of any unimodal water retention and hydraulic conductivity curves: Application to the Kosugi soil hydraulic model without using particle size distribution data. *Advances in Water Resources* 129, 118–130. <https://doi.org/10.1016/j.advwatres.2019.05.005>.
- Galagedara, L.W., Parkin, G.W., Redman, J.D., 2003. An analysis of the ground-penetrating radar direct ground wave method for soil water content measurement. *Hydrological Processes* 17(18), 3615–3628. <https://doi.org/10.1002/hyp.1351>.
- Green, W. H., Ampt, G. A., 1911. Studies on soil physics. *The Journal of Agricultural Sciences*, 4(1), 1-24. <https://doi.org/10.1017/S0021859600001441>.

- Huang, L., Shao, M.A., 2019. Advances and perspectives on soil water research in China's Loess Plateau. *Earth-Science Reviews* 199, 102962.
<https://doi.org/10.1016/j.earscirev.2019.102962>.
- Huisman, J.A., Sperl, C., Bouten, W., Verstraten, J.M., 2001. Soil water content measurements at different scales: accuracy of time domain reflectometry and ground-penetrating radar. *Journal of Hydrology* 245(1-4), 48-58.
- Huisman, J.A., Hubbard, S.S., Redman, J.D., Annan, A.P., 2003. Measuring soil water content with ground penetrating radar: A review. *Vadose Zone Journal* 2(4), 476–491.
<https://doi.org/10.2136/vzj2003.4760>.
- Indoria, A.K., Sharma, K.L., Reddy, K.S., 2020. Hydraulic properties of soil under warming climate. In: *Climate change and soil interactions*, Elsevier, pp. 473–508.
<https://doi.org/10.1016/B978-0-12-818032-7.00018-7>.
- Jajarmizadeh, M., Harun, S., Salarpour, M., 2012. A review on theoretical consideration and types of models in hydrology. *Journal of Environmental Science and Technology* 5(5), 249–261.
- Kowalsky, M.B., Finsterle, S., Peterson, J., Hubbard, S., Rubin, Y., Majer, E., Ward, A., Gee, G., 2005. Estimation of field-scale soil hydraulic and dielectric parameters through joint inversion of GPR and hydrological data. *Water Resources Research* 41(11).
<https://doi.org/10.1029/2005WR004237>.
- Lassabatère, L., Angulo-Jaramillo, R., Soria Ugalde, J.M., Cuenca, R., Braud, I., Haverkamp, R., 2006. Beerkan estimation of soil transfer parameters through infiltration experiments—BEST. *Soil Science Society of America Journal* 70(2), 521–532.
<https://doi.org/10.2136/sssaj2005.0026>.

- Li, S., Cui, P., Cheng, P., Wu, L., 2022. Modified green–ampt model considering vegetation root effect and redistribution characteristics for slope stability analysis. *Water Resources Management* 36(7), 2395–2410. <https://doi.org/10.1007/s11269-022-03149-6>.
- Liu, X., Chen, J., Cui, X., Liu, Q., Cao, X., Chen, X., 2019. Measurement of soil water content using ground-penetrating radar: A review of current methods. *International Journal of Digital Earth* 12(1), 95–118. <https://doi.org/10.1080/17538947.2017.1412520>.
- Lombardi, F., Ortuani, B., Facchi, A., Lualdi, M., 2022. Assessing the perspectives of ground penetrating radar for precision farming. *Remote Sensing* 14(23), 6066. <https://doi.org/10.3390/rs14236066>.
- Lunt, I.A., Hubbard, S.S., Rubin, Y., 2005. Soil moisture content estimation using ground-penetrating radar reflection data. *Journal of Hydrology* 307(1–4), 254–269. <https://doi.org/10.1016/j.jhydrol.2004.10.014>.
- Mangel, A.R., Moysey, S.M.J., Ryan, J.C., Tarbuton, J.A., 2012. Multi-offset ground-penetrating radar imaging of a lab-scale infiltration test. *Hydrology and Earth System Sciences* 16(11), 4009–4022. <https://doi.org/10.5194/hess-16-4009-2012>.
- Mohammadzadeh-Habili, J., Heidarpour, M., 2015. Application of the Green–Ampt model for infiltration into layered soils. *Journal of Hydrology* 527, 824–832. <https://doi.org/10.1016/j.jhydrol.2015.05.052>.
- Mualem, Y., 1976. A new model for predicting the hydraulic conductivity of unsaturated porous media. *Water Resources Research* 12(3), 513–522. <https://doi.org/10.1029/WR012i003p00513>.

- Pathirana, S., Lambot, S., Krishnapillai, M., Cheema, M., Smeaton, C., Galagedara, L., 2023. Ground-penetrating radar and electromagnetic induction: Challenges and opportunities in agriculture. *Remote Sensing* 15(11), 2932. <https://doi.org/10.3390/rs15112932>.
- Pathirana, S., Lambot, S., Krishnapillai, M., Smeaton, C., Cheema, M., Galagedara, L., 2024. Potential of ground-penetrating radar to calibrate electromagnetic induction for shallow soil water content estimation. *Journal of Hydrology* 633, 130957. <https://doi.org/10.1016/j.jhydrol.2024.130957>.
- Rezaei, M., Saey, T., Seuntjens, P., Joris, I., Boënné, W., Van Meirvenne, M., Cornelis, W., 2016. Predicting saturated hydraulic conductivity in a sandy grassland using proximally sensed apparent electrical conductivity. *Journal of Applied Geophysics* 126, 35–41. <https://doi.org/10.1016/j.jappgeo.2016.01.010>.
- Sanborn, P., Lamontagne, L., Hendershot, W., 2011. Podzolic soils of Canada: Genesis, distribution, and classification. *Canadian Journal of Soil Science* 91(5), 843–880. <https://doi.org/10.4141/cjss10025>.
- Schaap, M.G., van Genuchten, M.T., 2006. A modified Mualem–van Genuchten formulation for improved description of the hydraulic conductivity near saturation. *Vadose Zone Journal* 5(1), 27–34. <https://doi.org/10.2136/vzj2005.0005>.
- Scholer, M., Irving, J., Looms, M.C., Nielsen, L., Holliger, K., 2012. Bayesian Markov-chain-Monte-Carlo inversion of time-lapse crosshole GPR data to characterize the vadose zone at the Arrenæs Site, Denmark. *Vadose Zone Journal* 11(4), vzj2011.0153. <https://doi.org/10.2136/vzj2011.0153>.

- Singh, D., Mishra, A.K., Patra, S., Mariappan, S., Singh, N., Kar, S.K., 2023. Spatial variability of soil hydraulic and physical properties in erosive sloping agricultural fields. *Water Science and Engineering* 16(1), 57–66.
- Šimůnek, J., Huang, K., van Genuchten, M.T., 1998. The HYDRUS code for simulating the one-dimensional movement of water, heat, and multiple solutes in variably-saturated media. US Salinity Laboratory Research Report 144.
- Šimůnek, J., van Genuchten, M.T., Sejna, M., 2008. Development and applications of the HYDRUS and STANMOD software packages and related codes. *Vadose Zone Journal* 7(2), 587–600. <https://doi.org/10.2136/vzj2007.0077>.
- Topp, G.C., Davis, J.L., Annan, A.P., 1980. Electromagnetic determination of soil water content: Measurements in coaxial transmission lines. *Water Resources Research* 16(3), 574–582. <https://doi.org/10.1029/WR016i003p00574>.
- van Genuchten, M.T., 1980. A closed-form equation for predicting the hydraulic conductivity of unsaturated soils. *Soil Science Society of America Journal* 44(5), 892–898. <https://doi.org/10.2136/sssaj1980.03615995004400050002x>.
- Vereecken, H., Huisman, J.A., Pachepsky, Y., Montzka, C., van der Kruk, J., Bogena, H., Weihermüller, L., Herbst, M., Martinez, G., Vanderborght, J., 2014. On the spatio-temporal dynamics of soil moisture at the field scale. *Journal of Hydrology* 516, 76-96.
- Weiler, K.W., Steenhuis, T.S., Boll, J., Kung, K.J.S., 1998. Comparison of ground penetrating radar and time-domain reflectometry as soil water sensors. *Soil Science Society of America Journal* 62(5), 1237–1239. <https://doi.org/10.2136/sssaj1998.03615995006200050008x>.
- Willems, P., 2000. Probabilistic modeling of the emission receiving surface waters. PhD Thesis, Faculty of Engineering, Katholieke Universiteit Leuven, Belgium.

- Yasir, S.F., Jani, J., Mukri, M., 2019. The estimation of hydraulic properties from geophysical measurement of subsoil depend on regression equation. *Modern Applied Science* 13(6), 1–12. <https://doi.org/10.5539/mas.v13n6p1>.
- Yu, Y., Huisman, J.A., Klotzsche, A., Vereecken, H., Weihermüller, L., 2022. Coupled full-waveform inversion of horizontal borehole ground penetrating radar data to estimate soil hydraulic parameters: A synthetic study. *Journal of Hydrology* 610, 127817. <https://doi.org/10.1016/j.jhydrol.2022.127817>.
- Zajícová, K., Chuman, T., 2019. Application of ground penetrating radar methods in soil studies: A review. *Geoderma* 343, 116-129.
- Zhang, M., Feng, X., Bano, M., Xing, H., Wang, T., Liang, W., Zhou, H., Dong, Z., An, Y., Zhang, Y., 2022. Review of ground penetrating radar applications for water dynamics studies in unsaturated zone. *Remote Sensing* 14(23), 5993. <https://doi.org/10.3390/rs14235993>.
- Zou, C., Zhang, S., Jiang, X., Chen, F., 2023. Monitoring and characterization of water infiltration in soil unsaturated zone through an integrated geophysical approach. *Catena* 230, 107243. <https://doi.org/10.1016/j.catena.2023.107243>.

Co-authorship Statement for Review Paper

A manuscript based on Chapter 2, entitled “*Advances in Ground Penetrating Radar Application for Estimating Soil Hydraulic Properties: A Mini-Review*” has been submitted and published in the Canadian Biosystems Engineering Journal.³

Juwonlo Dahunsi, the thesis author, was the primary author and was responsible for the conceptualization and writing of the original manuscript. Sashini Pathirana, PhD Candidate, assisted with reviewing and editing the manuscript. Mumtaz Cheema and Mano Krishnapillai are co-supervisor and committee member, respectively, and were involved in the review and editing of the manuscript. Lakshman Galagedara, the supervisor, was responsible for the project conceptualization, funding acquisition, project administration, resource allocation, and supervision, and contributed to the review and editing of the manuscript.

³ Dahunsi, J., Pathirana, S., Cheema, M., Krishnapillai, M., Galagedara, L., 2023. Advances in Ground Penetrating Radar application for estimating soil hydraulic properties: A mini-review. Canadian Biosystems Engineering/Le génie des biosystèmes au Canada 65, 1.17–1.27. <https://doi.org/10.7451/CBE.2023.65.1.17>.

CHAPTER TWO

Advances in Ground Penetrating Radar Application for Estimating Soil Hydraulic

Parameters: A Mini-Review

Juwonlo Dahunsi ^a, Sashini Pathirana ^a, Manokararajah Krishnapillai ^a, Mumtaz Cheema ^a,

Lakshman Galagedara ^{a*}

^aSchool of Science and the Environment, Memorial University of Newfoundland, Corner Brook, NL A2H 5G4, Canada

*Correspondence: lgalagedara@mun.ca

Abstract

Information on soil water status and dynamics is needed for agricultural management, as well as engineering and environmental investigations. Water status and dynamics in the vadose zone are primarily influenced by two fundamental properties: soil water content (SWC) and soil hydraulic parameters (SHPs). The application of ground-penetrating radar (GPR) for monitoring and estimating these properties has received wider attention and has significantly advanced in recent years. While SWC estimation using GPR has been well-reviewed over the years, SHPs estimation has not received the same attention. Notably, there has been increasing research on SHPs estimation using GPR in the last decade. This paper reviews the recent studies and advances in applying GPR to study soil water dynamics and SHP estimation. We compared the progress and advantages of the three techniques (Borehole, Surface, and Off-ground), identified key issues affecting their application, and noted future research opportunities. By synthesizing these studies, this review paper aims to draw attention to evolving methodologies in GPR applications for

monitoring soil water dynamics and SHP estimation as good indicators of soil hydraulic resistance and how these opportunities can be harnessed to improve soil water management.

Keywords: Coupled inversion; Full waveform inversion (FWI); Ground-penetrating radar; infiltration; Soil hydraulic conductivity; Soil water dynamics.

2.1. Introduction

Reliable and timely information on the status and dynamics of soil water is essential for long-term agricultural sustainability and ecological management (Huang and Shao, 2019). However, deriving this information can be enigmatic due to the spatial and temporal heterogeneity of soil physical properties (Léger et al., 2014), which can also be affected by increasing land use changes and climate change impact (Hamidov et al., 2018; Sünnemann et al., 2023).

The physical properties of the soil, such as texture, structure, bulk density, porosity, and aggregate distribution, control soil physical processes like infiltration, percolation, and seepage. Consequently, these properties directly impact water storage, flow, and drainage within the soil (Li et al., 2019). These properties can be regarded as indicators of the physical resiliency of soil (de Andrade Bonetti et al., 2017), influencing soil hydraulic parameters (SHPs) and subsequently causing shifts in soil water dynamics and material transport within the soil (Hartmann et al., 2020). Common SHPs like saturated and unsaturated hydraulic conductivity, soil water retention, available water capacity, and infiltration capacity provide valuable insights into the current conditions and soil water dynamics. These SHPs are influenced by inherent soil properties such as soil texture, porosity, bulk density, organic matter, and surface and subsurface crusting (Indoria et al., 2020).

SHPs are subject to modification over time based on seasonal wetting-drying cycles, freeze-thaw cycles, management practices, and changes in vegetation and root distribution (Lu et al., 2020; Leuther and Schlüter, 2021). Moreover, SHPs are critical in partitioning rainfall or irrigated water into infiltration and surface runoff (Ghosh et al., 2019; Picciafuoco et al., 2019). They are also useful in predicting plant-water relationships (Indoria et al., 2020), assessing irrigation and drainage efficiency (Ali et al., 2014), and modeling soil water dynamics (Feki et al., 2020).

Conventional methods for SHP estimation, such as infiltrometers, Guelph permeameters, tension infiltrometers, and rainfall simulators (Verbist et al., 2013), are mostly intensive, invasive, expensive, and time-consuming. Additionally, these methods cannot provide the satisfactory spatial-temporal resolution needed for large-scale and continuous monitoring of soil water dynamics (Zou et al., 2023) to capture soil hydraulic resistance and overall resilience of soil.

Geophysical techniques are gaining popularity as a proxy method for characterizing shallow subsurface soil's physical and hydrologic properties with high temporal and spatial resolutions (Hubbard and Rubin, 2005; Zou et al., 2023). Although initially developed for engineering and geological applications, geophysical techniques have expanded their utility into various fields, including archeology, environmental science, oceanography, forestry and agricultural studies. Standard geophysical techniques used for agricultural applications are electromagnetic induction–EMI, electrical resistivity tomography–ERT, and ground-penetrating radar–GPR (Allred, 2008; Allred et al., 2010; Bitella et al., 2015; Lombardi et al., 2022). The application of these techniques can provide spatiotemporal information in the field, a crucial aspect essential for supporting site-specific management of agricultural resources and precision agriculture.

GPR is commonly used in soil hydrological studies because the propagation velocity of the GPR waves is very sensitive to changes in soil water content–SWC (Huisman et al., 2003; Slater and

Comas, 2009; Klotzsche et al., 2018). The GPR wave velocity is mainly influenced by the material's dielectric permittivity— K_r (Zajícová and Chuman, 2019), which is highly dependent on water content due to the significant difference between K_r of water (80) and all other materials (Galagedara et al., 2005a; Klotzsche et al., 2019a). Hence, GPR has been used in estimating SWC for over two decades (Chanzy et al., 1996; Galagedara et al., 2003a; Lunt et al., 2005; Mangel et al., 2022; Pathirana et al., 2023).

While GPR measurements are not directly related to SHPs, their potential to infer water and solute movement in soil has gained much attention owing to their sensitivity to fluid distribution (Kowalsky et al., 2005; Looms et al., 2008a; Yu et al., 2021; Zhang et al., 2022; Zou et al., 2023). When applied to monitoring soil water dynamics and estimating SHPs, GPR measurements rely on changes in SWC due to K_r differences (Rossi et al., 2015; Klotzsche et al., 2018; Klotzsche et al., 2019a).

The characterization of SHPs using GPR has mostly involved analysis of time-lapse GPR waves, specifically ground wave data, in both unsaturated and saturated soil samples (Weihnacht and Boerner, 2014; Klenk et al., 2015; Lombardi et al., 2022). The GPR-derived data is often coupled with soil hydrodynamic models (like the Richards equation) to estimate SHP (Léger et al., 2014; Pathirana et al., 2023).

Estimating SHPs using GPR employs comparable antenna positioning systems, techniques, measurement methods, survey strategies, and data processing methods like SWC estimation. Specifically, the three main GPR techniques (surface, borehole, and off-ground) have been used in studying soil water dynamics and SHP estimation in the last two decades (Kowalsky et al., 2005; Looms et al., 2008a; Lambot et al., 2010; Lai et al., 2012; Dagenbach et al., 2013; Zou et al., 2023).

A growing number of studies has emerged on soil hydraulic parametrization using GPR, with recent advancements focusing on the adoption of full waveform inversion (FWI) for increased accuracy (Yu et al., 2021), coupled inversion strategies (Yu et al., 2022) and integration of multiple geophysical data (Rossi et al., 2015). Other emerging methodologies are the assimilation of GPR data through various techniques (Cui et al., 2020), visualization and characterization of non-uniform flow in soils (Allroggen and Tronicke, 2015; Di Prima et al., 2022), and quantification of uncertainty in parameterization (Zhao et al., 2023), using diverse GPR techniques.

While there are extensive reviews addressing the general applications of GPR in soil studies (Liu et al., 2016; Lombardi et al., 2022; Pathirana et al., 2023) and specific ones focusing on SWC estimation (Huisman et al., 2003; Klotzsche et al., 2018; Liu et al., 2019), there are, to the best of our knowledge, only limited reviews on the application of GPR for SHP estimation. Zhang et al. (2022) recently reviewed GPR applications for soil water dynamic studies focusing on travel time and FWI methods.

This review focuses on comparing the application of the three GPR techniques—Borehole, Surface, and Off-ground—for predicting SHPs and their potential for studying soil water dynamics. The paper examines recent advancements in these techniques while also highlighting their current limitations. The analysis reveals an imbalance in strengths and weaknesses among the three methods and shows potential areas for improvement in accuracy, speed, and robustness.

2.2. Ground Penetrating Radar Principles and Methods

The GPR is a well-established geophysical technique that uses electromagnetic waves (EM) with frequencies commonly between 10 to 3600 MHz to image the subsurface (Lunt et al., 2005;

Dojack, 2012; Liu et al., 2019; Akinsunmade, 2021). The EM waves are propagated into the subsurface through the transmitter antenna, modified by the subsurface difference in K_r , electrical conductivity (σ), and magnetic permeability (μ). The receiving signals at the receiver antennae provide valuable information such as the two-way travel time, amplitude, waveform, and phase (Liu et al., 2019; Zajícová and Chuman, 2019). Detailed theoretical and empirical background on EM methods and GPR principles were reported in Huisman et al., 2003; Jol, 2008; Pathirana et al., 2023.

For agricultural applications, GPR is most extensively used in studying water-related issues. Many studies and reviews have been conducted on GPR applications for SWC, with well-developed methods for field-scale measurements. Different categories of radar system configurations, observation modes, and methodologies have been used in SWC measurement studies. More details on these categories can be seen in recent publications (Liu et al., 2019; Zhang et al., 2022; Pathirana et al., 2023). Notably, SWC estimation can be carried out using three forms of radar system configuration: surface (ground-coupled), borehole, and off-ground. Each radar system configuration has survey techniques selected based on a particular application's objective. Based on system architecture, GPR can be frequency domain or time domain (or pulsed radars). Time-domain GPR has the advantage of fast data acquisition and is more commercially available (Lombardi et al., 2022). Regarding SHP estimation, time-domain GPR is more commonly applied due to its ability to capture the propagation of EM waves through the subsurface with high spatial and temporal resolution (Allroggen and Tronicke, 2015). Consequently, it has shown great potential in monitoring vadose zone flow processes and imaging soil hydro-geophysical properties (Jadoon et al., 2012).

2.3. Surface GPR for Soil Hydraulic Parameters Estimation

Surface GPR primarily utilizes three survey techniques: fixed offset (FO), wide-angle reflection and refraction (WARR), and common midpoint (CMP) (Galagedara et al., 2005a; Liu et al., 2019; Pathirana et al., 2023; Zhang et al., 2022). As far as SHP estimation is concerned, the FO technique has been commonly used in monitoring infiltration (Saintenoy et al., 2008; Moysey, 2010; Lai et al., 2012; Leger et al., 2014; Klenk et al., 2015; Zou et al., 2023). Leger et al. (2014) assessed the application of the FO method to monitor the wetting front in sandy soils and estimate the Mualem-van Genuchten parameters. The results obtained by authors from the experiment closely aligned with laboratory and disk infiltrometer measurements.

Mangel et al. (2012) conducted a laboratory-scale infiltration and redistribution experiment to ascertain the effectiveness of multi-offset GPR (WARR) in monitoring infiltration fronts and capturing the temporal variability of SWC in dynamic systems. The authors acquired a 3-dimensional GPR dataset, interpreted as multi-offset or common-offset based on the distinctive automated time-lapse multi-offset adopted in the research. However, Galagedara et al. (2005a) evaluated the feasibility of using the FO and WARR methods for monitoring soil water dynamics under uniform irrigation and subsequent drainage. The authors suggested using the WARR survey to identify direct groundwaves and to select the best offsets for the FO method, which is suitable for a larger area (Galagedara et al., 2005a). Some studies have used the CMP method to characterize the subsurface vertical soil water dynamics. Steelman et al. (2012) acquired concurrent reflection profiles and CMP soundings for 26 months. Their results indicate that GPR-derived hydraulic estimates agreed with laboratory-derived estimates.

Surface GPR has generally been applied in various applications for studying soil water dynamics and SHPs estimation. For instance, many studies have used surface GPR for monitoring wetting

front depth (Saito et al., 2021) and hysteresis of water retention and hydraulic conductivity functions (Klenk et al., 2015; Léger et al., 2020). Further, it has been used for studying the transition zone above the water table by noting the shape of GPR reflection (Klenk et al., 2015) and for characterization of the unsaturated zone through wetting and drying (Moysey, 2010; Lai et al., 2012). In addition, surface GPR has recently been utilized to identify and describe non-uniform flow in soils. Di Prima et al. (2020) used a time-lapse GPR survey together with automated single-ring infiltration experiments to visualize three-dimensional (3D) wetting behaviors and identify the occurrence of preferential flow pathways and funneled flow in the subsurface.

Both sequential and coupled inversion techniques have also been applied to estimate SHPs from surface GPR. Busch et al. (2013) applied a coupled inversion approach that combines conventional ray-based analysis of time-lapse surface GPR data with a hydrological forward model to evaluate SHPs of synthetic and field GPR data from southern Ontario. The approach resulted in a better fit than an uncalibrated model using laboratory-derived SHPs. Ciu et al. (2020) utilized the Ensemble Smoother with Multiple Data Assimilation (ES-MDA), a stochastic approach, to estimate SHPs by updating the soil component. The findings showed that the approach achieves greater accuracy when simultaneously updating one, two, or three parameters. However, the error tends to increase when updating approximately five parameters together.

Recent developments in surface GPR application for SHP estimation involve integrating geophysical methods and data assimilation techniques for better characterization. Rossi et al. (2015) monitored a controlled infiltration experiment using ERT and GPR and determined SHPs using a sequential importance resampling (SIR) data assimilation process.

2.4. Borehole GPR for Soil Hydraulic Parameters Estimation

Many initial studies on monitoring soil water dynamics and estimating SHPs using GPR data focused on the borehole method (Galagedara et al., 2003b; Rucker and Ferré, 2004). Rucker and Ferré (2004) employed a procedure using the first arrival travel time measurements of borehole GPR to infer SHPs, and the method has gained wider application since then. The method's popularity in studying soil water dynamics can be credited to its high vertical resolution characteristics (Binley et al., 2001; Looms et al., 2008a) and heightened sensitivity to pore water distribution (Kowalsky et al., 2005). These attributes enhance spatial representativeness, making it well-suited for monitoring infiltration and recharge processes.

In the borehole GPR method, the transmitter is placed in one borehole, and the receiver is in another borehole, with water injection in between or around to initiate a change in soil moisture dynamics. This water injection can occur through a natural infiltration process, typically requiring observation over an extended period (Binley and Beven, 2003), a forced infiltration experiment using irrigation methods (Looms et al., 2008b; Kuroda et al., 2009) or a conventional infiltrometer (Di Prima et al., 2020).

Generally, three main acquisition methods are employed in borehole GPR: zero-offset profiling (ZOP), multi-offset gathering (MOG), and vertical radar profiling. ZOP, which is by far the most widely used acquisition strategy (Rejiba et al., 2012), uses the arrival time of the direct wave to calculate the velocity and soil permittivity (Zhang et al., 2022). The use of this method for SHP estimation is well documented in the literature (Rucker and Ferré, 2004; Kuroda et al., 2009; Scholer et al., 2011; Klotzsche et al., 2019a; Yu et al., 2022). The vertical radar profiling method (also known as the single-borehole technique) investigates the subsurface by only placing one antenna in a hole, thus reducing the soil disturbance level (Liu et al., 2019). Generally, it provides

increased penetration depth and resolution compared to the surface GPR technique. However, limited studies have used the vertical radar profiling borehole method to monitor water flow and transport (Tronicke and Hamann, 2014).

Conventionally, borehole GPR data has been processed through ray-based tomographic inversion approaches, leveraging the first arrival times for velocity information and the first cycle amplitude for attenuation information (Irving et al., 2007; Yu et al., 2022). However, this approach provides limited resolution due to the small amount of data considered and is subject to several uncertainties (Looms et al., 2008a). An additional constraint of the ray-based tomographic inversion approach involves challenges related to non-uniqueness and optimization issues when reconstructing subsurface images. This has led to the use of joint, hydro-geophysical inversion techniques, with GPR and hydrological data used to constrain each other (Kowalsky et al., 2005).

Generally, both stochastic and deterministic inversion approaches have been used to obtain vadose zone SHPs. Scholer et al. (2011) used the Bayesian Markov chain Monte Carlo (MCMC) stochastic inversion approach to study how different degrees of prior information (non-informative and informative) can be useful in estimating van-Genuchten-Mualem (VGM) parameters using ZOP cross-hole GPR data under steady-state conditions. The authors noted a significant improvement using informative priors based on soil property databases.

Sequential and coupled inversion strategies are the two commonly used hydro-geophysical inversion techniques to estimate SHP from time-lapse borehole GPR data (Yu et al., 2021). The sequential inversion strategy is a much simpler approach that combines GPR-estimated SWC data and a hydrological model to derive SHPs using inverse modeling (Huisman et al., 2010). The major drawback of this approach is that errors in GPR data interpretations, such as the straight-wave approximation, may quickly propagate into the derived SHPs (Yu et al., 2021). Coupled inversion,

however, avoids this error propagation by combining the hydrological model with a forward GPR data model, minimizing the mismatch between measured and modeled geophysical response (Yu et al., 2022).

An emerging technique for processing borehole GPR data is FWI, which considers the entire measured signal, including reflections and refractions. Yu et al. (2022) combined the benefits of both coupled inversion and FWI techniques, termed “a coupled full-waveform inversion (CFWI).” The experiment involved a synthetic infiltration event to estimate SHP from ZOG borehole GPR measurements. CFWI gave more accurate water retention and hydraulic conductivity function results than the coupled inversion of GPR travel times.

A flowchart showing the coupled inversion of travel times and FWI, as carried out by Yu et al. (2021 and 2022), is presented in Figure 2.1. Both approaches require minimizing the misfit between measured data and modeled data. However, while coupled inversion of travel time considers the first arrival data time of the measured data, CFWI considers the entire GPR waveform data of the measured data. Similarly, an initial simulation of vertical soil water profiles (θ^{mod}) using Hydrus-1D is required for both methods. Still, CFWI considers soil electrical conductivity (σ^{mod}) for GPR modeling, while coupled inversion of travel time considers dielectric permittivity profiles (ϵ^{mod}).

In addition, a few studies have also integrated borehole GPR data with other geophysical data to provide better estimates of SHPs. For instance, Looms et al. (2008a) and (2008b) developed a framework that integrated cross-borehole GPR travel time and ERT data to monitor tracer infiltration and reduce hydraulic parameter uncertainties, respectively.

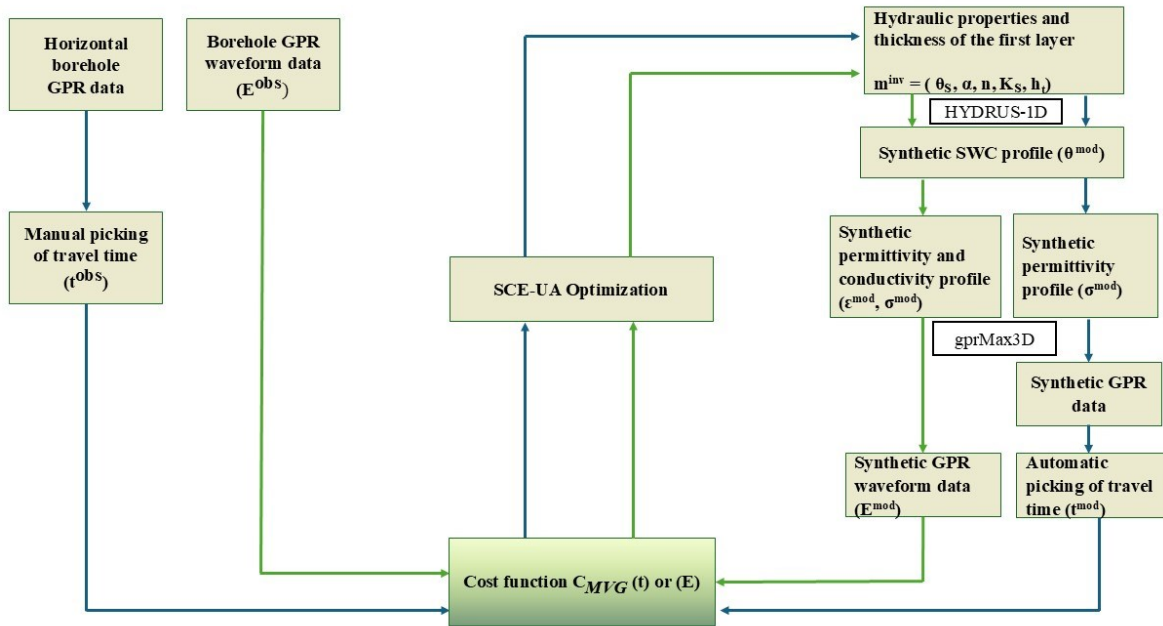


Figure 2.1. Flowchart of coupled inversion of ground penetrating radar (GPR) travel times (blue pathway) and coupled full-waveform inversion (CFWI) (green pathway) (Adapted from Yu et al., 2021 and 2022). SCE-UA = Shuffled Complex Evolution-University of Arizona

2.5. Off-ground GPR for Soil Hydraulic Parameters Estimation

Off-ground GPR (also known as air-borne) has also been applied to monitor soil water dynamics and to estimate SHPs. Off-ground GPR works by emitting EM waves from the air into the ground and measuring the reflection that bounces back from the soil surface (Zhang et al., 2022). This method's main advantage is its ability to rapidly provide spatially continuous measurements of soil properties (Ardekani, 2013). However, the technique is limited by penetration depth (approximately 1~2cm), depending on the soil conditions, height of measurement, antenna

frequency, and electromagnetic (EM) penetration capacity (Serbin and Or, 2003, 2004; Liu et al., 2019). The surface roughness and vegetation can also affect the potential of monitoring soil water dynamics using off-ground GPR (Lambot et al., 2006a).

Lambot et al.'s (2006, 2009, 2010) work form a significant foundation for applying off-ground GPR for SHP estimation. Lambot et al. (2009) utilized the off-ground GPR system to estimate shallow subsurface SHPs of unsaturated sandy soil using FWI in a coupled inversion strategy. Jadoon et al. (2012) extended these works to field conditions using off-ground GPR to estimate SHPs for single and dual porosity models using integrated FWI from air-launched GPR and one-dimensional vertical hydrodynamic inversion. The authors utilized a 200-800 MHz frequency range GPR and combined the roughness and antenna-medium models to generate plausible SHPs. Nonetheless, the application of off-ground GPR for SHPs is still limited by the constrained level of information that can be obtained from deeper soil layers due to significant dielectric contrast at the point where the soil meets the air, which reflects a large portion of energy (Klotzsche et al., 2018).

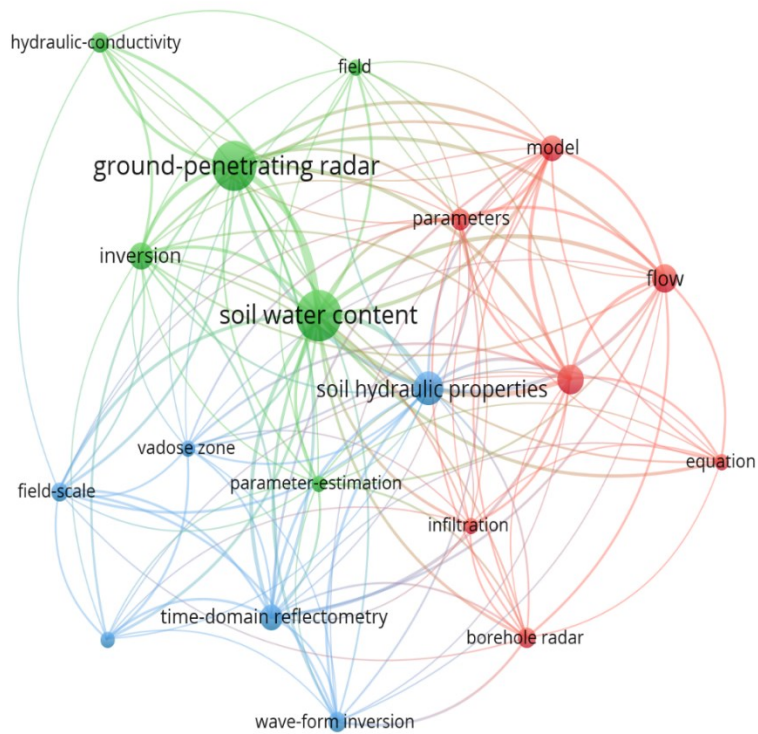


Figure 2.2. Network visualization map illustrating the primary areas of ground-penetrating radar (GPR) applications in studying water-related issues in the last 20 years (2004 -2023).

Table 2.1. Comparison of surface, borehole, and off-ground ground penetrating radar (GPR) potentials for soil hydraulic characterization showing advantages and limitations of each technique.

S/N	Characteristics	Surface GPR	Borehole GPR	Off-ground GPR	References
1	Investigation of depth and resolution of flow and transport process	Reasonable investigation depth and vertical resolution	Large investigation depth and higher vertical resolution	Smaller investigation depth and lower resolution	Huisman et al., 2003; Klotzsche et al., 2018
2	Invasiveness	Non-invasive	Invasive	Non-invasive	Steelman et al., 2012
3	Potential for large-scale characterization	Suitable for mapping	Not suitable	Highly suitable	Mangel et al., 2012
4	Common Measurement Method(s)	Reflected wave Groundwave	Ground wave	Surface reflections	Lambot et al., 2009; Zhang et al., 2019
5	Application of FWI	Well-suited. Effective in providing detailed near-surface imaging	FWI can significantly improve resolutions	Extensive work on this, but still challenging due to lower resolutions, surface roughness and the effects of	Lambot et al., 2009; Yang et al., 2013; Klotzsche et al., 2019b

				air-surface interactions.	
6	Combination with other geophysical methods	Can be easily combined with other surface techniques like electrical resistivity	Can be combined with other borehole techniques like cross-hole ERT	Potential for integration with other remote sensing techniques	Grasmueck and Viggiano, 2007; Looms et al., 2008b; Salako and Adepelumi, 2016

2.6. Discussion

The network visualization map illustrated the research trends spanning the last two decades in GPR applications in hydrology. Most research studies have focused on examining soil water content, as indicated by the larger circle, while comparatively fewer studies have explored SHPs, as shown in Figure 2.2. Particularly noteworthy in Figure 2.2 is the lack of studies (represented by smaller circles) in aspects such as inversion, parameter estimation, infiltration, and hydraulic conductivity. These aspects represent promising opportunities for future research to advance GPR applications within the field of soil hydrology. Furthermore, there is a noticeable inclination towards utilizing borehole radar for studies on SHPs, while investigations on surface and off-ground techniques remain limited. Based on the reviewed studies, the three GPR techniques have demonstrated successes and challenges, presenting comparative advantages and disadvantages, as elaborated in Table 2.1.

The most significant developments have been witnessed with GPR data processing and interpretation, particularly the use of FWI, which has been applied to surface GPR (Busch et al.,

2014), borehole GPR (Yu et al., 2021, 2022) and off-ground GPR (Lambot et al., 2009; Jadoon et al., 2012; Lambot and André, 2014). Lambot et al. (2010) emphasize that FWI, compared to surface reflection methods, has the advantage of filtering out antenna distortion effects, resulting in increased accuracy. Nonetheless, applying FWI requires careful consideration of several factors, including the initial model, data quality, and the frequency content of the GPR data.

Yu et al. (2020) recently combined ZOP borehole GPR measurements and surface GPR to investigate moisture dynamics in a forced infiltration event. The study found reasonable consistency between GPR results and SWC derived from time domain reflectometry (TDR). Similarly, some other studies have reported improved accuracy in SHP results when GPR is combined with other geophysical measurements. Zou et al. (2023) investigated a lab-scale water infiltration experiment using coupled time-lapse ERT data and GPR-derived permittivity with moisture sensor measurement. The authors concluded that the approach gave robust infiltration rate and hydraulic conductivity estimates and is feasible for monitoring the transient soil water dynamics in the shallow vadose zone. However, most of these studies have concentrated on combining GPR with only the ERT method (Looms et al., 2008; Rossi et al., 2015; Salako and Adepelumi, 2016), with limited work combining it with other geophysical techniques.

Additionally, there is a trend toward employing coupled inversion techniques to evaluate the agreement between observed geophysical measurements and hydrological models for estimating SHPs. Yu et al. (2021) noted that in comparison to sequential inversion techniques, the coupled inversion technique eliminates artifacts and could include other data sources within the inversion. However, the approach is still limited by its complex computational requirements and reliance on uncertain petrophysical relationships between geophysical measurements and hydrological models (Binley et al., 2015; Klotzsche et al., 2018).

Most of the research on SHPs estimation has been done in the laboratory or simulation/modelling to develop reliable models similar to pedo-transfer functions and experimental data (Lombardi et al., 2022; Zou et al., 2023). Attempts to replicate these methodologies on larger field-scale applications often face limitations and are constrained by time requirements. Additional time is needed to facilitate irrigation or infiltration until saturation and to collect and process spatially detailed data. Another challenge is the uncertainties in estimates due to inherent variability/complexity arising from the heterogeneity found under field conditions. Additionally, SHP estimates from these methods are still subject to high variability and show less accuracy when compared with standard methods. The reasons for this low precision and accuracy in results can be due to the assumptions and simplifications, like homogeneity and isotropy, included in the inversion model and the variability of the petrophysical properties (Jadoon et al., 2012). As a result, the characterization scales of hydrodynamic parameters and methodology should be considered while recording results.

2.7. Conclusions and Future Outlook

This mini-review discusses recent advances in estimating soil hydraulic parameters (SHPs) and studying soil water dynamics as crucial indicators of hydraulic resistance in soil, using ground penetrating radar (GPR) as a near-surface geophysical method. Specifically, the review focused on the potential and limitations of surface, boreholes, and off-ground GPR in estimating SHPs for water dynamic studies. Although surface and off-ground methods offer faster, scalable, and environmentally conscious properties due to their non-invasive nature, they do not provide the same level of spatial resolution for soil water dynamics as borehole GPR. Nonetheless, the invasive nature of the borehole GPR method undermines one of its primary advantages, namely non-

destructiveness, along with limited scalability, which are key considerations for the application of geophysical methods in soil studies.

In the future, more attention must be paid to improving the three methods for efficiency and accuracy. The off-ground GPR holds more potential for fast and large-scale characterization of SHPs, which are prerequisites for precision agriculture applications. Recent data collection and processing advancements using borehole and surface GPR methods should be replicated or modified with off-ground methods to improve usability and accuracy. Full-waveform inversion (FWI) has shown valuable and greater accuracy for GPR data processing and offers tremendous potential for SHP estimation, which can improve the spatial representativeness of surface GPR. However, the application of FWI is still complex and cannot be readily applied by non-experts. The future direction of GPR applications in soil studies needs to focus on automating some of the processes involved in FWI. Advances and integration of machine learning algorithms and artificial intelligence are expected to present a faster and more robust inversion process.

Further work combining other geophysical methods, such as electromagnetic induction, seismic surveys, and magnetometry with GPR, is expected to increase and improve the depth of measurement, accuracy, and the potential for enhanced SHP estimation.

The complexity of GPR data processing has challenges in its use as a fast and reliable method for SHP estimation. The standard inversion modelling method used to derive SHP estimates can be demanding and full of uncertainty and assumptions. Incorporating GPR data into infiltration processes using established calculation methods, such as the Beerkan Infiltration method, can offer simpler approaches for estimating SHPs.

Finally, there is a growing trend toward real-time and automated GPR data collection, analysis, and interpretation. This is anticipated to enable robust, rapid, and feasible large-scale subsurface characterization, including SHP estimation. This review concludes that with the introduction of more robust processing techniques like the coupled full-waveform inversion and the inclusion of artificial intelligence applications for faster data processing, there is a tremendous opportunity for more field research in improving SHP estimation accuracy and water dynamics studies, which can ultimately increase their application in soil water management and precision agriculture technologies.

2.8. Acknowledgements

The authors acknowledge the financial support provided by the Natural Sciences and Engineering Research Council of Canada, Discovery Grant (NSERC-DG: RGPIN-2019-04614), and the School of Graduate Studies, Memorial University of Newfoundland (MUN).

2.9. References

- Akinsunmade, A., 2021. GPR imaging of traffic compaction effects on soil structures. *Acta Geophysica* 69(2), 643–653. <https://doi.org/10.1007/s11600-020-00530-0>.
- Ali, M.H., Islam, A.K.M.R., Zaman, M.H., 2014. Improving soil hydraulic properties for better agricultural water management and crop production – A review. *International Journal of Engineering and Technical Research* 2, 30–34.
- Allred, B., 2008. *Handbook of agricultural geophysics (Books in soils, plants, and the environment)*. CRC Press, Boca Raton.
- Allred, B.J., Freeland, R.S., Farahani, H.J., Collins, M.E., 2010. Agricultural geophysics: Past, present, and future. *Symposium on the Application of Geophysics to Engineering and Environmental Problems* 23, 190–202. <https://doi.org/10.4133/1.3445432>.
- Allroggen, N., Tronicke, J., 2015. Analysis of time-lapse GPR data to visualize preferential flow paths. *8th International Workshop on Advanced Ground Penetrating Radar (IWAGPR)*, 1–3. <https://doi.org/10.1109/IWAGPR.2015.7292627>.
- Binley, A., Beven, K., 2003. Vadose zone flow model uncertainty as conditioned on geophysical data. *Groundwater* 41(2), 119-127.
- Binley, A., Hubbard, S.S., Huisman, J.A., Revil, A., Robinson, D.A., Singha, K., Slater, L.D., 2015. The emergence of hydrogeophysics for improved understanding of subsurface processes over multiple scales. *Water Resources Research* 51(6), 3837–3866. <https://doi.org/10.1002/2015WR017016>.

- Binley, A., Winship, P., Middleton, R., Pokar, M., West, J., 2001. High-resolution characterization of vadose zone dynamics using cross-borehole radar. *Water Resources Research* 37(11), 2639–2652. <https://doi.org/10.1029/2000WR000089>.
- Bitella, G., Rossi, R., Loperte, A., Satriani, A., Lapenna, V., Perniola, M., Amato, M., 2015. Geophysical techniques for plant, soil, and root research related to sustainability. In: *The sustainability of agro-food and natural resource systems in the Mediterranean Basin*, Springer International Publishing, pp. 353-372.
- Busch, S., van der Kruk, J., Vereecken, H., 2014. Improved characterization of fine-texture soils using on-ground GPR full-waveform inversion. *IEEE Transactions on Geoscience and Remote Sensing* 52(7), 3947–3958. <https://doi.org/10.1109/TGRS.2013.2278297>.
- Busch, S., Weihermüller, L., Huisman, J.A., Steelman, C.M., Endres, A.L., Vereecken, H., van der Kruk, J., 2013. Coupled hydrogeophysical inversion of time-lapse surface GPR data to estimate hydraulic properties of a layered subsurface. *Water Resources Research* 49(12), 8480–8494. <https://doi.org/10.1002/2013WR013992>.
- Chanzy, A., Tarussov, A., Bonn, F., Judge, A., 1996. Soil water content determination using a digital ground-penetrating radar. *Soil Science Society of America Journal* 60(5), 1318–1326. <https://doi.org/10.2136/sssaj1996.03615995006000050005x>.
- Cui, F., Bao, J., Cao, Z., Li, L., Zheng, Q., 2020. Soil hydraulic parameters estimation using ground penetrating radar data via ensemble smoother with multiple data assimilation. *Journal of Hydrology* 583, 124552. <https://doi.org/10.1016/j.jhydrol.2020.124552>.

- Dagenbach, A., Buchner, J.S., Klenk, P., Roth, K., 2013. Identifying a parameterisation of the soil water retention curve from on-ground GPR measurements. *Hydrology and Earth System Sciences* 17(2), 611–618. <https://doi.org/10.5194/hess-17-611-2013>.
- de Andrade Bonetti, J., Anghinoni, I., de Moraes, M.T., Fink, J.R., 2017. Resilience of soils with different texture, mineralogy and organic matter under long-term conservation systems. *Soil and Tillage Research* 174, 104–112. <https://doi.org/10.1016/j.still.2017.06.008>.
- Di Prima, S., Giannini, V., Ribeiro Roder, L., Giadrossich, F., Lassabatere, L., Stewart, R.D., Abou Najm, M.R., Longo, V., Campus, S., Winiarski, T., Angulo-Jaramillo, R., Del Campo, A., Capello, G., Biddoccu, M., Roggero, P.P., Pirastru, M., 2022. Coupling time-lapse ground penetrating radar surveys and infiltration experiments to characterize two types of non-uniform flow. *Science of The Total Environment* 806, 150410. <https://doi.org/10.1016/j.scitotenv.2021.150410>.
- Di Prima, S., Winiarski, T., Angulo-Jaramillo, R., Stewart, R.D., Castellini, M., Abou Najm, M.R., Ventrella, D., Pirastru, M., Giadrossich, F., Capello, G., Biddoccu, M., Lassabatere, L., 2020. Detecting infiltrated water and preferential flow pathways through time-lapse ground-penetrating radar surveys. *Science of The Total Environment* 726, 138511. <https://doi.org/10.1016/j.scitotenv.2020.138511>.
- Dojack, L., 2012. Ground penetrating radar theory, data collection, processing, and interpretation: A guide for archaeologists. University of British Columbia. <https://doi.org/10.14288/1.0086065>.
- Feki, M., Ravazzani, G., Barontini, S., Ceppi, A., Mancini, M., 2020. A comparative assessment of the estimates of the saturated hydraulic conductivity of two

- anthropogenic soils and their impact on hydrological model simulations. *Soil and Water Research* 15(3), 135–147. <https://doi.org/10.17221/33/2019-SWR>.
- Galagedara, L.W., Parkin, G.W., Redman, J.D., 2003. An analysis of the ground-penetrating radar direct ground wave method for soil water content measurement. *Hydrological Processes* 17(18), 3615–3628. <https://doi.org/10.1002/hyp.1351>.
- Galagedara, L.W., Parkin, G.W., Redman, J.D., Endres, A.L., 2003. Assessment of soil moisture content measured by borehole GPR and TDR under transient irrigation and drainage. *Journal of Environmental and Engineering Geophysics* 8(2), 77–86. <https://doi.org/10.4133/JEEG8.2.77>.
- Galagedara, L.W., Parkin, G.W., Redman, J.D., von Bertoldi, P., Endres, A.L., 2005a. Field studies of the GPR ground wave method for estimating soil water content during irrigation and drainage. *Journal of Hydrology* 301(1), 182–197. <https://doi.org/10.1016/j.jhydrol.2004.06.031>.
- Ghosh, B., Pekkat, S., 2019. A critical evaluation of the variability induced by different mathematical equations on hydraulic conductivity determination using disc infiltrometer. *Acta Geophysica* 67, 863–877. <https://doi.org/10.1007/s11600-019-00266-6>.
- Hamidov, A., Helming, K., Bellocchi, G., Bojar, W., Dalgaard, T., Ghaley, B.B., Hoffmann, C., Holman, I., Holzkämper, A., Krzeminska, D., Kværnø, S.H., Lehtonen, H., Niedrist, G., Øygarden, L., Reidsma, P., Roggero, P.P., Rusu, T., Santos, C., Seddaiu, G., Schönhart, M., 2018. Impacts of climate change adaptation options on soil functions: A review of European case studies. *Land Degradation & Development* 29(8), 2378–2389. <https://doi.org/10.1002/ldr.3006>.

- Hartmann, A., Weiler, M., Blume, T., 2020. The impact of landscape evolution on soil physics: Evolution of soil physical and hydraulic properties along two chronosequences of proglacial moraines. *Earth System Science Data* 12(4), 3189–3204. <https://doi.org/10.5194/essd-12-3189-2020>.
- Huang, L., Shao, M., 2019. Advances and perspectives on soil water research in China's Loess Plateau. *Earth-Science Reviews* 199, 102962. <https://doi.org/10.1016/j.earscirev.2019.102962>.
- Hubbard, S.S., Rubin, Y., 2005. Introduction to hydrogeophysics. In: Rubin, Y., Hubbard, S.S. (Eds.), *Hydrogeophysics*, Springer Netherlands, pp. 3–21. https://doi.org/10.1007/1-4020-3102-5_1.
- Huisman, J.A., Hubbard, S.S., Redman, J.D., Annan, A.P., 2003. Measuring soil water content with ground penetrating radar: A review. *Vadose Zone Journal* 2(4), 476–491. <https://doi.org/10.2136/vzj2003.4760>.
- Indoria, A.K., Sharma, K.L., Reddy, K.S., 2020. Hydraulic properties of soil under warming climate. In: *Climate change and soil interactions*, Elsevier, pp. 473–508. <https://doi.org/10.1016/B978-0-12-818032-7.00018-7>.
- Jadoon, K.Z., Weihermüller, L., Scharnagl, B., Kowalsky, M.B., Bechtold, M., Hubbard, S.S., Vereecken, H., Lambot, S., 2012. Estimation of soil hydraulic parameters in the field by integrated hydrogeophysical inversion of time-lapse ground-penetrating radar data. *Vadose Zone Journal* 11(4), vzj2011.0177. <https://doi.org/10.2136/vzj2011.0177>.
- Jol, H.M., 2008. *Ground penetrating radar theory and applications*. Elsevier, Amsterdam.

- Klenk, P., Jaumann, S., Roth, K., 2015. Quantitative high-resolution observations of soil water dynamics in a complicated architecture using time-lapse ground-penetrating radar. *Hydrology and Earth System Sciences* 19(3), 1125–1139. <https://doi.org/10.5194/hess-19-1125-2015>.
- Klotzsche, A., Jonard, F., Looms, M.C., van der Kruk, J., Huisman, J.A., 2018. Measuring soil water content with ground penetrating radar: A decade of progress. *Vadose Zone Journal* 17(1), 1–9. <https://doi.org/10.2136/vzj2018.03.0052>.
- Klotzsche, A., Lärm, L., Vanderborght, J., Cai, G., Morandage, S., Zörner, M., Vereecken, H., van der Kruk, J., 2019a. Monitoring soil water content using time-lapse horizontal borehole GPR data at the field-plot scale. *Vadose Zone Journal* 18(1), 190044. <https://doi.org/10.2136/vzj2019.05.0044>.
- Klotzsche, A., Vereecken, H., van der Kruk, J., 2019b. Review of crosshole ground-penetrating radar full-waveform inversion of experimental data: Recent developments, challenges, and pitfalls. *Geophysics* 84(6), H13–H28. <https://doi.org/10.1190/geo2018-0597.1>.
- Kowalsky, M.B., Finsterle, S., Peterson, J., Hubbard, S., Rubin, Y., Majer, E., Ward, A., Gee, G., 2005. Estimation of field-scale soil hydraulic and dielectric parameters through joint inversion of GPR and hydrological data. *Water Resources Research* 41(11). <https://doi.org/10.1029/2005WR004237>.
- Kuroda, S., Jang, H., Kim, H.J., 2009. Time-lapse borehole radar monitoring of an infiltration experiment in the vadose zone. *Journal of Applied Geophysics* 67(4), 361–366. <https://doi.org/10.1016/j.jappgeo.2008.07.005>.

- Lai, W.W.L., Kou, S.C., Poon, C.S., 2012. Unsaturated zone characterization in soil through transient wetting and drying using GPR joint time–frequency analysis and grayscale images. *Journal of Hydrology* 452–453, 1–13. <https://doi.org/10.1016/j.jhydrol.2012.03.044>.
- Lambot, S., André, F., 2014. Full-wave modeling of near-field radar data for planar layered media reconstruction. *IEEE Transactions on Geoscience and Remote Sensing* 52(5), 2295–2303. <https://doi.org/10.1109/TGRS.2013.2259243>.
- Lambot, S., Antoine, M., Vanclooster, M., Slob, E.C., 2006. Effect of soil roughness on the inversion of off-ground monostatic GPR signal for non-invasive quantification of soil properties. *Water Resources Research* 42(3). <https://doi.org/10.1029/2005WR004416>.
- Lambot, S., Slob, E., Minet, J., Jadoon, K.Z., Vanclooster, M., Vereecken, H., 2010. Full-waveform modeling and inversion of ground-penetrating radar data for non-invasive characterization of soil hydrogeophysical properties. In: Rossel, R.A.V., McBratney, A.B., Minasny, B. (Eds.), *Proximal soil sensing*, Springer Netherlands, pp. 299–311. https://doi.org/10.1007/978-90-481-8859-8_25.
- Lambot, S., Slob, E., Rhebergen, J., Lopera, O., Jadoon, K.Z., Vereecken, H., 2009. Remote estimation of the hydraulic properties of a sand using full-waveform integrated hydrogeophysical inversion of time-lapse, off-ground GPR data. *Vadose Zone Journal* 8(3), 743–754. <https://doi.org/10.2136/vzj2008.0058>.
- Léger, E., Saintenoy, A., Coquet, Y., 2014. Hydrodynamic parameters of a sandy soil determined by ground-penetrating radar inside a single ring infiltrometer. *Water Resources Research* 50(7), 5459–5474. <https://doi.org/10.1002/2013WR014226>.

- Léger, E., Saintenoy, A., Coquet, Y., Tucholka, P., Zeyen, H., 2020. Evaluating hydrodynamic parameters accounting for water retention hysteresis in a large sand column using surface GPR. *Journal of Applied Geophysics* 182, 104176. <https://doi.org/10.1016/j.jappgeo.2020.104176>.
- Leuther, F., Schlüter, S., 2021. Impact of freeze–thaw cycles on soil structure and soil hydraulic properties. *SOIL* 7(1), 179–191. <https://doi.org/10.5194/soil-7-179-2021>.
- Li, H., Liao, X., Zhu, H., Wei, X., Shao, M., 2019. Soil physical and hydraulic properties under different land uses in the black soil region of Northeast China. *Canadian Journal of Soil Science* 99(4), 406–419. <https://doi.org/10.1139/cjss-2019-0039>.
- Liu, X., Chen, J., Cui, X., Liu, Q., Cao, X., Chen, X., 2019. Measurement of soil water content using ground-penetrating radar: A review of current methods. *International Journal of Digital Earth* 12(1), 95–118. <https://doi.org/10.1080/17538947.2017.1412520>.
- Liu, X., Dong, X., Leskovar, D.I., 2016. Ground penetrating radar for underground sensing in agriculture: A review. *International Agrophysics* 30(4), 533–543. <https://doi.org/10.1515/intag-2016-0010>.
- Lombardi, F., Ortuani, B., Facchi, A., Lualdi, M., 2022. Assessing the perspectives of ground penetrating radar for precision farming. *Remote Sensing* 14(23), 6066. <https://doi.org/10.3390/rs14236066>.
- Looms, M.C., Binley, A., Jensen, K.H., Nielsen, L., Hansen, T.M., 2008a. Identifying unsaturated hydraulic parameters using an integrated data fusion approach on cross-borehole geophysical data. *Vadose Zone Journal* 7(1), 238–248. <https://doi.org/10.2136/vzj2007.0087>.

- Looms, M.C., Jensen, K.H., Binley, A., Nielsen, L., 2008b. Monitoring unsaturated flow and transport using cross-borehole geophysical methods. *Vadose Zone Journal* 7(1), 227–237. <https://doi.org/10.2136/vzj2006.0129>.
- Lu, J., Zhang, Q., Werner, A.D., Li, Y., Jiang, S., Tan, Z., 2020. Root-induced changes of soil hydraulic properties—A review. *Journal of Hydrology* 589, 125203. <https://doi.org/10.1016/j.jhydrol.2020.125203>.
- Lunt, I.A., Hubbard, S.S., Rubin, Y., 2005. Soil moisture content estimation using ground-penetrating radar reflection data. *Journal of Hydrology* 307(1), 254–269. <https://doi.org/10.1016/j.jhydrol.2004.10.014>.
- Mahmoudzadeh Ardekani, M.R., 2013. Off- and on-ground GPR techniques for field-scale soil moisture mapping. *Geoderma* 200–201, 55–66. <https://doi.org/10.1016/j.geoderma.2013.02.010>.
- Mangel, A.R., Linneman, D., Sprinkle, P., Jaysaval, P., Thomle, J., Strickland, C., 2022. Multifrequency electromagnetic geophysical tools for evaluating the hydrologic conditions and performance of evapotranspiration barriers. *Journal of Environmental Management* 303, 114123. <https://doi.org/10.1016/j.jenvman.2021.114123>.
- Mangel, A.R., Moysey, S.M.J., Ryan, J.C., Tarbuton, J.A., 2012. Multi-offset ground-penetrating radar imaging of a lab-scale infiltration test. *Hydrology and Earth System Sciences* 16(11), 4009–4022. <https://doi.org/10.5194/hess-16-4009-2012>.
- Moysey, S.M., 2010. Hydrologic trajectories in transient ground-penetrating-radar reflection data. *Geophysics* 75(4), WA211–WA219. <https://doi.org/10.1190/1.3463416>.
- Pathirana, S., Lambot, S., Krishnapillai, M., Cheema, M., Smeaton, C., Galagedara, L., 2023. Ground-penetrating radar and electromagnetic induction: Challenges and

opportunities in agriculture. *Remote Sensing* 15(11).
<https://doi.org/10.3390/rs15112932>.

Picciafuoco, T., Morbidelli, R., Flammini, A., Saltalippi, C., Corradini, C., Strauss, P., Blöschl, G., 2019. A pedotransfer function for field-scale saturated hydraulic conductivity of a small watershed. *Vadose Zone Journal* 18(1), 1–15.
<https://doi.org/10.2136/vzj2019.02.0018>.

Rossi, M., Manoli, G., Pasetto, D., Deiana, R., Ferraris, S., Strobbia, C., Putti, M., Cassiani, G., 2015. Coupled inverse modeling of a controlled irrigation experiment using multiple hydro-geophysical data. *Advances in Water Resources* 82, 150–165.
<https://doi.org/10.1016/j.advwatres.2015.03.008>.

Rucker, D.F., Ferré, T.P.A., 2004. Parameter estimation for soil hydraulic properties using zero-offset borehole radar: Analytical method. *Soil Science Society of America Journal* 68(5), 1560–1567. <https://doi.org/10.2136/sssaj2004.1560>.

Saintenoy, A., Schneider, S., Tcholka, P., 2008. Evaluating ground penetrating radar use for water infiltration monitoring. *Vadose Zone Journal* 7(1), 208–214.
<https://doi.org/10.2136/vzj2007.0132>.

Salako, A.O., Adepelumi, A.A., 2016. Evaluation of hydraulic conductivity of subsoil using electrical resistivity and ground penetrating radar data: Example from Southwestern Nigeria. *International Journal of Geo-Engineering* 7(1), 1–26.
<https://doi.org/10.1186/s40703-016-0018-7>.

Scholer, M., Irving, J., Binley, A., Holliger, K., 2011. Estimating vadose zone hydraulic properties using ground penetrating radar: The impact of prior information. *Water Resources Research* 47(10). <https://doi.org/10.1029/2011WR010409>.

- Scholer, M., Irving, J., Looms, M.C., Nielsen, L., Holliger, K., 2012. Bayesian Markov-Chain-Monte-Carlo inversion of time-lapse crosshole GPR data to characterize the vadose zone at the Arrenaes Site, Denmark. *Vadose Zone Journal* 11(4), vzj2011.0153. <https://doi.org/10.2136/vzj2011.0153>.
- Serbin, G., Or, D., 2003. Near-surface soil water content measurements using horn antenna radar. *Vadose Zone Journal* 2(4), 500. <https://doi.org/10.2136/vzj2003.0500>.
- Serbin, G., Or, D., 2004. Ground-penetrating radar measurement of soil water content dynamics using a suspended horn antenna. *IEEE Transactions on Geoscience and Remote Sensing* 42(8), 1695–1705. <https://doi.org/10.1109/TGRS.2004.831693>.
- Slater, L., Comas, X., 2009. The contribution of ground penetrating radar to water resource research. In: *Ground penetrating radar: Theory and applications*, Elsevier, Amsterdam, pp. 203-246. <https://doi.org/10.1016/B978-0-444-53348-7.00007-7>.
- Steelman, C.M., Endres, A.L., Jones, J.P., 2012. High-resolution ground-penetrating radar monitoring of soil moisture dynamics: Field results, interpretation, and comparison with unsaturated flow model. *Water Resources Research* 48(9). <https://doi.org/10.1029/2011WR011414>.
- Sünnemann, M., Beugnon, R., Breikreuz, C., Buscot, F., Cesarz, S., Jones, A., Lehmann, A., Lochner, A., Orgiazzi, A., Reitz, T., Rillig, M.C., Schädler, M., Smith, L.C., Zeuner, A., Guerra, C.A., Eisenhauer, N., 2023. Climate change and cropland management compromise soil integrity and multifunctionality. *Communications Earth & Environment* 4(1), 394. <https://doi.org/10.1038/s43247-023-01047-2>.

- Tronicke, J., Hamann, G., 2014. Vertical radar profiling: Combined analysis of travel times, amplitudes, and reflections. *Geophysics* 79(4), H23–H35. <https://doi.org/10.1190/geo2013-0428.1>.
- Weihnacht, B., Boerner, F., 2014. Measurement of retention functions with hysteresis using ground-penetrating radar. *Near Surface Geophysics* 12(4), 539–548. <https://doi.org/10.3997/1873-0604.2014001>.
- Yang, X., Klotzsche, A., Meles, G., Vereecken, H., van der Kruk, J., 2013. Improvements in crosshole GPR full-waveform inversion and application on data measured at the Boise Hydrogeophysics Research Site. *Journal of Applied Geophysics* 99, 114–124. <https://doi.org/10.1016/j.jappgeo.2013.08.007>.
- Yu, Y., Huisman, J.A., Klotzsche, A., Vereecken, H., Weihermüller, L., 2022. Coupled full-waveform inversion of horizontal borehole ground penetrating radar data to estimate soil hydraulic parameters: A synthetic study. *Journal of Hydrology* 610, 127817. <https://doi.org/10.1016/j.jhydrol.2022.127817>.
- Yu, Y., Klotzsche, A., Weihermüller, L., Huisman, J.A., Vanderborght, J., Vereecken, H., van der Kruk, J., 2020. Measuring vertical soil water content profiles by combining horizontal borehole and dispersive surface ground penetrating radar data. *Near Surface Geophysics* 18(3), 275–294.
- Yu, Y., Weihermüller, L., Klotzsche, A., Lärm, L., Vereecken, H., Huisman, J.A., 2021. Sequential and coupled inversion of horizontal borehole ground penetrating radar data to estimate soil hydraulic properties at the field scale. *Journal of Hydrology* 596, 126010. <https://doi.org/10.1016/j.jhydrol.2021>.

Co-authorship Statement for Study One

A manuscript based on Chapter 3, entitled “*Estimating Soil Hydraulic Conductivity from Time-lapsed Ground-penetrating Radar Data in Podzolic Soils using the Green-Ampt Model*,” has been submitted to the Journal of Hydrology and is currently under review (Dahunsi, J., Pathirana, S., Cheema, M., Krishnapillai, M., & Galagedara, L. 2024) (Journal of Hydrology, revision requested).⁴

An abstract based on the findings of Chapter 3, entitled “*Application of Ground-penetrating Radar Travel-Time to Beerkan Infiltration Procedure for Soil Hydraulic Characterization*,” has been submitted and presented at the Canadian Society for Bioengineering / La Societe Canadienne de Genie Agroalimentaire et de Bioenginierie (CSBE/SCGAB) Annual General Meeting (AGM) and Technical Conference 2024.⁵

Juwonlo Dahunsi, the thesis author, was the primary author and was responsible for proposal development, methodology, data collection, processing, analysis, modeling, and writing of the original manuscript. Sashini Pathirana, PhD student, supported the data collection, data processing

⁴ Dahunsi, J., Pathirana, S., Cheema, M., Krishnapillai, M., Galagedara, L., 2024. Estimating soil hydraulic conductivity from time-lapse ground-penetrating radar data in Podzolic soils using the Green-Ampt model. Journal of Hydrology–HYDROL62404 (revision requested).

⁵ Dahunsi, J., Pathirana, S., Cheema, M., Krishnapillai, M., Galagedara, L., 2024. Application of ground-penetrating radar travel-time to Beerkan infiltration procedure for soil hydraulic characterization. CSBE/SCGAB AGM and Technical Conference 2024 on “Engineering Responses to Wicked Problems” July 7 - 10, Winnipeg, Manitoba, Canada.

<https://doi.org/10.13140/RG.2.2.19459.72487>

review, and editing of the manuscript. Mumtaz Cheema and Mano Krishnapillai are co-supervisors and committee members, respectively, and provided input on the research proposal and methodology and assisted with the review and editing of the manuscripts. Lakshman Galagedara, the supervisor, was responsible for the project conceptualization, funding acquisition, project administration, resource allocation, supervision, supported the development of methodology and investigation, and contributed to the review and editing of the manuscript.

CHAPTER THREE

Estimating Soil Hydraulic Conductivity from Time-lapsed Ground-penetrating Radar Data in Podzolic Soils using the Green-Ampt Model

Juwonlo Dahunsi^a, Sashini Pathirana^a, Mumtaz Cheema^a, Manokararajah Krishnapillai^a,
Lakshman Galagedara^{a,*}

^a School of Science and the Environment, Memorial University of Newfoundland, Corner Brook,
NL A2H 5G4, Canada

*Corresponding author

E-mail addresses: jedahunsi@mun.ca (J. Dahunsi), epsathirana@mun.ca (S. Pathirana),
macheema@mun.ca (M. Cheema), n62mk@mun.ca (M. Krishnapillai), lgalagedara@mun.ca (L.
Galagedara)

Abstract

Efficient soil water management and prediction of contaminant transport requires a deep understanding of spatial and temporal variation in soil hydraulic parameters (SHPs). The growing interest in using ground-penetrating radar (GPR) for large-scale and non-destructive estimation of SHPs demands more effective approaches. This study evaluates the potential for monitoring soil water content (SWC) variation using GPR time-laps data and predicting field-saturated hydraulic conductivity (K_{fs}) by employing the Green-Ampt (GA) model. At two locations in a podzolic soil site in western Newfoundland, Canada, a surface GPR system with a center frequency of 500 MHz was used to monitor infiltration experiments employing equal volumes of water and with a limited

duration (Beerkan method). The downward movement of the wetting zone during infiltration was monitored by collecting time-lapsed GPR traces every 5 s. Variations in SWC estimated from GPR (GPR-SWC) and soil moisture probes (SMP-SWC) (installed to a depth of 0.20 m) were used as parameters in the GA model to estimate K_{fs} . Findings from this study show that GPR provided consistent information on the dielectric constant during the infiltration experiment at both locations ($r = 0.902$). The average K_{fs} value ($1.35 \times 10^{-5} \pm 5.45 \times 10^{-6}$ m/s) estimated using the GPR-SWC in the GA model was in a similar magnitude to the theoretical value for the tested soil type and in close range to BEST estimates and Guelph permeameter measured values, although all approaches were significantly different. Further research is needed to validate this approach across various soil types and conditions.

Keywords: Soil water content, Beerkan infiltration, Direct ground wave, Soil hydraulic properties, Dielectric constant.

3.1. Introduction

The accurate prediction of soil hydraulic parameters (SHPs) is crucial for modeling hydrological processes and is needed for various agricultural and environmental applications (Fernández-Gálvez et al., 2019; Rahmati et al., 2019; Castellini et al., 2021). Several methods have been developed to estimate SHPs (saturated and unsaturated hydraulic conductivities (K_s and $K[\theta]$), water retention characteristics, and infiltration capacity) in field experiments, laboratory experiments, and pedo-transfer functions (PTFs). Although field experiments are likely to produce more realistic results, they tend to be time-consuming, labor-intensive, invasive, and costly (Rezaei et al., 2016; Albalasmeh et al., 2022). Laboratory and PTF methods, despite sharing some of these shortcomings, often fail to reflect the field conditions accurately (Gribb et al., 2009). Collectively,

most of these methods lack the capacity to provide the spatiotemporal variation needed for continuous monitoring of SHPs, a need that is becoming increasingly critical due to global climate and land use changes. (Hartmann et al., 2020; Fu et al., 2021).

There has been a growing interest in applying geophysical methods to estimate the soil hydrological and hydraulic properties over the past two decades to address these limitations (Cao et al., 2020). Geophysical techniques are advantageous since they are non-invasive, cost-effective, and capable of repeatedly capturing spatiotemporal variability of soil properties and state variables on a large scale (Liu et al., 2019; Pathirana et al., 2023). Specifically, ground-penetrating radar (GPR) has been applied in hydrological studies due to its high sensitivity to water, reflected in its dielectric constant (K_r) measurement. GPR uses high-frequency electromagnetic waves (ranging from 10 to 3600 MHz) to image the subsurface (Zhang et al., 2022; Pathirana et al., 2023). It has been extensively applied to estimate soil water content (SWC), often yielding results comparable to those obtained from established methods such as the gravimetric method and Time Domain Reflectometry (TDR) (Huisman et al., 2002; Wijewardana and Galagedara, 2010; Pathirana et al., 2024).

Although GPR measurement is not directly related to SHPs, its sensitivity to fluid distribution has made it a potential technique for estimating SHPs (Kowalsky et al., 2005). With established relationships such as empirical models (Topp et al., 1980) and volumetric mixing formula (Birchak et al., 1974) used to convert GPR attributes to SWC, the quantification of soil water dynamics using GPR has become relevant. Consequently, significant progress has been made in the last two decades in applying GPR for the estimation of SHPs using different techniques (Lambot et al., 2006; Jadoon et al., 2012; Scholer et al., 2012; Busch et al., 2013; Rossi et al., 2015; Léger et al., 2016; Yu et al., 2021, 2022; Zou et al., 2023). Several of these studies utilized travel-time data

collected during irrigation and infiltration experiments, while others have employed more advanced techniques, such as Full-Waveform Inversion (FWI).

Significantly, most of these studies monitored infiltration procedures over longer periods. For example, Scholer et al. (2012) estimated SHPs at the field scale by inverting GPR data collected during a forced infiltration experiment that spanned 20 days and used approximately 95,000 L of water. Zou et al. (2023) characterized subsurface water flow dynamics by using a combination of time-lapse Electrical Resistivity Tomography (ERT) and GPR with soil moisture probe (SMP) measurements in a laboratory-scale water infiltration experiment that lasted about 84 h. Similarly, Yu et al. (2022) employed a 6 h infiltration event to estimate SHPs through coupled full-waveform inversion of horizontal borehole GPR data.

The development of simple infiltration methods, such as the Beerkan Estimation of Soil Transfer (BEST) parameter method, provides a more economical and rapid way to perform infiltration in the field and laboratory conditions (Lassabatère et al., 2006). This procedure allows for simple measurement of SHPs using cumulative infiltration data collected through a single ring (e.g., a can) and additional information such as particle size distribution (PSD), soil bulk density, and initial water content (Angulo-Jaramillo et al., 2019; Fernández-Gálvez et al., 2019). The method has since gained popularity due to the robustness of its theory and the minimal water and time needed.

Theoretical models have also been used to estimate SHPs. The Green-Ampt (GA) model, a widely used approach to describe the infiltration process, conceptualizes water movement from a ponded surface into the soil (Green and Ampt, 1911; Baiamonte, 2019). It is a physical infiltration model that applies the principle of mass conservation and Darcy's law to describe one-dimensional vertical flow through a uniform soil column (Mohammadzadeh-Habili and Heidarpour, 2015). This

model assumes continuous ponding in soils with uniform antecedent moisture content will lead to a sharp wetting front between the upper saturated zone and the lower unsaturated zone (wetting front) as the infiltrated water moves down the profile (Lee et al., 2020). The GA model is known for its simple structure and requires fewer parameters compared to other infiltration models (Li et al., 2022). While the GA model is appreciated for its simplicity and ease of application, its accuracy in predicting SHPs highly depends on site-specific conditions. The GA model has been particularly effective for coarse-textured soils exhibiting sharply defined wetting fronts (Baiamonte, 2019), such as boreal podzolic soils, typically sandy and/or stony.

One of the benefits of the GA model is its physical basis, allowing its parameters to be independently estimated from SHPs (Mohammadzadeh-Habili and Khalili, 2021). As a result, several methods have been proposed over the years to estimate the hydraulic conductivity, wetting front suction, and water content of the wetting zone, theoretically and through laboratory and field experiments (Vigo et al., 2021). Specifically, using soil porosity as an estimate of water content behind the wetting front (*i.e.*, saturated water content) during ponded infiltration can often lead to overestimation (Ma et al., 2010; Mohammadzadeh-Habili and Khalili, 2021). Consequently, several direct and indirect methods have been developed to estimate water content changes at the wetting zone accurately. For instance, Mohammadzadeh-Habili and Heidarpour (2015) conducted a laboratory experiment using constant head infiltration tests to monitor the wetting profile's advancement in a two-layered soil. The authors observed that the wetness increment behind the wetting front is less than saturation due to air entrapment in the wetting zone. Similarly, Meng and Yang (2019) introduced a wet zone partition function (comprising a saturation zone and a transient unsaturated zone) to more accurately depict the water content in the wetting zone, and they found that their approach provided a more accurate representation of the infiltration process.

Although these studies have provided valuable insights into the need for accurate estimates of the moisture content in the wetting zone for the GA model, only a few studies have investigated integrating geophysical methods like GPR-estimated water content changes for the GA model. This is understandable, given the existing limitations in the capacity of GPR to provide accurate estimates of SWC variation (Ma et al., 2017) and the difficulty in accurately detecting the advancement of the wetting front depth using GPR (Zou et al., 2023).

The present study explores the potential of GPR-DGW in estimating SWC variation and predicting field-saturated hydraulic conductivity (K_{fs}) by integrating the estimated SWC variation into the GA model. The specific objectives of this study were to: 1) explore the potential of GPR to capture soil water content variation during a limited duration infiltration experiment and 2) estimate K_{fs} using the SWC variation estimated from GPR time-lapse data in the GA model and assess the accuracy of the estimates. Overall, this study integrates the potential of using a geophysical approach (GPR) with the potential for large-scale characterization of K_{fs} and a limited-duration infiltration procedure (Beerkan Infiltration) to estimate SHPs in boreal podzolic soil.

3.2. Methodology

3.2.1. Study area

The study was carried out at the Western Agriculture Center and Research Station, Pasadena (49°04'20"N, 57°33'35"W), Newfoundland, Canada. This area is characterized by a humid continental climate, with an average annual precipitation of 1113 mm and an annual mean temperature of 4°C (<https://climate.weather.gc.ca/>). The selected area is an uncultivated (fallow) grassland with no farming activities during the last eight years. The groundwater table depth in the

area is more than 1 m with a 2-5% slope (Badewa et al., 2018; Illawathure et al., 2020). Specific locations for the experiment were flattened to minimize the runoff effect during infiltration experiments. The soil texture of the top 0.15 m depth was loamy sand (sand = 83.0 % (± 1.25); silt = 14.6 % (± 1.21); clay = 2.4 % (± 0.04); n = 9), with the average bulk density of 1.31 (± 0.01 ; n = 9) g/cm³. Based on the Canadian soil classification, the soils in this area are dominated by the orthic humic podzol (Soil Classification Working Group, 1998).

3.2.2. Field data collection

3.2.2.1. Site preparation and moisture probe installation

Two random locations on the site were selected for the infiltration experiment (Locations 1 and 2). The selected locations were carefully cleaned (removed surface debris) and leveled with minimum disturbances to ensure a uniform surface. One of the locations (Location 1) had SMPs (SM100, Spectrum Technologies, Aurora, IL, USA) installed horizontally at 5 cm, 10 cm, 15 cm, and 20 cm depth to monitor the movement of water and variation in SWC along the profile during the experiment. After installing these probes, the soil was backfilled and allowed to settle under natural conditions for a few weeks before starting the infiltration experiment. The probes were programmed to collect and store time-lapse SWC data every minute using a WatchDog 1400 micro station data logger (Spectrum Technologies, Aurora, IL, USA). The SMPs were calibrated using the laboratory-measured SWC employing the gravimetric method, and the relationship is provided in Fig 3.10 (Appendix 2). The second location (Location 2) was without any installation.

3.2.2.2. Beerkan Infiltration experiments

Infiltration experiments were carried out at the two locations using the Beerkan method (Lassabatère et al., 2006). The infiltration experiments were conducted on three different days as

replicates to consider possible variability and improve the accuracy of the results. For each experiment, a small inner diameter (i.e., 10 cm) metal ring was inserted to a depth of 1 cm into the soil to avoid lateral loss of ponded water (Angulo-Jaramillo et al., 2019). Ring insertion was done gently using a rubber hammer and ensuring the upper end of the ring was leveled using a leveler.

A known equal volume of water (200 mL in this experiment) was poured into the ring at the start of the measurement, and the elapsed time for complete infiltration was recorded. A small transparent plastic piece was placed inside the ring to minimize soil disturbance, and water was added to the top. Once the initial volume had infiltrated, the known volume of water was immediately added, and the cumulative infiltration time was recorded. The procedure was repeated until steady-state infiltration was achieved, defined as having zero or minimal difference in infiltration time across three consecutive readings (Lassabatère et al., 2006; Alagna et al., 2019). These experiments required about 10-20 readings to achieve the steady-state condition.

3.2.2.3. GPR data collection

Each infiltration experiment was monitored with a 500 MHz center frequency GPR transducer (PulseEKKOPro Sensors and Software Inc., Mississauga, Canada). The transmitter and receiver transducers were placed on either side of the Beerkan infiltration ring (Figure 3.1). Time-lapse GPR traces were collected at 5 s intervals and 32 staking during the entire infiltration experiment using the fixed offset (0.43 m offset) method survey mode and a time window of 50 ns. Common midpoint measurements were carried out before and after the infiltration experiment to calibrate the time-zero (t_0) and find the average direct ground wave velocity.

3.2.2.4. Other data collections

The Guelph permeameter (GP) is a widely accepted and reliable method for measuring field-saturated hydraulic conductivity (K_{fs}). For this study, GP measurements were carried out on the site using the 1003-100 GP, following the manufacturer's manual (Soilmoisture Equipment Corp., Santa Barbara, California). The GP was inserted in a 6 cm diameter by 15 cm deep hole prepared using a soil auger, sizing auger, and prep brush. The permeameter maintained a constant depth of water in the hole, initially set at 5 cm and subsequently at 10 cm, using a constant pressure head inside the tube. The rate of water level in the reservoir was monitored until a steady-state rate was attained (i.e., no significant changes in flow rate over three consecutive time intervals). The K_{fs} was calculated using the steady-state flow rate and the equations provided in Reynolds and Elrick (1986).

The bulk density and particle size distribution obtained from the field were used to calculate K_{fs} estimates according to BEST-Intercept (Yilmaz et al., 2010) and BEST-Steady (Bagarello et al., 2014) procedures. The BEST procedure for soil hydraulic characterization is based on the van Genuchten (1980) relationship for the water retention curve, in conjunction with the Burdine (1953) condition, and the Brooks and Corey (1964) relationship for hydraulic conductivity, $K(\theta)$. Details of the theory behind both algorithms and the reason for their selection are provided in Appendix 1. The average measured K_{fs} obtained from GP, BEST-Intercept, and BEST-Steady were used to evaluate the accuracy of estimates from this approach.



Figure. 3.1. Experimental set-up for the Beeken infiltration experiment and data collection using 500 MHz ground-penetrating radar (GPR) transducers. a) side view and b) top-down view.

3.2.3. GPR data processing

GPR data collected during the infiltration experiment were t_0 corrected and processed by applying filters and gain functions. After this initial processing, the direct ground wave (DGW) travel times were picked using Picker V2 software (Sensors and Software Inc., Mississauga, Canada).

The DGW velocity (V_{DGW}) was calculated using the measured DGW travel time and the transducer offset. The dielectric constant (K_r) was calculated using Equation (3.1).

$$K_r = \left(\frac{c}{V_{DGW}} \right)^2 \quad \text{Equation 3.1}$$

where c is the speed of electromagnetic waves in the free space (0.3 m/ns). The K_r obtained was converted to SWC (v/v) using the Topp et al. (1980) Equation (3.2).

$$SWC = -5.3 \times 10^{-2} + 2.92 \times 10^{-2}K_r - 5.5 \times 10^{-4}K_r^2 + 4.3 \times 10^{-6}K_r^3 \quad \text{Equation 3.2}$$

SWC data were also collected using FieldScout TDR 350 (Spectrum Technologies, Aurora, IL, USA) before each infiltration experiment to identify GPR-DGW precisely.

3.2.4. Estimating wetting front depth

Several methods that have been used to determine the sampling depth of the DGW in GPR studies include theoretical modeling, which is based on factors such as antenna frequency, soil dielectric properties, and antenna separation (van Overmeeren et al., 1997); wave-length-based numerical modeling (forward modeling), which relates GPR wavelength to the depth of soil influence (Du, 1996; Sperl, 1999; Galagedara et al., 2005b); and empirical field measurements that compare soil moisture monitored at different depths with GPR-derived dielectric constant (Steelman and Endres, 2011).

The empirical field measurement approach was considered more suitable for this study for several reasons. First, unlike theoretical and numerical approaches, which often assume a uniform soil profile, the empirical field measurement approach can accommodate variability in soil properties and water movement. Hence, this approach is assumed to provide more realistic estimates of the cumulative sampling depth under field conditions where heterogeneity is common. Second, this approach reflects the dynamic nature of the infiltration experiment and links the GPR's response with the observed changes in SWC during the wetting process. Finally, the empirical field measurement approach allows for direct validation of GPR-SWC measurements by comparing them with ground-truth data from SMPs.

While Steelman and Endres (2011) found cumulative sampling depth for sandy soil using a similar antenna frequency (450 MHz) to be approximately 20 cm, this finding was based on measurements obtained at relatively coarse intervals (i.e., 0 - 10 cm, 10 - 20 cm, 20 - 30 cm, 30 - 40 cm, 40 - 50

cm). The coarse intervals could limit the precision of the cumulative sampling depth estimation by failing to capture finer-scale variations. Hence, this study, although focused on the 20 cm range, utilizes finer depth resolution with SMPs installed at 0 - 5cm, 5 - 10 cm, 10 - 15 cm, and 15 - 20 cm.

An additional advantage of this approach is the concurrent use of SMPs to monitor the advancement of the wetting front down the profile during the infiltration. The wetting front represents the transition zone between saturated and unsaturated soil as water infiltrates and its depth provides crucial information about water movement in the soil profile (Hillel, 2003). Previous studies have shown the effectiveness of SMPs in determining the arrival of the wetting front (Fattahi Nafchi et al., 2023; Zou et al., 2023). Consequently, this study adopts the cumulative sampling depth derived from GPR measurements as a practical proxy for the wetting front depth, since it will be practically impossible for GPR to effectively capture SWC variation beyond the cumulative sampling depth.

3.2.5. Estimation of saturated hydraulic conductivity using the Green-Ampt model

According to the GA model, the one-dimensional vertical cumulative infiltration (as a function of time) can be obtained using Equation (3.3), the infiltration rate using Equation (3.3), and the wetting front depth using Equation (3.5).

$$F(t) = K_s t + \psi \Delta \theta \ln \left(1 + \frac{F(t)}{\psi \Delta \theta} \right) \quad \text{Equation 3.3}$$

$$f(t) = K_s \left(\frac{\psi \Delta \theta}{F(t)} + 1 \right) \quad \text{Equation 3.4}$$

$$L = \frac{F(t)}{\Delta \theta} \quad \text{Equation 3.5}$$

Where;

$F(t)$ = Cumulative infiltration, cm

K_s = Saturated hydraulic conductivity, cm/s

t = Time (s)

ψ = Suction head at the “sharp” wetting front, cm

$\Delta\theta$ = Increase in moisture content as the wetting front passes (cm^3/cm^3)

$f(t)$ = Infiltration rate, cm/s

L = Wetted depth, cm

Full details and mathematical derivations of the equations are provided in Chow et al. (1988) and Green and Ampt (1911).

For this study, SWC variation from SMPs (SMP-SWC) and those estimated using GPR- K_r (GPR-SWC) were used as a parameter in the GA model. The average GPR-DGW sampling depth (Steelman and Endres, 2011) was considered the wetting front depth. $F(t)$ was estimated using Equation (3.5), while the K_{fs} were estimated using Equation (3.3) by inserting the GPR-SWC and SMP-SWC and the steady-state time. The mean value for the suction head of loamy sand textured soil, 6.13 cm, according to Rawls et al. (1983), were used for all the calculations.

3.2.6. Statistical analysis

At Location 1, regression analysis was conducted between the average GPR- K_r and average SMP-SWC (v/v) at different depths. We adopted Steelman and Endres (2011) approach to inferring the average DGW sampling depth by using the cumulative sampling depth with the highest coefficient of determination (R^2 value). Bar charts were used to describe and compare the K_{fs} values obtained using SWC changes estimated with GPR-DGW and SMPs. One-sampled t-tests were used to statistically assess the difference in the K_{fs} estimates from the theoretical value for the soil type at the study site (Saxton and Rawls, 2006).

At Location 2 (without SMPs), a similar approach was used to estimate K_{fs} from changes in GPR-SWC. The estimated K_{fs} with GPR time-lapse data from both locations were subsequently compared with K_{fs} of theoretical values, BEST estimates, and GP.

3.3. Results and Discussion

3.3.1. Monitoring of soil water content variation during infiltration

The downward movement of water monitored by the SMPs during the infiltration campaigns at Location 1 is shown in Figure 3.2. Notably, the probes sequentially responded to SWC (v/v) changes as infiltrated water migrated down the profile. Initial water contents were within the 0.15 to 0.18 cm³/cm³ range, while the steady-state water contents achieved at the end of infiltration were within the 0.25 – 0.28 cm³/cm³ range. Similar initial and steady-state SWCs were reported by Badewa et al. (2018) under natural moisture conditions and by Pathirana et al. (2024) under irrigated conditions on the same site. In general, soils with higher sand percentages and low organic matter (OM) content, like the podzolic soils of study site, tend to have lower steady-state SWC. Moreover, it is difficult to attain saturation on this site unless water is applied at very high rates due to the low retention capacity and relatively larger macropore content in sandy soil. Therefore, when the SWC is slightly above the field capacity in the studied site, soil water flow comes under the strong influence of the gravitational component of the water potential, draining quickly by internal drainage before saturation can be reached.

It can also be deduced from Figure 3.2 that a steady state was attained around 120 – 400 s during the infiltration campaigns. This is also expected, as sandy soils generally absorb water rapidly and reach steady-state fast due to large pore spaces and fairly uniform porosity. Also, as illustrated in

Figure 3.2, the SWC at the surface (top 5 cm) drops quickly after reaching a peak value (just above the field capacity). On the other hand, measured SWC at other depths seems to maintain comparatively uniform values after reaching the peak state. A possible explanation for the drop in SWC at the surface might be due to hydraulic redistribution after reaching the peak stage (i.e. water moving from wetter to drier areas).

The variation of GPR-SWC and SMP-SWC during the infiltration experiments is shown in Figure 3.3. Throughout the infiltration campaigns, the SWC estimated from SMPs was higher than the SWC estimated from GPR-DGW. This can be attributed to the difference in the sampling volume of both methods and the infiltrating area. Galagedara et al. (2003) noted that GPR measures the average SWC between the antennas and to a certain depth in between, depending on the wavelength, resulting in a large sampling volume. On the other hand, SMPs are on a point scale and consider a smaller sampling volume. Hence, it is easier for the SMPs to respond promptly during infiltration since the probes are just below the infiltrating front. Moreover, this study used GPR over a transducer offset of 43 cm (due to its size) with only a wetting coverage distance (diameter of the ring) of about 10 cm, leaving an unwetted distance of around 15 cm on each side. These two drier areas (approximately $2/3$ of the offset) result in drier-biased values for SWC estimated by GPR and might have contributed to the underestimation. The above reason can also partly explain why, for the most part, the curve of SWC variation estimated from GPR was smooth and showed gradual changes, while SWC variation monitored by the moisture probes exhibited sharp peaks (Figure 3.3).

In addition, Figure 3.4 presents a GPR profile illustrating the increase in the DGW's travel time with increasing water addition to the soil. This demonstrates the capability of GPR to effectively

capture the spatial-temporal dynamics of water content in the soil as the infiltration continues. Only a profile from one of the trials is presented here for brevity.

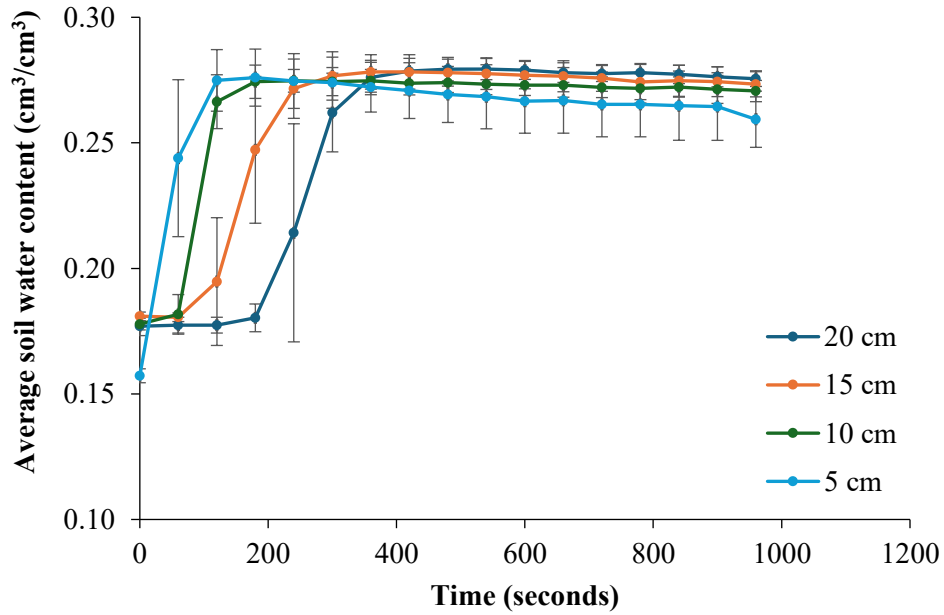


Figure 3.2. Variation in average soil water content (SWC, v/v) monitored by soil moisture probes (SMPs) at 5 cm, 10 cm, 15 cm, and 20 cm depths.

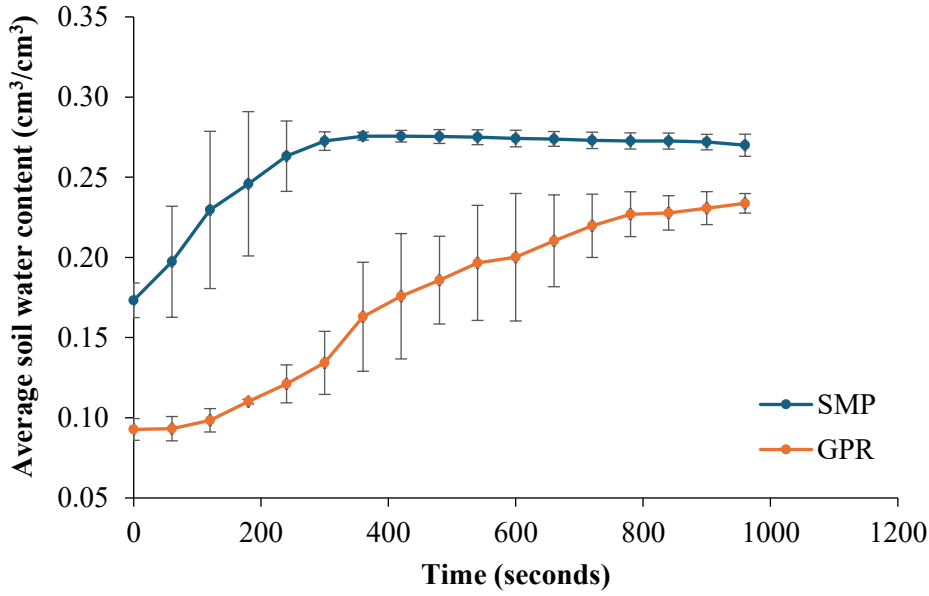


Figure 3.3. Comparison of average soil water content (SWC, v/v) variation estimated and monitored by ground-penetrating radar (GPR) and soil moisture probes (SMPs), respectively.

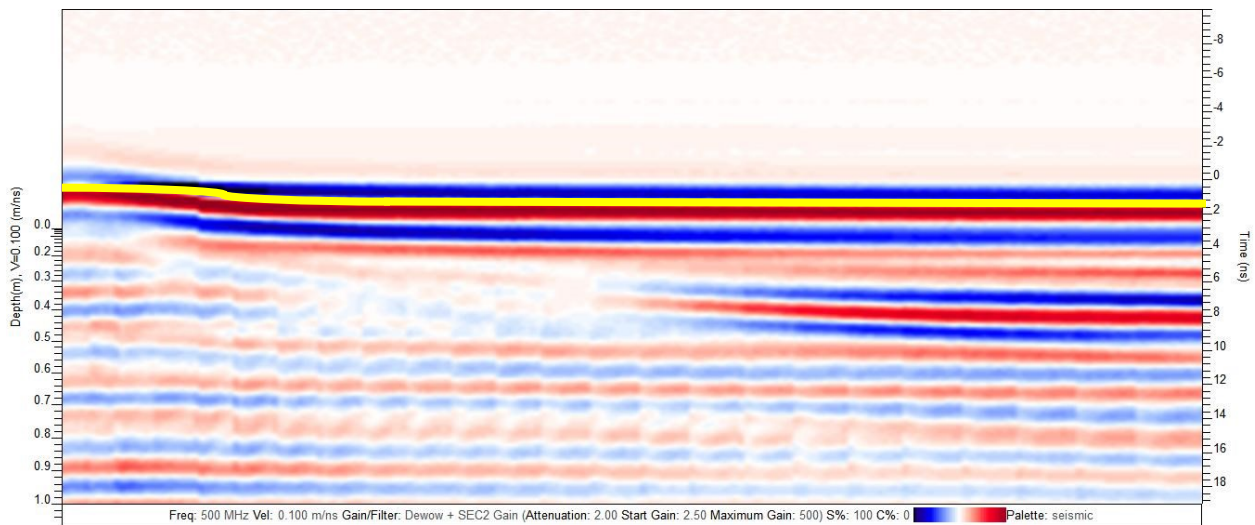


Figure 3.4. Ground-penetrating radar (GPR) radargrams obtained during one of the infiltration experiments at Location 1.

3.3.2. Estimating wetting front depth using the relationship between soil water content monitored by moisture probes and ground-penetrating radar

Adopting the empirical field measurement approach, site-specific third-order polynomial relationships were developed using the average K_r measurements and SWC measured by SMPs at different depths to obtain the average DGW cumulative sampling depth (Figure 3.5). The relationship between SWC and the K_r of soils has also been expressed using different third-order polynomial relationships (Topp et al., 1980; Nadler et al., 1991; Roth et al., 1992; Curtis, 2001).

As shown in Figure 3.5, the 15 cm depth equation provided the best relationship ($R^2 = 0.9622$), although the value was very close to the 20 cm depth ($R^2 = 0.9597$). Nonetheless, the 15 cm depth was selected as it showed slightly higher precision.

According to Liu et al. (2019), the propagation of the DGW is mainly influenced by three factors: frequency, soil type, and interferences from the soil reflection interface. The lower the frequency, the deeper the penetration depth. Steelman and Endres (2011) estimated sampling depths of 20 cm for both 450 and 900 MHz antennas at a sandy site. Additionally, Grote et al. (2010a) reported a sampling depth range of 12 - 30 cm for sandy soils, depending on frequency and soil moisture conditions.

This study used an antenna frequency of 500 MHz and found a similar sampling depth based on the comparison of K_r to SMP data at four depths. Based on these findings, the 15 cm cumulative sampling depth was selected and used as the wetting front depth for the GA modeling.

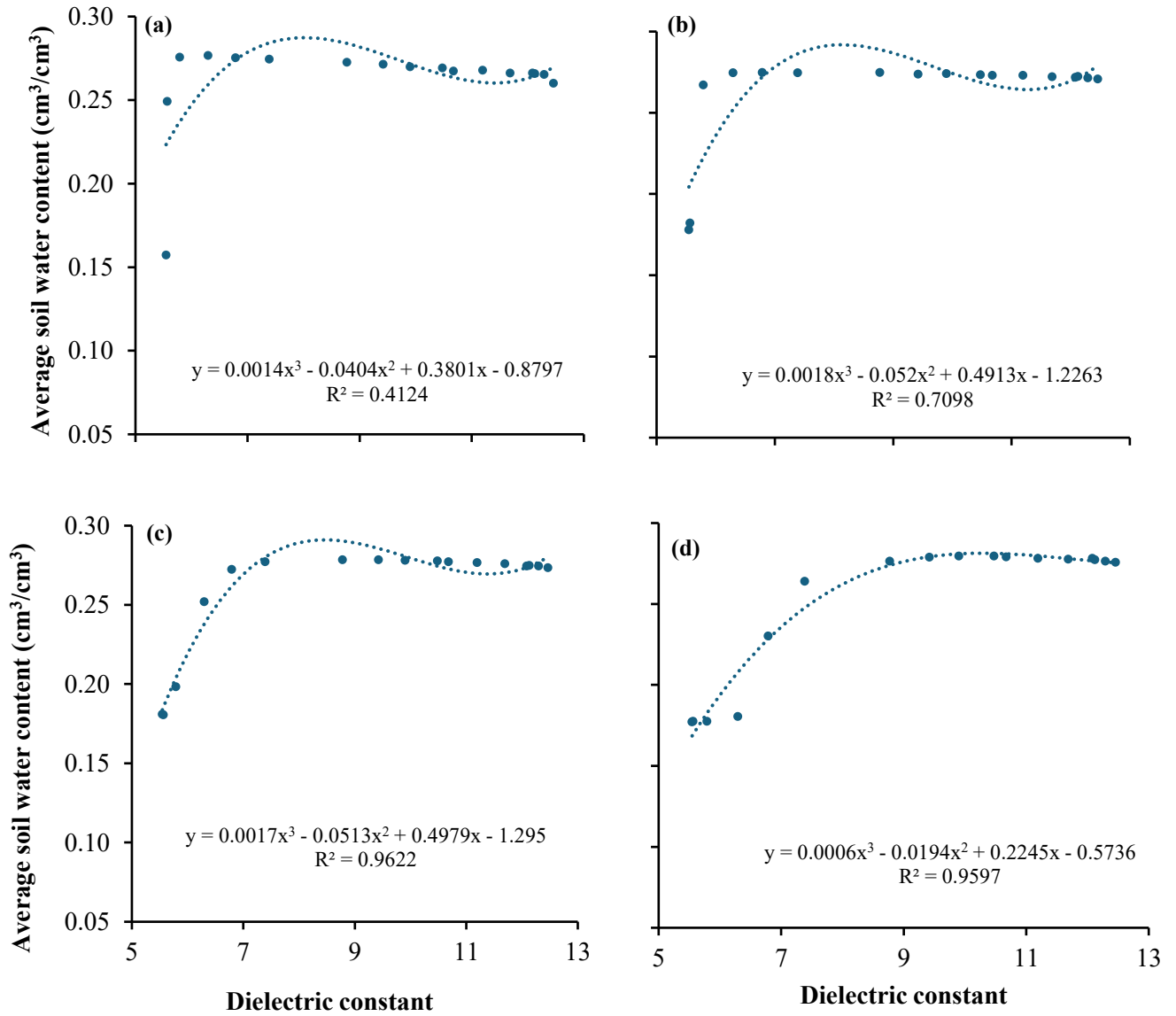


Figure 3.5. Site-specific calibrated relationships between soil moisture probes soil water content (SMPs-SWC, v/v) and average ground-penetrating radar dielectric constant (GPR- K_r) at different depths: a) 5 cm, b) 10 cm, c) 15 cm, and d) 20 cm.

3.3.3. Estimating field-saturated hydraulic conductivity using SWC variations and wetting front depth in the Green-Ampt model

Applying the GA model to SWC variation from GPR (GPR-SWC) and SMPs (SMP-SWC) and using the steady-state times and a wetting front depth of 15 cm as parameters yielded K_{fs} estimates within the expected range for the soil type at the study site (loamy sand). For instance, an average K_{fs} value of $1.45 \times 10^{-5} \text{ m/s} \pm 8.33 \times 10^{-6} \text{ m/s}$ was estimated using the GPR-SWC in the GA model. However, it appeared that the GA model underestimated these K_{fs} from GPR-SWC compared to those estimated from SMP-SWC ($2.10 \times 10^{-5} \pm 1.01 \times 10^{-6} \text{ m/s}$). Since the same wetting front depth and suction head were used in both estimations, the difference between K_{fs} estimates from both methods can be attributed to the differences in estimated SWC variation and steady-state times. A previous study has described the influence of the initial soil water content in the GA models as being negligible (Mohammadzadeh-Habili and Khalili, 2021). Thus, most differences could be associated with the steady-state SWC and the time to reach the steady-state condition. The underestimation of water changes by GPR can be attributed to the large sampling volume and extended dry areas (unwetted distance) within the transducer offset. The unwetted distance (*i.e.*, the 33 cm antenna separation not covered by the ring), considered in GPR-SWC changes estimation, is a major shortcoming of this study that could be improved in future research work.

Also, as noted in the previous section, the extended steady-state time is due to GPR's gradual changes in water content, as against the earlier peaks in SMP-measured SWC changes.

Further, this study considered the DGW, which can only account for a shallow sampling depth (up to 0.20 m). Since the considered soil is sandy and water drains faster, this posed challenges to the ability of GPR to acquire cumulative SWC estimation accurately, which is needed to obtain the

steady-state condition. In addition, Liu et al. (2019) noted that DGWs are rapidly attenuated and can be easily affected by a higher noise-to-signal ratio.

Nonetheless, when compared with the traditional GA model K_s parameter for the soil type at the study site (loamy sand) and estimated K_s value from Saxton and Rawls (2006) (2.69×10^{-5} m/s) (taken as theoretical value), both K_{fs} estimates from the GPR-SWC and SMPs-SWC estimates are in-between those values (Figure 3.6). The results of a two-sample t-test conducted to compare mean K_{fs} values estimated using the GPR-SWC and SMPs-SWC revealed no significant difference between estimates from both approaches ($p = 0.549$). Overall, this approach conferred K_{fs} values within the range estimated from other methods, highlighting its potential for estimating K_{fs} .

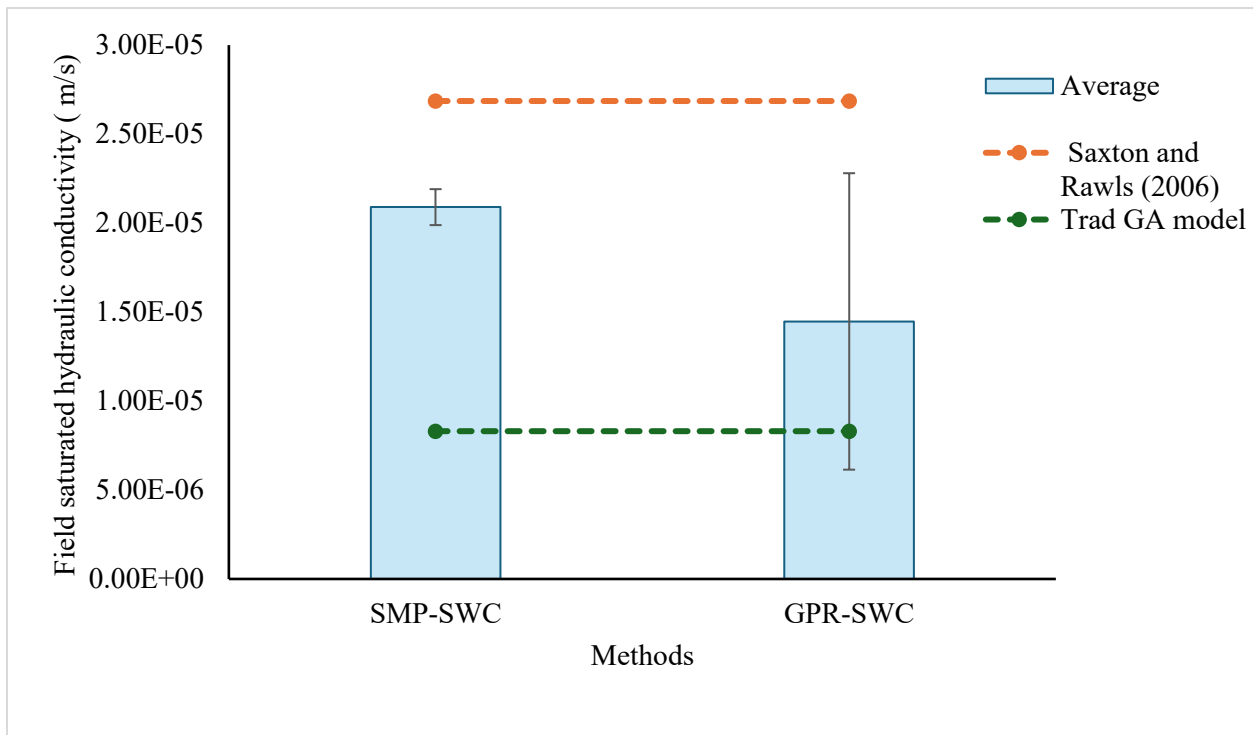


Figure 3.6. Comparison of field-saturated hydraulic conductivity (K_{fs}) estimates derived from using the Green-Ampt (GA) model for ground-penetrating radar soil water content (GPR-SWC, v/v), and soil moisture probes soil water content (SMPs-SWC, v/v), with Saxton and Rawls (2006) estimates and traditional GA parameters as benchmarks.

3.3.4. Soil water content variations at the two locations

A similar infiltration experiment at Location 2 (without SMPs) at the same site was used to evaluate the consistency of K_r changes with infiltration. First, a Pearson correlation between the average K_r from both locations gave a strong and positive relationship ($r = 0.902$; Figure 3.7). This showed a relative similarity in the K_r collected at both locations using equal-volume infiltration trials, suggesting the relevance of using GPR data for evaluating soil water dynamics. Further, the variation in SWC estimated from the K_r from both locations also showed similar consistency with time (Figure 3.8).

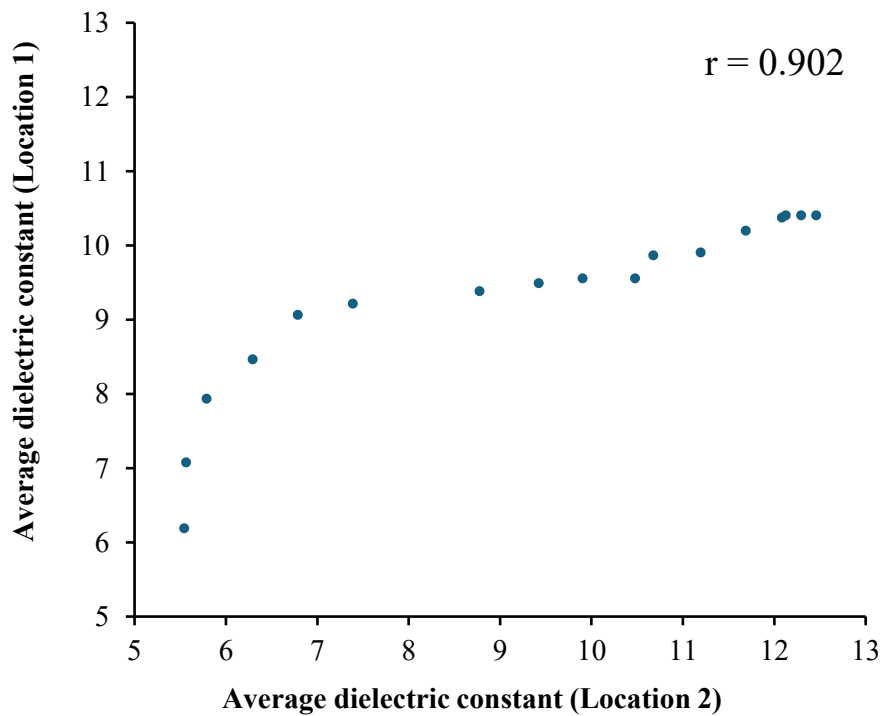


Figure 3.7. Correlation between average dielectric constant (K_r) obtained at Locations 1 and 2.

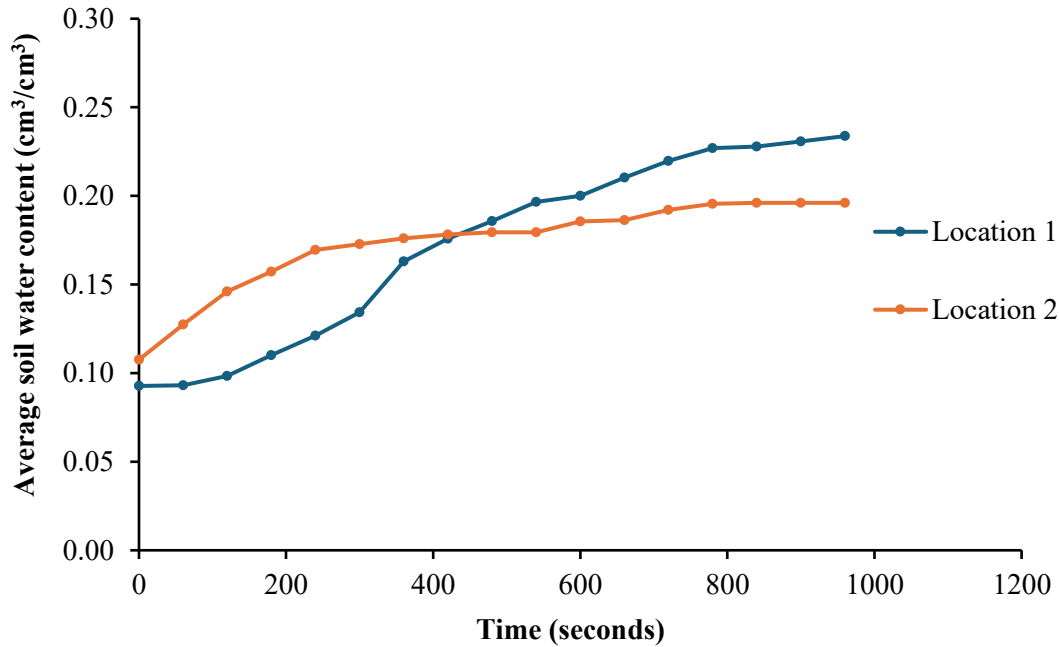


Figure 3.8. Comparison of average ground-penetrating radar soil water content (GPR-SWC, v/v) variations at Locations 1 and 2 with infiltration time.

3.3.5. Estimating field-saturated hydraulic conductivity using SWC variations from both locations

At Location 2, the average K_{fs} estimated using GPR-SWC variation as parameters in the GA model was $1.25 \times 10^{-5} \pm 1.36 \times 10^{-6}$ m/s. This is also closer to the expected range for the soil type at the study site and showed no significant difference from K_{fs} estimates from location 1 based on the two-sample t-test ($p = 0.721$). Considering both locations, the average K_{fs} estimated using the GPR-SWC was $1.35 \times 10^{-5} \pm 5.45 \times 10^{-6}$ m/s.

In comparison with average values from the BEST methods (BEST-Intercept and BEST-Steady) and GP-measured K_{fs} from the study site, this approach appears to underestimate K_{fs} values, although they remain within the same order of magnitude (Figure 3.9). Indeed, all the methods

considered gave different values. Also, the one-sampled t-test conducted using K_{fs} value (2.67×10^{-5} m/s) as the hypothesized mean revealed that all approaches are significantly different from the hypothesized mean ($p < 0.05$).

Soil hydraulic conductivity is a highly variable property dependent on several factors, including measurement methods (Verbist et al. 2013). Similar challenges have led to discrepancies in K_s estimates even with conventional methods. Lee et al. (1985) compared the performance of three different conventional measurements (air-entry permeameter, GP, and the falling head permeameter) in different soils, including loamy sand soils. The authors highlighted the relevance of sampling volume and geometrical difference of the different methods in the K_{fs} values obtained. Verbist et al. (2013) also compared six different methods (single-ring (SR) and double-ring (DR) infiltrometers, the constant head well infiltrometer (CH), the inverse auger (IA) hole, the tension infiltrometer (TI) and the rainfall simulator (RFS) to determine K_{fs} in stony soils and found that technique selection has effects on measured value. The authors were, however, unclear how much of the differences can be attributed to the stony nature of the soil or the structural disturbances caused by methods like SR and DR infiltrometers that might have affected the infiltration rates.

Since this approach provided estimates that fall within the expected range for the soil type in the study site, its utilization for large-scale mapping of SHPs non-destructively (since even smaller distractions, like insertion of rings to the surface, could change the infiltration and thus K_{fs}) is feasible and can be reported and considered in relation to estimates from the same approach.

While this study was conducted on a field scale and built on similar previous studies that have been conducted to study soil water dynamics on a laboratory scale, we did not exactly overcome all the challenges posed by heterogeneity and variability in the field. Infiltration at the field level is often characterized by different situations, such as lateral and preferential flow, that can

contribute to variability in its quantification. From a research perspective, more laboratory studies might be needed to explore the approach under less-varied conditions; however, since most hydrological experiments conducted in the laboratory are to be upscaled and replicated on the field eventually, a continuous iteration of laboratory and field exploration might be a better approach.

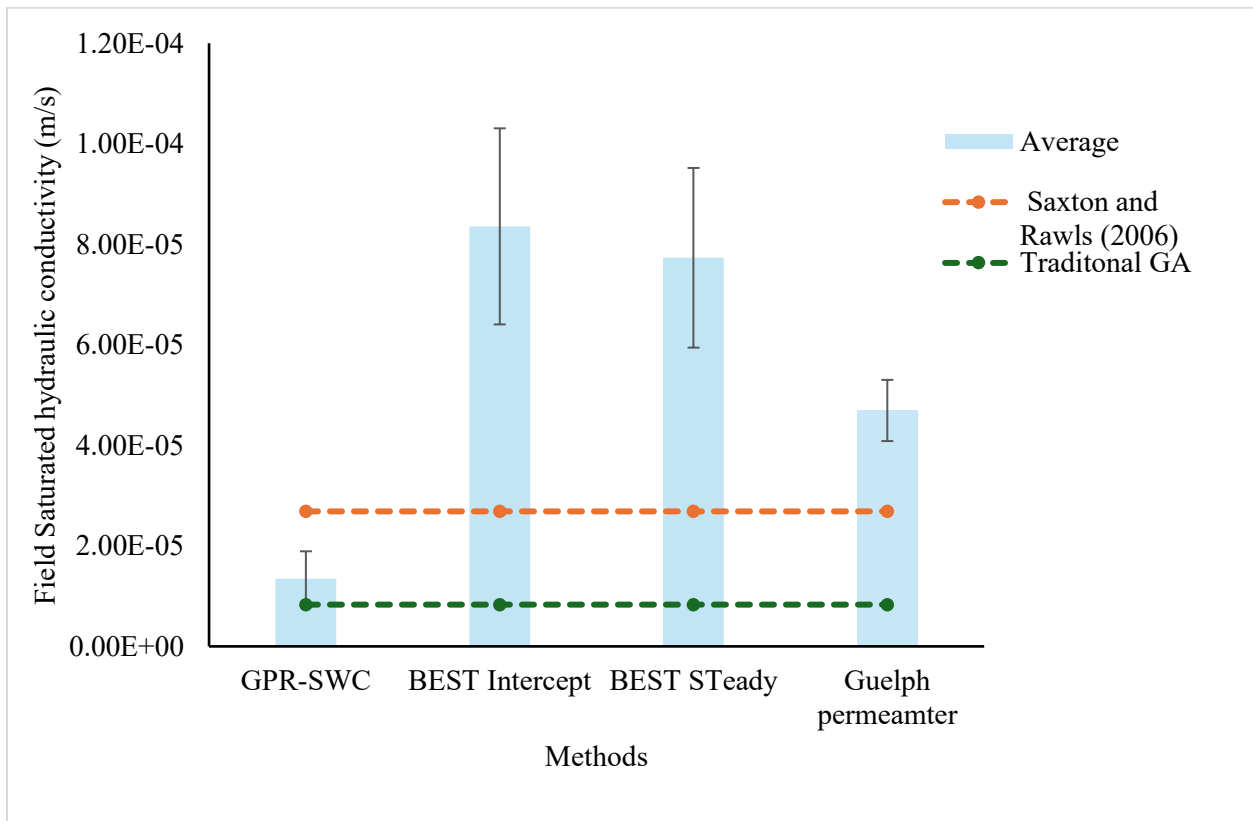


Figure 3.9. Comparison of field-saturated hydraulic conductivity (K_{fs}) estimates derived from ground-penetrating radar soil water content variations (GPR-SWC, v/v), BEST-Intercept, BEST-Steady, and Guelph permeamter (GP), with Saxton and Rawls (2006) estimates and traditional Green-Ampt (GA)- K_s parameters as benchmarks.

3.4. Conclusions

This study explored the potential of using time-lapse ground-penetrating radar direct ground wave (GPR-DGW) travel time measurement to monitor soil water dynamics during an infiltration experiment. It also examined the estimation of field-saturated hydraulic conductivity (K_{fs}) by incorporating GPR-monitored soil water content (GPR-SWC) in the Green-Ampt (GA) model. The infiltration experiment was conducted using the Beerkan method, which involved applying a constant and limited volume of water at specific intervals.

The findings revealed that GPR-DGW effectively provided continuous and reliable information on soil water content (SWC) changes during the infiltration experiments. GPR also showed consistency in measuring the dielectric constant, and SWC changes at two different locations.

The study also highlighted that GPR-SWC changes can serve as a useful parameter for estimating K_{fs} . The observed underestimation of K_{fs} from this approach compared to theoretical values and conventional methods was attributed to the relatively large sampling volume and the inclusion of extended dry areas during the infiltration by the GPR method. Despite this underestimation, this approach yielded values that are still within the expected ranges for the soil type at the study site. These results could be relevant when reported according to the method utilized, similar to other soil hydraulic conductivity estimation/measurement methods. Overall, these findings suggest that GPR-DGW can be a valuable tool for large-scale monitoring of soil water dynamics and estimation of SHPs.

Future research endeavors should aim to improve the monitoring of SWC changes more accurately for the estimation of K_{fs} by the GPR-DGW approach. This could be achieved using rings with large diameters (e.g., double rings) and GPR antenna systems with smaller areas to reduce the sampling area and minimize dry areas to be considered. Further studies are needed to explore this approach

under different moisture levels and soil types. Utilizing GPR or integrating different geophysical techniques may help derive additional parameters in the GA model. Considering the advancement in GPR data processing, investigating this approach using more advanced techniques, such as the Full-Waveform Inversion (FWI), could improve the accuracy of SHP estimates. In addition, future research could explore the use of 3D GPR for more accurate field monitoring of SWC changes during infiltration experiments.

3.5. Acknowledgments

The authors acknowledge the financial support provided by the Natural Sciences and Engineering Research Council of Canada, Discovery Grant (NSERC-DG: RGPIN-2019-04614), Industry, Energy and Innovation of the Government of Newfoundland and Labrador, IET Grant: 5404-1962-102, and the School of Graduate Studies, Memorial University of Newfoundland (MUN). The authors would also like to thank the Department of Fisheries, Forestry, and Agriculture, Government of Newfoundland and Labrador, for providing access to the research field, and members of the Soil Hydrology and Agrophysics research group, Grenfell Campus Memorial University of Newfoundland, for their assistance during data collection and their valuable suggestions and feedback that improved the quality of the manuscript.

3.6. References

- Alagna, V., Bagarello, V., Di Prima, S., Guaitoli, F., Iovino, M., Keesstra, S., Cerdà, A., 2019. Using Beerkan experiments to estimate hydraulic conductivity of a crusted loamy soil in a Mediterranean vineyard. *Journal of Hydrology and Hydromechanics* 67(2), 191–200. <https://doi.org/10.2478/johh-2018-0023>.
- Albalasmeh, A., Mohawesh, O., Gharaibeh, M., Deb, S., Slaughter, L., El Hanandeh, A., 2022. Artificial neural network optimization to predict saturated hydraulic conductivity in arid and semi-arid regions. *CATENA* 217, 106459. <https://doi.org/10.1016/j.catena.2022.106459>.
- Angulo-Jaramillo, R., Bagarello, V., Di Prima, S., Gosset, A., Iovino, M., Lassabatere, L., 2019. Beerkan Estimation of Soil Transfer parameters (BEST) across soils and scales. *Journal of Hydrology* 576, 239–261. <https://doi.org/10.1016/j.jhydrol.2019.06.007>.
- Badewa, E., Unc, A., Cheema, M., Kavanagh, V., Galagedara, L., 2018. Soil moisture mapping using multi-frequency and multi-coil electromagnetic induction sensors on managed podzols. *Agronomy* 8(10), Article 10. <https://doi.org/10.3390/agronomy8100224>.
- Bagarello, V., Di Prima, S., Iovino, M., 2014. Comparing alternative algorithms to analyze the beerkan infiltration experiment. *Soil Science Society of America Journal* 78(3), 724–736. <https://doi.org/10.2136/sssaj2013.06.0231>.
- Baiamonte, G., 2019. SCS curve number and green-ampt infiltration models. *Journal of Hydrologic Engineering* 24(10), 04019034. [https://doi.org/10.1061/\(ASCE\)HE.1943-5584.0001838](https://doi.org/10.1061/(ASCE)HE.1943-5584.0001838).

- Birchak, J.R., Gardner, C.G., Hipp, J.E., Victor, J.M., 1974. High dielectric constant microwave probes for sensing soil moisture. *Proceedings of the Institute of Electrical and Electronics Engineers* 62(1), 93-98.
- Brooks, R.H., Corey, C.T., 1964. Hydraulic properties of porous media. Hydrology Paper 3. Colorado State University, Fort Collins.
- Burdine, N., 1953. Relative permeability calculations from pore size distribution data. *Journal of Petroleum Technology* 5(03), 71-78.
- Busch, S., Weihermüller, L., Huisman, J.A., Steelman, C.M., Endres, A.L., Vereecken, H., van der Kruk, J., 2013. Coupled hydrogeophysical inversion of time-lapse surface GPR data to estimate hydraulic properties of a layered subsurface. *Water Resources Research* 49(12), 8480–8494. <https://doi.org/10.1002/2013WR013992>.
- Cao, Q., Song, X., Wu, H., Gao, L., Liu, F., Yang, S., Zhang, G., 2020. Mapping the response of volumetric soil water content to an intense rainfall event at the field scale using GPR. *Journal of Hydrology* 583, 124605. <https://doi.org/10.1016/j.jhydrol.2020.124605>.
- Castellini, M., Di Prima, S., Moret-Fernández, D., Lassabatere, L., 2021. Rapid and accurate measurement methods for determining soil hydraulic properties: A review. *Journal of Hydrology and Hydromechanics* 69(2), 121–139. <https://doi.org/10.2478/johh-2021-0002>.
- Chow, V.T., Maidment, D.R., Mays, L.W., 1988. *Applied Hydrology*. McGraw-Hill Series in Water Resources and Environmental Engineering.
- Curtis, J.O., 2001. Moisture effects on the dielectric properties of soils. *IEEE Transactions on Geoscience and Remote Sensing* 39(1), 125-128.
- Du, S., 1996. Determination of water content in the subsurface with the ground wave of ground penetrating radar. Ph.D. thesis, Ludwig-Maximilians-Universität, Munich, Germany.

- Fattahi Nafchi, R., Valiyari-Eskandari, M., Raeisi Vanani, H., Ostad-Ali-Askari, K., Bahrami, A., 2023. Evaluation of wetting front detector to estimate the dimensions of wetting front in the drip irrigation. *Journal of Engineering and Applied Science* 70(1), 126 <https://doi.org/10.1186/s44147-023-00295-5>.
- Fernández-Gálvez, J., Pollacco, J.A.P., Lassabatere, L., Angulo-Jaramillo, R., Carrick, S., 2019. A general Beerkan Estimation of Soil Transfer parameters method predicting hydraulic parameters of any unimodal water retention and hydraulic conductivity curves: Application to the Kosugi soil hydraulic model without using particle size distribution data. *Advances in Water Resources* 129, 118–130. <https://doi.org/10.1016/j.advwatres.2019.05.005>.
- Fu, Z., Hu, W., Beare, M., Thomas, S., Carrick, S., Dando, J., Langer, S., Müller, K., Baird, D., Lilburne, L., 2021. Land use effects on soil hydraulic properties and the contribution of soil organic carbon. *Journal of Hydrology* 602, 126741. <https://doi.org/10.1016/j.jhydrol.2021.126741>.
- Galagedara, L.W., Parkin, G.W., Redman, J.D., Endres, A.L., 2003. Assessment of soil moisture content measured by borehole GPR and TDR under transient irrigation and drainage. *Journal of Environmental and Engineering Geophysics* 8(2), 77–86. <https://doi.org/10.4133/JEEG8.2.77>.
- Galagedara, L.W., Redman, J.D., Parkin, G.W., Annan, A.P., Endres, A.L., 2005b. Numerical modeling of GPR to determine the direct ground wave sampling depth. *Vadose Zone Journal* 4(4), 1096–1106.
- Green, W. H., Ampt, G. A., 1911. Studies on soil physics. *The Journal of Agricultural Sciences*, 4(1), 1-24. <https://doi.org/10.1017/S0021859600001441>.

- Gribb, M.M., Forkutsa, I., Hansen, A., Chandler, D.G., McNamara, J.P., 2009. The effect of various soil hydraulic property estimates on soil moisture simulations. *Vadose Zone Journal* 8(2), 321–331. <https://doi.org/10.2136/vzj2008.0088>.
- Grote, K., Crist, T., Nickel, C., 2010a. Experimental estimation of the GPR groundwave sampling depth. *Water Resources Research* 46(10). <https://doi.org/10.1029/2009WR008403>.
- Hartmann, A., Weiler, M., Blume, T., 2020. The impact of landscape evolution on soil physics: Evolution of soil physical and hydraulic properties along two chronosequences of proglacial moraines. *Earth System Science Data* 12(4), 3189–3204. <https://doi.org/10.5194/essd-12-3189-2020>.
- Haverkamp, R., Ross, P.J., Smettem, K.R.J., Parlange, J.Y., 1994. Three-dimensional analysis of infiltration from the disc infiltrometer: 2. Physically based infiltration equation. *Water Resources Research* 30(11), 2931–2935.
- Hillel, D., 2003. *Introduction to Environmental Soil Physics*. Elsevier, Amsterdam.
- Huisman, J.A., Snepvangers, J.J.J.C., Bouten, W., Heuvelink, G.B.M., 2002. Mapping spatial variation in surface soil water content: Comparison of ground-penetrating radar and time domain reflectometry. *Journal of Hydrology* 269(3), 194–207. [https://doi.org/10.1016/S0022-1694\(02\)00239-1](https://doi.org/10.1016/S0022-1694(02)00239-1).
- Illawathure, C., Cheema, M., Kavanagh, V., Galagedara, L., 2020. Distinguishing capillary fringe reflection in a GPR profile for precise water table depth estimation in a boreal podzolic soil field. *Water* 12(6), 1670. <https://doi.org/10.3390/w12061670>.
- Jadoon, K.Z., Weihermüller, L., Scharnagl, B., Kowalsky, M.B., Bechtold, M., Hubbard, S.S., Vereecken, H., Lambot, S., 2012. Estimation of soil hydraulic parameters in the field by

- integrated hydrogeophysical inversion of time-lapse ground-penetrating radar data. *Vadose Zone Journal* 11(4), vzt2011.0177. <https://doi.org/10.2136/vzj2011.0177>.
- Kowalsky, M.B., Finsterle, S., Peterson, J., Hubbard, S., Rubin, Y., Majer, E., Ward, A., Gee, G., 2005. Estimation of field-scale soil hydraulic and dielectric parameters through joint inversion of GPR and hydrological data. *Water Resources Research* 41(11). <https://doi.org/10.1029/2005WR004237>.
- Lambot, S., Slob, E.C., Vanclooster, M., Vereecken, H., 2006. Closed loop GPR data inversion for soil hydraulic and electric property determination. *Geophysical Research Letters* 33(21). <https://doi.org/10.1029/2006GL027906>.
- Lassabatère, L., Angulo-Jaramillo, R., Soria Ugalde, J.M., Cuenca, R., Braud, I., Haverkamp, R., 2006. Beerkan estimation of soil transfer parameters through infiltration experiments—best. *Soil Science Society of America Journal* 70(2), 521–532. <https://doi.org/10.2136/sssaj2005.0026>.
- Lee, D.M., Elrick, D.E., Reynolds, W.D., Clothier, B.E., 1985. A comparison of three field methods for measuring saturated hydraulic conductivity. *Canadian Journal of Soil Science* 65(3), 563–573. <https://doi.org/10.4141/cjss85-060>.
- Lee, S., Chu, M.L., Schmidt, A.R., 2020. Effective green-ampt parameters for two-layered soils. *Journal of Hydrologic Engineering* 25(4), 04020004. [https://doi.org/10.1061/\(ASCE\)HE.1943-5584.0001897](https://doi.org/10.1061/(ASCE)HE.1943-5584.0001897).
- Léger, E., Saintenoy, A., Tucholka, P., Coquet, Y., 2016. Hydrodynamic parameters of a sandy soil determined by ground-penetrating radar monitoring of porchet infiltrations. *IEEE Journal of Selected Topics in Applied Earth Observations and Remote Sensing* 9(1), 188–200. <https://doi.org/10.1109/JSTARS.2015.2464231>.

- Li, S., Cui, P., Cheng, P., Wu, L., 2022. Modified green–ampt model considering vegetation root effect and redistribution characteristics for slope stability analysis. *Water Resources Management* 36(7), 2395–2410. <https://doi.org/10.1007/s11269-022-03149-6>.
- Liu, X., Chen, J., Cui, X., Liu, Q., Cao, X., Chen, X., 2019. Measurement of soil water content using ground-penetrating radar: A review of current methods. *International Journal of Digital Earth* 12(1), 95–118. <https://doi.org/10.1080/17538947.2017.1412520>.
- Ma, D., Zhang, J., Horton, R., Wang, Q., Lai, J., 2017. Analytical method to determine soil hydraulic properties from vertical infiltration experiments. *Soil Science Society of America Journal* 81(6), 1303–1314. <https://doi.org/10.2136/sssaj2017.02.0061>.
- Ma, Y., Feng, S., Su, D., Gao, G., Huo, Z., 2010. Modeling water infiltration in a large layered soil column with a modified green–ampt model and HYDRUS-1D. *Computers and Electronics in Agriculture* 71, S40–S47. <https://doi.org/10.1016/j.compag.2009.07.006>.
- Meng, S., Yang, Y., 2019. Infiltration simulation with improved green-ampt model coupled with the wet zone partition function. *Journal of Hydrologic Engineering* 24(5), 04019014. [https://doi.org/10.1061/\(ASCE\)HE.1943-5584.0001782](https://doi.org/10.1061/(ASCE)HE.1943-5584.0001782).
- Minasny, B., McBratney, A.B., 2007. Estimating the water retention shape parameter from sand and clay content. *Soil Science Society of America Journal* 71(4), 1105-1110.
- Mohammadzadeh-Habili, J., Heidarpour, M., 2015. Application of the green–ampt model for infiltration into layered soils. *Journal of Hydrology* 527, 824–832. <https://doi.org/10.1016/j.jhydrol.2015.05.052>.
- Mohammadzadeh-Habili, J., Khalili, D., 2021. Development of the green-ampt infiltration rate model and relationship of the ga model parameters with soil hydraulic parameters. *Journal*

- of Hydrologic Engineering 26(11), 04021033. [https://doi.org/10.1061/\(ASCE\)HE.1943-5584.0002130](https://doi.org/10.1061/(ASCE)HE.1943-5584.0002130).
- Nadler, A., Dasberg, S., Lapid, I., 1991. Time domain reflectometry measurements of water content and electrical conductivity of layered soil columns. Soil Science Society of America Journal 55(4), 938-943.
- Pathirana, S., Lambot, S., Krishnapillai, M., Cheema, M., Smeaton, C., Galagedara, L., 2023. Ground-penetrating radar and electromagnetic induction: challenges and opportunities in agriculture. Remote Sensing 15(11), Article 11. <https://doi.org/10.3390/rs15112932>.
- Pathirana, S., Lambot, S., Krishnapillai, M., Smeaton, C., Cheema, M., Galagedara, L., 2024. Potential of ground-penetrating radar to calibrate electromagnetic induction for shallow soil water content estimation. Journal of Hydrology 633, 130957. <https://doi.org/10.1016/j.jhydrol.2024.130957>.
- Rahmati, M., Latorre, B., Lassabatere, L., Angulo-Jaramillo, R., Moret-Fernández, D., 2019. The relevance of Philip theory to Haverkamp quasi-exact implicit analytical formulation and its uses to predict soil hydraulic properties. Journal of Hydrology 570, 816–826. <https://doi.org/10.1016/j.jhydrol.2019.01.038>.
- Rawls, W.J., Brakensiek, D.L., Miller, N., 1983. Green-ampt infiltration parameters from soils data. Journal of Hydraulic Engineering 109(1), 62–70. [https://doi.org/10.1061/\(ASCE\)0733-9429\(1983\)109:1\(62\)](https://doi.org/10.1061/(ASCE)0733-9429(1983)109:1(62)).
- Reynolds, W.D., Elrick, D.E., 1986. A method for simultaneous in situ measurement in the vadose zone of field-saturated hydraulic conductivity, sorptivity and the conductivity-pressure head relationship. Groundwater Monitoring & Remediation 6(1), 84–95. <https://doi.org/10.1111/j.1745-6592.1986.tb01229.x>.

- Rezaei, M., Saey, T., Seuntjens, P., Joris, I., Boëne, W., Van Meirvenne, M., Cornelis, W., 2016. Predicting saturated hydraulic conductivity in a sandy grassland using proximally sensed apparent electrical conductivity. *Journal of Applied Geophysics* 126, 35–41. <https://doi.org/10.1016/j.jappgeo.2016.01.010>.
- Rossi, M., Manoli, G., Pasetto, D., Deiana, R., Ferraris, S., Strobbia, C., Putti, M., Cassiani, G., 2015. Coupled inverse modeling of a controlled irrigation experiment using multiple hydro-geophysical data. *Advances in Water Resources* 82, 150–165. <https://doi.org/10.1016/j.advwatres.2015.03.008>.
- Roth, C.H., Malicki, M.A., Plagge, R., 1992. Empirical evaluation of the relationship between soil dielectric constant and volumetric water content as the basis for calibrating soil moisture measurements by TDR. *Journal of Soil Science* 43(1), 1–13. <https://doi.org/10.1111/j.1365-2389.1992.tb00115.x>.
- Saxton, K.E., Rawls, W.J., 2006. Soil water characteristic estimates by texture and organic matter for hydrologic solutions. *Soil Science Society of America Journal* 70(5), 1569–1578. <https://doi.org/10.2136/sssaj2005.0117>.
- Smettem, K.R.J., Parlange, J.Y., Ross, P.J., Haverkamp, R., 1994. Three-dimensional analysis of infiltration from the disc infiltrometer: 1. A capillary-based theory. *Water Resources Research* 30(11), 2925–2929.
- Soil Classification Working Group, 1998. *The Canadian System of Soil Classification*, 3rd ed. Agriculture and Agri-Food Canada Publication, Ottawa.
- Sperl, C., 1999. Determination of spatial and temporal variation of soil water content in an agro-ecosystem with ground-penetrating radar (in German). Ph.D. thesis, Technische Universität München, Germany

- Steelman, C.M., Endres, A.L., 2011. Comparison of petrophysical relationships for soil moisture estimation using GPR ground waves. *Vadose Zone Journal* 10(1), 270–285. <https://doi.org/10.2136/vzj2010.0040>.
- Topp, G.C., Davis, J.L., Annan, A.P., 1980. Electromagnetic determination of soil water content: Measurements in coaxial transmission lines. *Water Resources Research* 16(3), 574–582.
- van Genuchten, M.T., 1980. A closed-form equation for predicting the hydraulic conductivity of unsaturated soils. *Soil Science Society of America Journal* 44(5), 892–898.
- van Overmeeren, R.A., Sariowan, S.V., Gehrels, J.C., 1997. Ground penetrating radar for determining volumetric soil water content: Measurement results of comparative measurements at two sites. *Journal of Hydrology* 197, 316–338.
- Verbist, K.M.J., Cornelis, W.M., Torfs, S., Gabriels, D., 2013. Comparing methods to determine hydraulic conductivities on stony soils. *Soil Science Society of America Journal* 77(1), 25–42. <https://doi.org/10.2136/sssaj2012.0025>.
- Vigo, Á. del, Zubezu, S., Juana, L., 2021. Infiltration models and soil characterisation for hemispherical and disc sources based on Green-Ampt assumptions. *Journal of Hydrology* 595, 125966. <https://doi.org/10.1016/j.jhydrol.2021.125966>.
- Wijewardana, Y.G.N.S., Galagedara, L.W., 2010. Estimation of spatio-temporal variability of soil water content in agricultural fields with ground penetrating radar. *Journal of Hydrology* 391(1), 24–33. <https://doi.org/10.1016/j.jhydrol.2010.06.036>.
- Yilmaz, D., Lassabatere, L., Angulo-Jaramillo, R., Deneele, D., Legret, M., 2010. Hydrodynamic characterization of basic oxygen furnace slag through an adapted best method. *Vadose Zone Journal* 9(1), 107. <https://doi.org/10.2136/vzj2009.0039>.

- Yu, Y., Huisman, J.A., Klotzsche, A., Vereecken, H., Weihermüller, L., 2022. Coupled full-waveform inversion of horizontal borehole ground penetrating radar data to estimate soil hydraulic parameters: A synthetic study. *Journal of Hydrology* 610, 127817. <https://doi.org/10.1016/j.jhydrol.2022.127817>.
- Yu, Y., Weihermüller, L., Klotzsche, A., Lärm, L., Vereecken, H., Huisman, J.A., 2021. Sequential and coupled inversion of horizontal borehole ground penetrating radar data to estimate soil hydraulic properties at the field scale. *Journal of Hydrology* 596, 126010. <https://doi.org/10.1016/j.jhydrol.2021.126010>.
- Zhang, M., Feng, X., Bano, M., Xing, H., Wang, T., Liang, W., Zhou, H., Dong, Z., An, Y., Zhang, Y., 2022. Review of ground penetrating radar applications for water dynamics studies in unsaturated zone. *Remote Sensing* 14(23), 5993. <https://doi.org/10.3390/rs14235993>.
- Zou, C., Zhang, S., Jiang, X., Chen, F., 2023. Monitoring and characterization of water infiltration in soil unsaturated zone through an integrated geophysical approach. *CATENA* 230, 107243. <https://doi.org/10.1016/j.catena.2023.107243>.

Appendices

Appendix 1

BEST Theory

The BEST procedure for soil hydraulic characterization is based on the van Genuchten (1980) relationship for the water retention curve, in conjunction with the Burdine (1953) condition, and the Brooks and Corey (1964) relationship for hydraulic conductivity, $K(\theta)$.

$$\frac{\theta - \theta_r}{\theta_s - \theta_r} = \left[1 + \left(\frac{h}{h_g} \right)^n \right]^{-m} \quad \text{Equation 3.6a}$$

$$m = 1 - \frac{2}{n} \quad \text{Equation 3.6b}$$

$$\frac{K(\theta)}{K_s} = \left(\frac{\theta - \theta_r}{\theta_s - \theta_r} \right)^\eta \quad \text{Equation 3.6c}$$

$$\eta = \frac{2}{m \times n} + 2 + p \quad \text{Equation 3.6d}$$

where n , m , and η are shape parameters, with $n > 2$ (Minasny and McBratney, 2007), p is a tortuosity parameter (set equal to 1 following Burdine's (1953) condition), and h_g (pressure head, length units, L), θ_s (saturated soil water content, L^3L^{-3}), θ_r (residual soil water content, L^3L^{-3}) and K_s (saturated soil hydraulic conductivity, LT^{-1}) are scale parameters.

In the BEST procedure, θ_r is assumed to be zero, and θ_s can be measured at the end of the infiltration or calculated as total soil porosity. The shape parameter n can be estimated using the PTF that uses the particle-size distribution of soil fraction (<2 mm) (Lassabatere et al., 2006) or the indirect procedure proposed by Minasny and McBratney (2007) that uses only

the sand and clay content of the soils. The scale parameters K_s and h_g are derived from the inverse analysis of the infiltration data.

The three-dimensional cumulative infiltration, I (L), and steady-state infiltration rate, i_s (LT⁻¹) can be approached by the following explicit transient two-term expressions (Haverkamp et al., 1994; Lassabatère et al., 2006):

$$I(t) = S\sqrt{t} + (AS^2 + BK_s)t \quad \text{Equation 3.7a}$$

$$i(t) = \frac{S}{2\sqrt{t}} + (AS^2 + BK_s) \quad \text{Equation 3.7b}$$

$$I_{+\infty}(t) = (AS^2 + K_s)t + C \frac{S^2}{K_s} \quad \text{Equation 3.7c}$$

$$i_s = AS^2 + K_s \quad \text{Equation 3.7d}$$

Where t (T) is the time, S (LT^{-1/2}) is soil sorptivity, and A (L⁻¹), B and C are constants that can be defined for specific case of a Brooks and Corey (1964) relationship as:

$$A = \frac{\gamma}{r(\theta_s - \theta_0)} \quad \text{Equation 3.8a}$$

$$B = \frac{2-\beta}{3} \left[1 - \left(\frac{\theta_0}{\theta_s} \right)^\eta \right] + \left(\frac{\theta_0}{\theta_s} \right)^n \quad \text{Equation 3.8b}$$

$$C = \frac{1}{2 \left[1 - \left(\frac{\theta_0}{\theta_s} \right)^\eta \right]^{(1-\beta)}} \ln \left(\frac{1}{\beta} \right) \quad \text{Equation 3.8c}$$

where β and γ are coefficients that are commonly set at 0.6 and 0.75, respectively, θ_0 for < 0.25 θ_s (Haverkamp et al., 1994; Smettem et al., 1994).

Three common algorithms have been used to analyze the measured infiltration and estimate K_s and S : Best-Slope, Best-Intercept, and Best-Steady (Bagarello et al., 2014; Angulo-Jaramillo et al., 2019)

Best-Slope

The Best-Slope algorithm, developed by Lassabatere et al. (2006), estimates S by fitting the transient cumulative infiltration data on Equation (3a), with S function and experimental steady-state infiltration rate replacing K_s .

$$K_s = i_s^{exp} - AS^2 \quad \text{Equation 3.9}$$

The fit is carried out by minimizing the classical objective function for cumulative infiltration:

$$f(S, K, k) = \sum_{i=1}^k [I^{exp}(t_i) - I_{est}(t_i)]^2 \quad \text{Equation 3.10}$$

where k is the number of data points considered for the transient state, and I^{exp} is the measured and the I_{est} estimated cumulative infiltration, respectively. Once S has been estimated, the K_s can be derived using Equation (5). The values of S and K_s calculated are only considered valid when the experimental time (t_k) is lower than t_{max} .

Best-Intercept

The Best-Intercept algorithm, developed by Yilmaz et al. (2010), proposed an alternative to the above constraint by using the intercept ($b_{+\infty}^{end}$) of the asymptotic expansion, $I_{+\infty}(t)$ (from equation 3c), as defined by the following equation:

$$I_{+\infty}(t) = (AS^2 + K_s)t + C \frac{S^2}{K_s} \quad \text{Equation 3.11}$$

Therefore, the following equation is used to derive K_s :

$$K_s = C \frac{S^2}{b_{+\infty}^{end}} \quad \text{Equation 3.12}$$

Best-Steady

The third approach is more holistic, using both the intercept and the slope of the straight line fitted on the data to describe the steady-state conditions on the I vs. t plot.

$$S = \sqrt{\frac{i_s^{exp}}{A + \frac{C}{b_{+\infty}^{end}}}} \quad \text{Equation 3.13}$$

K_s can be calculated using equations (3.9) or (3.12).

A number of studies have noted its possibility of giving erroneous K_s values, particularly when the $i_s \gg AS^2$ (Yilmaz et al., 2010; Bagarello et al., 2014). Hence, Best-Intercept and Best-Steady were used in this study.

Appendix 2

Calibration of Soil Moisture Probes (SMPs)

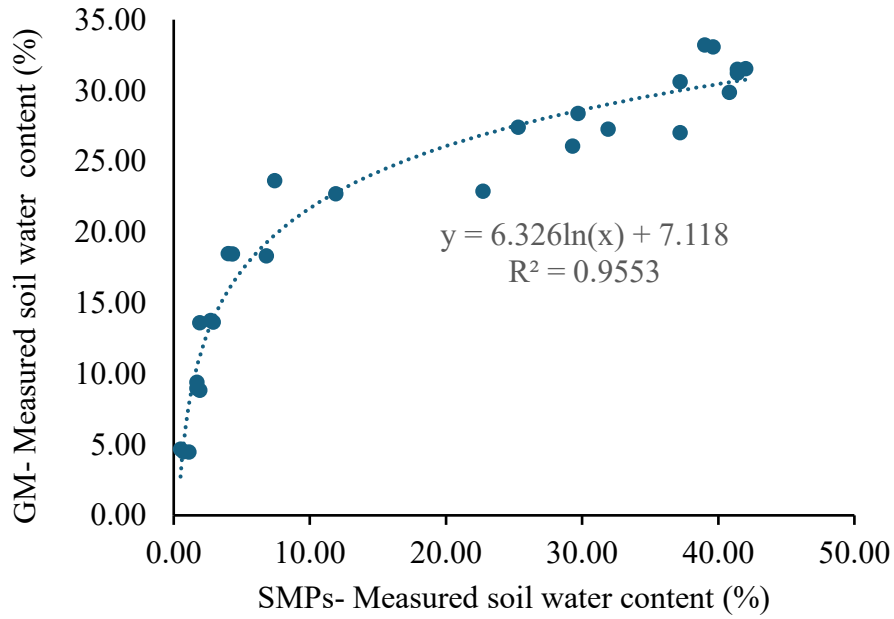


Figure 3.10. Calibration of Soil Moisture Probes (SMPs) for measuring soil water content.

GM- Gravimetric Method; SMPs – Soil Moisture Probes

Co-authorship Statement for Study Two

A manuscript based on Chapter 4, entitled “*Using Hydrus-1D Modeling to Predict Soil Hydraulic Parameters of Podzolic Soils from Time-lapsed Ground-penetrating Radar Data*,” will be submitted for publication in the “Geoderma Regional Journal.”

Juwonlo Dahunsi, the thesis author, was the primary author and was responsible for proposal development, methodology, data collection, investigation, analysis, modeling, and writing of the original manuscript. Sashini Pathirana, PhD student, assisted with the data collection, processing and review and editing of the manuscript. Mumtaz Cheema and Mano Krishnapillai are co-supervisor and committee member, respectively, and provided input on the research proposal, methodology, and validation and assisted with the review and editing of the manuscripts. Lakshman Galagedara, the supervisor, was responsible for the project conceptualization, funding acquisition, project administration, resource allocation, supervision, supported the development of methodology and investigation, and contributed to the review and editing of the manuscript.

CHAPTER FOUR

Using Hydrus-1D Modeling to Predict Soil Hydraulic Parameters of Podzolic Soils from Time-lapsed Ground-penetrating Radar Data

Juwonlo Dahunsi^a, Sashini Pathirana^a, Manokararajah Krishnapillai^a, Mumtaz Cheema^a,
Lakshman Galagedara^{a,*}

^a School of Science and the Environment, Memorial University of Newfoundland, Corner Brook,
NL A2H 5G4, Canada.

*Corresponding author

*Correspondence: lgalagedara@mun.ca

Abstract

Understanding soil hydraulic parameters (SHPs) is crucial for many agricultural and environmental applications. In this study, ground-penetrating radar (GPR) direct ground wave (DGW) was utilized as a non-invasive technique to monitor infiltration in the field and laboratory settings. Time-lapse GPR data was combined with Hydrus-1D inverse modeling to predict Mualem-van Genuchten (M-vG) parameters and to simulate water flow dynamics in boreal podzolic soil. The field experiment was conducted at a site in Western Agriculture Center and Research Station, Pasadena, Newfoundland, Canada. Bulk soil samples from this location were also collected to fill a 102 L container for the respective laboratory infiltration experiment. In both cases, Beerkan infiltration experiments were conducted using known equal water volume and monitored with 500 MHz center frequency GPR. The collected DGW travel time was converted

to soil water content (SWC) variation and used in the Hydrus-1D simulation. Calibration was carried out through the inverse modeling of the first experiments, and validation was done using forward modeling of two additional experiments. Calibrated M-vG parameters obtained from the inverse modeling of the GPR data are comparable with estimates from Rosetta neural network prediction for the soil type at the study site. The validation results reveal a good correlation between the simulated and measured SWC variation with a root mean square error of 0.0199–0.0365 cm³/cm³ and Nash-Sutcliffe modeling efficiency of 0.2955–0.8273. The approach presented in this study offers a non-invasive method for large-scale characterization of soil water dynamics and SHPs.

Keywords: Beerkan infiltration, Direct ground wave, Forward modeling, Inverse modeling, Soil water content, Mualem-van Genuchten parameters.

4.1. Introduction

Monitoring soil hydraulic parameters (SHPs) is important for various environmental and agricultural applications (Yu et al., 2022; Ramos et al., 2023). They directly or indirectly impact plant water availability, the transport of water and associated contaminants through the vadose zone, groundwater recharge, and surface runoff generation, among other soil processes (Moysey, 2010). They also have crucial implications for the development and applications of hydrological models over different environmental and agricultural problems (Leger et al., 2014; Kishne et al., 2017; Lu et al., 2020).

Several mathematical expressions have been used to represent SHPs and vadose zone flow (Kosugi et al., 2002). The Mualem-van Genuchten (M-vG) function (Mualem, 1976; van Genuchten, 1980)

is widely recognized among these expressions. The function combines soil water retention parameters introduced by van Genuchten (1980) with the pore-size distribution model introduced by Mualem (1976) for hydraulic conductivity (Schaap and van Genuchten, 2006). Due to its flexibility and accuracy in describing vadose zone flow and transport, the M-vG function has been incorporated into several hydrological models.

The Hydrus-1D model is one of the most widely used hydrological models incorporating the M-vG function. It allows for robust water, heat, and solute transport simulation in saturated and unsaturated zones (Šimůnek et al., 2009) and has been applied in various soil hydrodynamics studies (Šimůnek et al., 2016; Radcliffe and Šimůnek, 2018; Iqbal et al., 2019). However, the effectiveness of the simulation, like other models, often depends on the accurate estimation of SHPs under local conditions (Dragonetti et al., 2022).

The determination of the soil water retention parameters is usually carried out using laboratory experiments such as HYPROP, pressure plate, or water hanging column (Richards, 1941; Schindler et al., 2010; Dane and Topp, 2020). Also, the hydraulic conductivity function is often estimated in the laboratory and field using infiltration tests and permeameters (Reynolds et al., 2008; Verbist et al., 2013). However, many of these methods are tedious, invasive, time-consuming, and unable to capture high-resolution spatio-temporal variations in the SHPs (Rezaei et al., 2016; Zou et al., 2023).

Non-invasive geophysical methods like ground-penetrating radar (GPR), electromagnetic induction (EMI), and electrical resistivity tomography (ERT) offer advantages with some of these limitations (Vereecken et al., 2014). The sensitivity of their physical properties to soil water content (SWC) has made relevant techniques in hydrological studies (Binley et al., 2015). GPR is one of the most used near-surface geophysical methods applied in soil hydrology because of the high

sensitivity of GPR wave velocity to SWC changes (Klotzsche et al., 2018). It emits high-frequency electromagnetic waves into the soil, which the receiver antenna receives at varying times, depending on the dielectric properties of the material (Huisman et al., 2003; Zajícová and Chuman, 2019).

The waves received and interpreted from the receiver antenna are in three main forms: air wave, direct ground wave (DGW), and reflected wave (Galagedara et al., 2003a). The DGW is a direct wave that propagates directly from the transmitter to the receiver just beneath the soil surface (Huisman et al., 2001). It has been used extensively to estimate SWC (Huisman et al., 2002; Galagedara et al. 2003a; Weihermüller et al., 2007; Steelman and Endres, 2011; Pathirana et al., 2024) and monitor spatio-temporal variability of SWC (Galagedara et al., 2003b, 2005; Grote et al., 2010b; Wijewardana and Galagedara, 2010) at around upper 0 ~ 30 cm of the soil.

Although GPR techniques do not directly measure SHPs, their ability to infer soil water movement has attracted considerable interest due to their sensitivity to fluid distribution (Kowalsky et al., 2005; Zhang et al., 2022). Hence, integrating GPR-derived parameters into hydrological models has become a relevant approach for monitoring soil water dynamics and estimating SHPs.

Recent studies have integrated GPR-derived parameters with the Hydrus-1D model to monitor soil water dynamics and estimate M-vG parameters using different approaches. For instance, Jadoon et al. (2012) employed a two-layer single- and dual-porosity model to carry out a one-dimensional vertical inversion of time-lapse GPR data using Hydrus-1D, successfully estimating M-vG parameters in the shallow layers of a silty loam soil. In another study, Leger et al. (2014) simulated infiltration experiments with Hydrus-1D and converted simulated SWC snapshots into permittivity profiles using the Complex Refractive Index Method (CRIM). The authors then applied the Shuffled Complex Algorithm to optimize the inversion of both modeling and experimental data,

obtaining M-vG parameters for sandy soil that were comparable to those derived from laboratory and disk infiltrometer experiments. Similarly, Yu et al. (2022) estimated M-vG parameters using a coupled full-waveform inversion (CFWI) approach by minimizing the discrepancy between measured and simulated travel times. In the study, Hydrus-1D first simulated vertical soil water dynamics, and the resulting SWC information was then used to simulate travel times with gprMax3D.

Despite the progress and successes achieved so far, several challenges persist, limiting the use of GPR-derived SWC variation in hydrological models to estimate SHPs accurately. Few or no studies have integrated GPR-DGW information into the Hydrus-1D model for estimating SHPs despite its potential advantage in effectively capturing water movement down the profile during infiltration/irrigation events. In addition, many of these approaches have not been thoroughly evaluated across different scales (i.e., lab and field scales), different infiltration/irrigation events, and diverse soil types and conditions, particularly in soils like podzols, which are characterized by their sandy, stony, and shallow nature.

This study investigates the use of GPR-DGW data and the Hydrus-1D model for obtaining M-vG parameters and simulating soil water dynamics in boreal podzolic soils. The objectives were to: i) obtain M-vG parameters through the inverse modeling of SWC variation obtained from GPR-DGW and the Hydrus-1D model, ii) validate and evaluate the potential of the Hydrus-1D model for simulating soil water dynamics based on the inverted M-vG parameters.

4.2. Methodology

4.2.1. Experimental set-up

The field experiment was conducted at the Western Agriculture Center and Research Station, Pasadena (49.004'22" N 57.033'44" W), Newfoundland, Canada. The soil texture of the site was determined as loamy sand (sand = 83.0 % (± 1.25); silt = 14.6 % (± 1.21); clay = 2.4 % (± 0.04); $n = 9$), with the average bulk density of 1.31 (± 0.01 ; $n = 9$) g/cm³. Three locations on the site were used for the infiltration experiment.

Infiltration experiments were conducted on the field using the Beerkan method (Lassabatère et al., 2006). A ring of 10 cm diameter was inserted to a depth of 1 cm at the locations for the experiment after being cleared and leveled. A known volume of water (200 mL) was poured into the ring, followed by successive additions of equal water volume after the previous pour had infiltrated. The cumulative infiltration time was recorded, and the experiment ended after a steady infiltration was achieved (zero or minimal difference in infiltration time). A surface GPR system with a center frequency transducer of 500 MHz (PulseEKKOPro, Sensors and Software Inc., Mississauga, Canada) was used to monitor the infiltration experiments. Other details concerning the experiment setup on the field have been provided in the previous chapter of this thesis (Chapter 3).

A similar experiment was conducted in the laboratory to monitor Beerkan infiltration experiments under controlled conditions. A plastic container with an internal volume of 102 L, as shown in Figure 4.1, was used for this experiment. This volume was selected to ensure enough space to place GPR antennae and to allow adequate space for the wetting front advancement. Draining holes with a diameter of about 1 cm were drilled in the bottom of the box to allow for free drainage. Bulk soil was retrieved from the field experiment's location at the top 0.15 m. The retrieved soils were air-dried and sieved using a 4 mm sieve before being carefully packed into the box. The soils were packed at 10 cm layer increments, with moderate compaction needed. The required soil mass for the box was calculated based on the in-situ bulk density and the volume of the container, with

a bulk density of 1.403 g/cm^3 achieved after packing (moisture factor considered). The total depth of the soil packing was about 40 cm.

For the laboratory experiments, infiltration was conducted using an 8 cm diameter ring, inserted 1 cm deep into the soil. A known volume of 100 mL of water was used for the laboratory experiment, and the infiltration procedure was similar to what was carried out in the field. The infiltration experiments were carried out over three days and monitored with GPR transducers. Specifically, the monitoring was done using 500 MHz GPR transducers to replicate the field set-up and outcomes. However, the antenna separation was reduced to 33 cm to fit the container's volume.

The study utilized the GPR- direct ground wave (DGW) travel time. Previous studies have demonstrated the relevance of the GPR-DGW in capturing SWC and its variation (Galagedara et al., 2005a; Steelman and Endres, 2011; Pathirana et al., 2024). Details concerning the processing of the GPR data collected and its conversion to SWC variation have also been provided in Chapter 3 of this thesis.



Figure 4.1. Data collection set-up for the Beerkan infiltration experiment monitored by ground-penetrating radar (GPR).

4.2.2. Hydrus-1D modeling

Hydrus-1D was used for the numerical simulation of the infiltration experiment. According to Simunek et al. (2008), Hydrus-1D can simulate one-dimensional water, heat, and solute transport in variably saturated porous media. For water flow, the model solves Richard's equation (Equation 4.1).

$$\frac{\partial \theta}{\partial t} = \frac{\partial}{\partial z} \left[K(\psi) \left(\frac{\partial \psi}{\partial z} + 1 \right) \right] \quad \text{Equation 4.1}$$

Where θ is volumetric soil water content (cm^3/cm^3), t = time (seconds), Z is the vertical space coordinate (cm), K is the hydraulic conductivity (cm/sec), ψ is matric potential head (cm).

The model uses the van Genuchten relationship (Equation 4.2) to describe the water retention curve (van Genuchten, 1980) and the Mualem relationship (Equation 4.3) to describe the hydraulic conductivity (Mualem, 1976).

$$\theta(h) = \begin{cases} \theta_r + \frac{\theta_s - \theta_r}{1 + |\alpha h^n|^m} & h < 0 \\ \theta_s & h \geq 0 \end{cases} \quad \text{where } m = 1 - \frac{1}{n}, n > 1 \quad \text{Equation 4.2}$$

Where θ_r is the residual water content [$\text{L}^{-3}\text{L}^{-3}$], θ_s is the saturated water content [$\text{L}^{-3}\text{L}^{-3}$], h is the water pressure head [L], α [L^{-1}] and n [-] are shape parameters.

$$K(h) = \begin{cases} K_{sr} S_e^{1/2} \left[1 - (1 - S_e^m)^{1/m} \right]^2 & h < 0 \\ K_s & h \geq 0 \end{cases} \quad \text{where } m = 1 - \frac{1}{n}, n > 1 \quad \text{Equation 4.3}$$

Where S_e (effective saturation) = $(\theta - \theta_r) / (\theta_s - \theta_r)$, K_s is the saturated hydraulic conductivity [LT^{-1}], S_e is the effective saturation [-], and r is the pore connectivity parameter [-], equal to 0.5.

For this study, simulation was carried out in two steps: (i) inverse modeling of M-vG parameters using SWC variation measured by time-lapse GPR data for the first experiment and Marquardt-Levenberg parameter estimation algorithm of the Hydrus-1D for calibration, and (ii) forward simulation of water flow of the second and third experiments using the inverted M-vG parameters for validation. For both the field and laboratory experiments, initial M-vG parameters were defined based on the Rosetta neural network prediction model (Schaap et al., 2001) using the particle size distribution and bulk density for the soil ($\theta_r = 0.0458 \text{ cm}^3/\text{cm}^3$, $\theta_s = 0.439 \text{ cm}^3/\text{cm}^3$, $\alpha = 0.0385$, $n = 1.8106$, $K_s = 2.77 \cdot 10^{-2} \text{ cm/sec}$). Initial soil water was set as the initial water content measured from GPR-DGW data.

The simulations assumed that the infiltration experiments were on bare soil; hence, the relevance of root water uptake was neglected. Further, evaporation was not considered in the simulation processes because typical evaporation rates are much lower than the infiltration rate (Yu et al., 2022).

The upper boundary condition was set as a variable pressure head (h), with an initial value of $h = 0$, according to the nature of the Beerkan infiltration experiment (Minasny and McBratney, 2007), while the lower boundary consideration was set as free drainage. Initial and simulation times were set according to the experimental times recorded during the infiltration experiments. The soil was assumed to be a single homogenous soil column with one layer, and a vertical 1-D simulation was carried out (Šimůnek et al., 2008). A depth of 15 cm was considered for the simulation based on the direct ground wave sampling depth for 500 MHz center frequency (Steelman and Endres, 2011) that has been earlier determined in the field study discussed in the previous chapter.

Dragonetti et al. (2022) conducted a similar hydrological modeling process to estimate SHPs from infiltration experiments monitored using EMI. Likewise, Pinheiro et al. (2019) used SWC variation

measured by gamma-ray beam attenuation for the inverse optimization of SHPs through a similar approach. A flowchart outlining the overall modeling process for this study is presented in Figure 4.2. Additional details on Hydrus-1D simulation procedures can be found in Šimůnek et al. (2009).

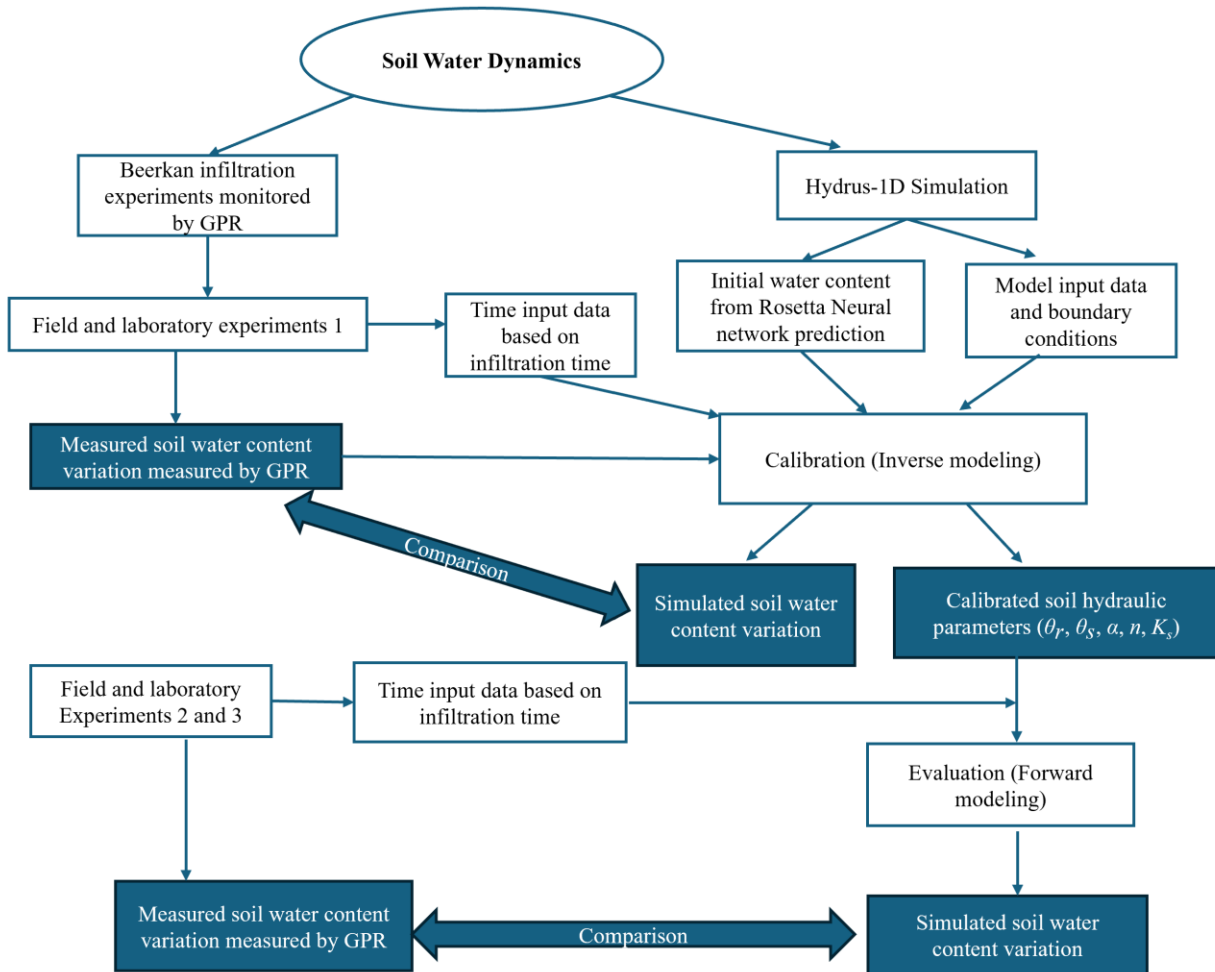


Figure 4.2. Flow chart presenting the integration of ground-penetrating radar (GPR) monitored infiltration experiment and Hydrus-1D simulation. The shaded rectangles represent key results in the workflow that are later presented and discussed in this paper.

4.2.3. Model evaluation

The M-vG parameters derived from the Hydrus-1D inversion of SWC variation, as observed in time-lapse GPR data collected during the infiltration experiments, were compared with results from HYPROP, Guelph Permeameter, and Rosetta neural network prediction for the soil type at the study site.

The simulated and observed SWC variations during calibration were evaluated graphically by plotting them against time. For validation, scatter plot with a 1:1 line was used. The agreement between simulated and observed data was further evaluated statistically using the root mean square error (RMSE) and Nash-Sutcliffe efficiency (NSE). In addition, the coefficient of determination (R^2) and Levene's test were used to assess the relationship between the two variables and compare the variances, respectively. Levene's test was specifically selected due to the non-normal distribution of most measured and simulated SWC variations. The equations for the RMSE and NSE (Nash and Sutcliffe, 1970) are defined below (Equation 4.4 and 4.5).

$$RMSE = \sqrt{\sum_{i=1}^n \frac{(P_i - O_i)^2}{n}} \quad \text{Equation 4.4}$$

$$NSE = 1 - \frac{\sum_{i=1}^n (O_i - P_i)^2}{\sum_{i=1}^n (O_i - O)^2} \quad \text{Equation 4.5}$$

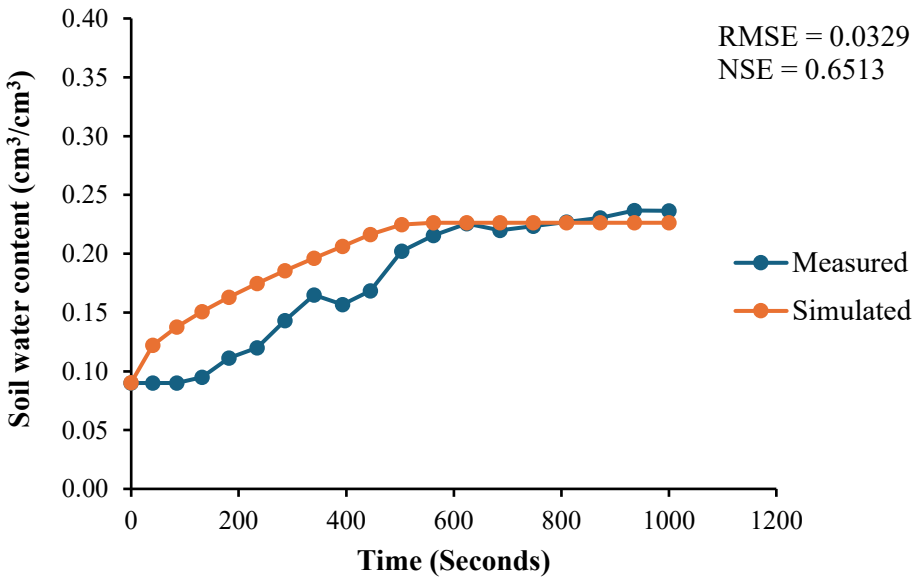
Where P_i is the predicted water content corresponding to the observed water content O_i (cm^3/cm^3), O is the mean of the observed values, and n is the number of data pairs.

4.3. Results and Discussion

4.3.1. Soil water content variation (inverse modeling for calibration)

For the field experiment calibration, Figure 4.3a compares the SWC variation measured by GPR and the simulated SWC variation derived from inverting the measured SWC variation from the first experiment. The measured and simulated SWC variation reaches a maximum level of around 0.21 - 0.23 cm^3/cm^3 . The relatively low RMSE (0.0329 cm^3/cm^3) indicates minor differences between the measured GPR-SWC variation and the simulated SWC variation data. The moderately well NSE (0.6513) suggests that the model is reasonably effective, but there is room for improvement in fully capturing the dynamics of the observed water content variation on the field.

a)



b)

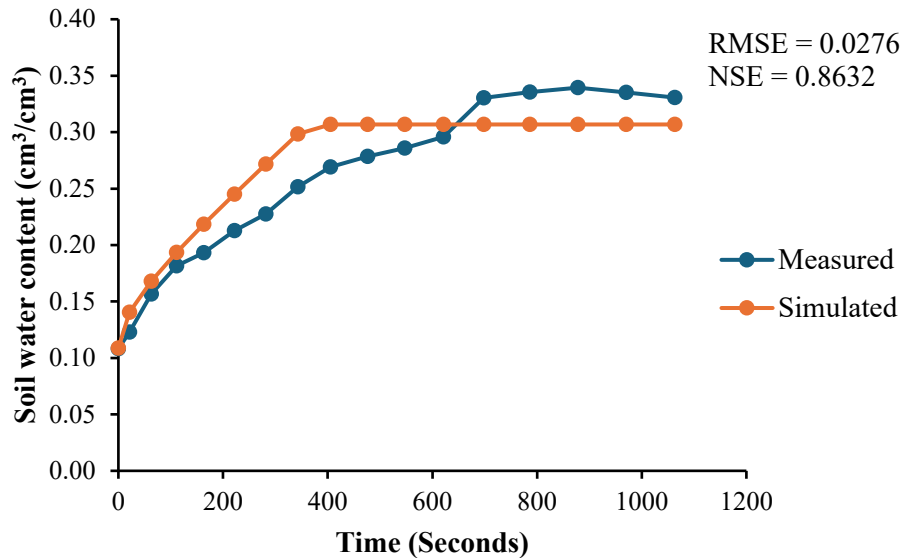


Figure 4.3. Measured and simulated soil water content (SWC) variation for the calibration using the first a) field and b) laboratory experiments versus time. RMSE - root mean square errors (cm^3/cm^3); NSE - Nash-Sutcliffe efficiency.

For the laboratory experiment, Figure 4.3b shows the measured and simulated SWC variations based on the calibration of the first experiment. Statistical analysis revealed an RMSE of $0.0276 \text{ cm}^3/\text{cm}^3$ and NSE of 0.8632 for the laboratory experiment, indicating that the Hydrus-1D inversion offers a similar and relatively more accurate representation of the water flow observed by GPR measurements under laboratory conditions compared to the field experiment. The better agreement between simulated and measured data in the laboratory experiment may be due to the more uniform flow conditions.

Additionally, in comparison to the field experiment, there was an observed increase in the maximum soil water content reached for both measured and simulated SWC in the laboratory

experiment ($0.30 - 0.33 \text{ cm}^3/\text{cm}^3$). This difference could be attributed to the varying GPR offset distances used in the two measurements (field experiment = 43 cm; laboratory experiment = 33 cm), resulting in differences in their sampling volume and the SWC variation measurement and simulation outcomes. Another factor could be the macroscopic arrangement of the solids. Field experiments often exhibit significant variability, and in this case, the Podzolic soils in the study area, known for being sandy, stony, and shallow (Sanborn et al., 2011), likely contribute to an irregular macroscopic arrangement, leading to non-uniform and preferential water flow. Such flow patterns can be caused by various forms of soil heterogeneity, including multi-porosity and multi-permeability systems (Lassabatere et al., 2019; Di Prima et al., 2022).

However, in the laboratory experiment, the soil was passed through a 4 mm sieve before being packed into the container according to its bulk density and volume. This process likely reduced macropores, increased the specific surface area, and improved pore connectivity, which may have minimized non-uniform and preferential flows, enhancing the soil's water retention capacity.

4.3.2. Inverted soil hydraulic parameters

The calibrated M-vG parameters from the inverse simulation of the field and laboratory experiment are presented in Table 4.1, alongside parameters obtained from other methods. The calibrated values are also in close range to those predicted by the Rosetta neural networks integrated within the Hydrus-1D package, based on the particle size distribution and bulk density for the tested soil. The slight increase in the calibrated values of K_s , n , and α , derived from the laboratory experiment compared to the field experiment might be due to increased SWC and more uniform wetting of the soil particles.

Table 4.1. Inverted hydraulic parameters from the field and laboratory experiments compared to other methods.

Methods	θ_r (cm ³ /cm ³)	θ_s or Max (cm ³ /cm ³)	α (cm ⁻¹)	n	K_s (cm/sec)
Field Experiment	0.04037	0.22630	0.04252	1.66660	0.00259
Laboratory Experiment	0.02500	0.30680	0.12200	1.94300	0.00647
HYPROP	0.09000	0.38500	0.05140	4.14000	-
Rosetta neural network prediction	0.04580	0.43930	0.03850	1.81600	0.00271
Guelph Permeameter					0.00469

θ_r = residual water content, θ_s or Max = saturated or maximum water content, α and n are shape parameters, K_s = saturated hydraulic conductivity.

In the laboratory experiment, the soil was closer to saturation, and this had the potential to reduce resistance to flow and lead to increased K_s . Similarly, the parameter α (inverse of air-entry value) is closely related to the soil's ability to retain water, and when soil is saturated or close to saturation, the air-entry value decreases, which causes an increase in α value. Distribution sizes influence the parameter n and can be higher with measurements under conditions with less soil compaction (Vogel et al., 2000), such as in the laboratory experiment.

When comparing these estimates with those from other studies, it is important to consider the soil texture (loamy sand) and the specific modeling conditions. For instance, in a similar study by Mangel et al. (2012), closely calibrated SHPs ($\theta_r = 0.04 \text{ cm}^3/\text{cm}^3$, $\theta_s = 0.35 \text{ cm}^3/\text{cm}^3$, $\alpha = 0.045$, $n = 2.10$, $K_s = 0.035 \text{ cm}/\text{sec}$) were obtained from Hydrus-1D inversion using data from a lab-scale infiltration experiment in a sand tank. Similarly, Leger et al. (2014) reported comparable hydraulic parameter estimates in sandy soil using the Hydrus-1D inversion procedure and the Shuffled Complex Evolution (SCE-UA) algorithm to invert M-vG parameters from GPR data acquired during a single ring infiltration experiment.

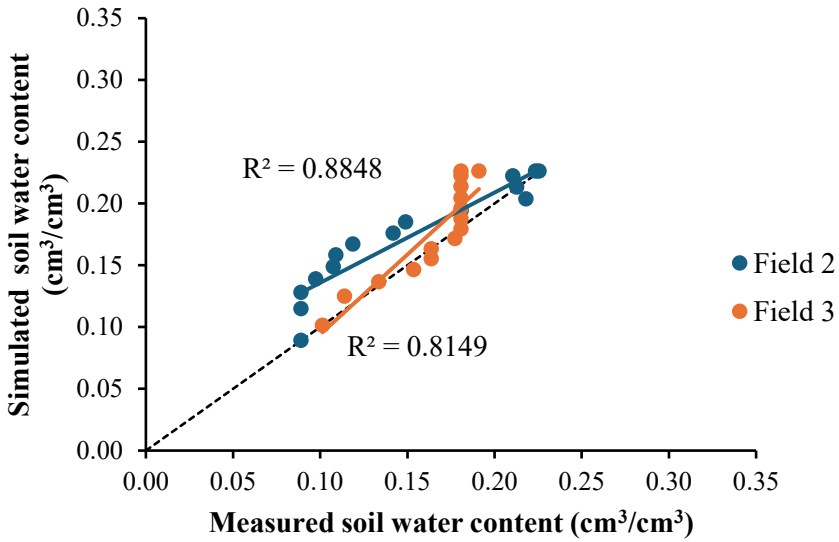
In another study comparing the performance of Hydrus-1D to simulate water movement in water-repellent soils with wettable soils, Wang et al. (2018) measured θ_r , θ_s and K_s in wettable sandy soil as $0.010 \text{ cm}^3/\text{cm}^3$, $0.390 \text{ cm}^3/\text{cm}^3$, and $0.004 \text{ cm}/\text{sec}$, respectively. Using Hydrus-1D simulation, they calibrated soil hydraulic parameters α and n as 0.080 and 1.650, respectively, for the same soil type, which are also in close agreement with the estimates estimated in this study.

A key limitation of this study is the inability to achieve saturated soil conditions due to the sandy soil's high permeability. In sandy soils, internal drainage is rapid because of the large macropores, which increases the possibility of non-uniform flow. Consequently, it was difficult to achieve saturation with the intermittent and slow rate of water application required during the Beerkan infiltration procedure. Therefore, the simulation for this study relied on the maximum soil water content observed. Although this had minimal impact on the accuracy of the water flow and SHP estimates in this study, as reflected in the consistency of the results above, enhancing GPR's capability to measure SWC variation up to saturation could potentially improve the SHP estimates derived from the simulation.

4.3.3. Soil water content variation (forward modeling for validation)

The calibrated M-vG parameters were applied to simulate soil water flow in forward modeling for two additional field and laboratory experiments. Comparisons between these simulations with GPR-derived SWC variation are shown in Figures 4.4a and 4.4b scatter plots, respectively. The scatter plots and regression analyses showed strong correlations between the simulated and measured data, with R^2 of 0.8848 and 0.8149 for Fields 2 and 3, respectively. The laboratory experiments also produced similar results with R^2 of 0.8630 and 0.8397 experiments for Labs 2 and 3, respectively, indicating the model's effectiveness. Although the initial and final SWC values closely align with the reference line, many intermediate values lie above them, indicating a slight overestimation of SWC during the Hydrus simulation. This overestimation may have resulted because the maximum SWC measured by GPR was used in place of the saturated SWC, which could have restricted the simulated water flow and introduced systematic error. In a study by Gribb et al. (2009), using maximum SWC derived from time domain reflectometry (TDR) improved the accuracy of SWC simulations from Hydrus-1D, enhancing the model's performance. Despite this improvement, minor discrepancies between simulated and actual field measurements persisted. These differences could be attributed to several factors, including measurement precision and assumptions made during the model calibration.

a)



b)

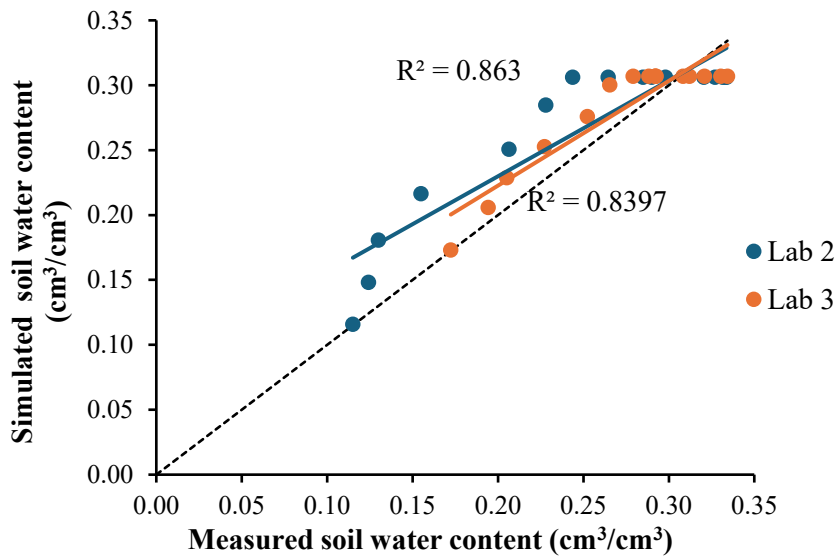


Figure 4.4. Scatter plots of simulated soil water content (SWC) variation using calibrated hydraulic parameters versus measured SWC variation from ground-penetrating radar for a) field and b) laboratory experiments. The solid lines correspond to the 1:1 line, and the dashed lines correspond to the linear regression lines.

Table 4.2 compares the RMSE and NSE values for the measured and simulated data. For both field experiments, the low RMSE values suggest good accuracy in the model's predictions (Table 2). However, while the NSE value of the second and third laboratory experiments (0.7794 and 0.8273, respectively) and the second field experiment (0.6856) indicate a good agreement between the measured and simulated data, the third field experiment had a relatively lower NSE value of 0.2955. This reduced agreement in the third field experiment's validation may be due to the lower SWC variation observed by GPR during the infiltration.

Table 4.2. RMSE and NSE values for the validation of the simulated results.

Validation	RMSE	NSE
Field		
Experiment 2	0.0299	0.6856
Experiment 3	0.0220	0.2955
Laboratory		
Experiment 2	0.0365	0.7794
Experiment 3	0.0199	0.8273

RMSE - root mean square errors (cm^3/cm^3); NSE - Nash-Sutcliffe modeling efficiency.

Furthermore, as shown in Figure 4.4a, the SWC variation for the third experiment ranged from 0.101 - 0.191 cm^3/cm^3 , whereas the first and second field experiments had wider ranges. This

outcome underscores the importance of accurate and reliable GPR-SWC variations for robust and efficient simulation. Validation using the laboratory experiments yielded relatively low RMSEs and high NSE values (Table 4.2), suggesting that the model effectively captured variability. The laboratory experiments had wider SWC ranges and recorded more uniform flow simulations, which may have contributed to improved efficiency compared to the field simulation.

Despite this, Levene's test results for homogeneity of variances revealed no significant differences between the simulated and measured data, with p-values of 0.160, 0.119, 0.218, and 0.395 for field experiments 2 and 3 and laboratory experiments 2 and 3, respectively.

Another notable observation is the improved water flow simulation, which shows better variation and more accurate steady-state conditions compared to the GPR-observed data. This improvement in the simulated results could be valuable for determining parameters like infiltration rates or constant flux in steady-state conditions.

Given the improvements observed in simulated water flow from calibrated hydraulic parameters using GPR data, there is potential for non-invasive mapping of SHPs on a watershed scale. This could be achieved by integrating GPR and Hydrus-1D models with large-scale hydrological models, such as SWAT (Soil and Water Assessment Tool), to predict regional soil water movement. This approach could also be extended to predict contaminant transport by incorporating additional data on contaminant characteristics.

4.4. Conclusions

In this study, soil water content (SWC) variations, estimated from time-lapse ground-penetrating radar direct ground wave (GPR-DGW) data, were coupled with the Hydrus-1D model to invert

Mualem-van Genuchten (M-vG) parameters and validate water flow dynamics. The results demonstrated that reliable M-vG parameters could be obtained through Hydrus-1D inverse modeling using SWC variations monitored by GPR-DGW. In addition, the inverted M-vG parameters were useful in simulating water flow dynamics, closely matching the measured values.

The combination of GPR and Hydrus-1D for monitoring soil water dynamics and estimating soil hydraulic parameters (SHPs) offers several benefits, including rapid, low-cost, and non-destructive data collection, the ability to improve variation analysis from time-lapse GPR data, and the potential for large-scale SHP characterization. However, the accuracy of estimates from this approach depends largely on the reliability of the GPR data collected and processed, as well as the effectiveness of the simulation model.

Future research under similar coarse-textured soil types could explore the use of dual-porosity models, which allow for improved water flow simulation, especially under field conditions, by accounting for macropores and preferential flow paths. Additionally, advanced GPR data processing techniques such as full waveform inversion could enhance the accuracy of soil water content variation estimates. Further, employing Hydrus 2D/3D simulation models could improve the simulation of the soil water dynamics and enable better visualizations of flow paths.

In conclusion, this study found that GPR-DGW can provide valuable insights into soil water dynamics that can be integrated into hydrological models for SHPs estimation, and this study represents a significant step in that direction.

4.5. Acknowledgments

This paper is based upon work supported by the Natural Sciences and Engineering Research Council of Canada, Discovery Grant (NSERC-DG: RGPIN-2019-04614), Industry, Energy and Innovation of the Government of Newfoundland and Labrador, IET Grant: 5404-1962-102, and the School of Graduate Studies, Memorial University of Newfoundland (MUN). The authors thank the Department of Fisheries, Forestry, and Agriculture, Government of Newfoundland and Labrador, for the provision and clearing of the research field, and members of the Soil Hydrology and Agrophysics research group, Grenfell Campus-Memorial University of Newfoundland, for their valuable suggestions and feedback that helped improve the manuscript.

4.6. References

- Binley, A., Hubbard, S.S., Huisman, J.A., Revil, A., Robinson, D.A., Singha, K., Slater, L.D., 2015. The emergence of hydrogeophysics for improved understanding of subsurface processes over multiple scales. *Water Resources Research* 51(6), 3837-3866.
- Dane, J.H., Topp, C.G. (Eds.), 2020. *Methods of Soil Analysis, Part 4: Physical Methods, Vol. 20*. John Wiley & Sons, New York.
- Di Prima, S., Giannini, V., Roder, L.R., Giadrossich, F., Lassabatere, L., Stewart, R.D., Abou Najm, M.R., Longo, V., Campus, S., Winiarski, T., Angulo-Jaramillo, R., 2022. Coupling time-lapse ground penetrating radar surveys and infiltration experiments to characterize two types of non-uniform flow. *Science of The Total Environment* 806, 150410.
- Dragonetti, G., Farzamian, M., Coppola, A., Basile, A., Monteiro Santos, F., 2022. In-situ estimation of soil hydraulic and hydrodispersive properties by inversion of Electromagnetic Induction measurements and soil hydrological modeling. *Hydrology and Earth System Sciences Discussions* 1-38.
- Galagedara, L.W., Parkin, G.W., Redman, J.D., 2003a. An analysis of the ground-penetrating radar direct ground wave method for soil water content measurement. *Hydrological Processes* 17(18), 3615-3628.
- Galagedara, L.W., Parkin, G.W., Redman, J.D., Endres, A.L., 2003b. Assessment of soil moisture content measured by borehole GPR and TDR under transient irrigation and drainage. *Journal of Environmental & Engineering Geophysics* 8(2), 77-86.
- Galagedara, L.W., Parkin, G.W., Redman, J.D., Von Bertoldi, P., Endres, A.L., 2005a. Field studies of the GPR ground wave method for estimating soil water content during irrigation and drainage. *Journal of Hydrology* 301(1-4), 182-197.

- Gribb, M.M., Forkutsa, I., Hansen, A., Chandler, D.G., McNamara, J.P., 2009. The effect of various soil hydraulic property estimates on soil moisture simulations. *Vadose Zone Journal* 8(2), 321-331.
- Grote, K., Anger, C., Kelly, B., Hubbard, S., Rubin, Y., 2010b. Characterization of soil water content variability and soil texture using GPR groundwave techniques. *Journal of Environmental & Engineering Geophysics* 15(3), 93-110.
- Huisman, J.A., Sperl, C., Bouten, W., Verstraten, J.M., 2001. Soil water content measurements at different scales: accuracy of time domain reflectometry and ground-penetrating radar. *Journal of Hydrology* 245(1-4), 48-58.
- Huisman, J.A., Snepvangers, J.J.J.C., Bouten, W., Heuvelink, G.B.M., 2002. Mapping spatial variation in surface soil water content: comparison of ground-penetrating radar and time domain reflectometry. *Journal of Hydrology* 269(3-4), 194-207.
- Huisman, J.A., Hubbard, S.S., Redman, J.D., Annan, A.P., 2003. Measuring soil water content with ground penetrating radar: A review. *Vadose Zone Journal* 2(4), 476-491.
- Iqbal, M., Kamal, M.R., Che Man, H., Wayayok, A., 2020. HYDRUS-1D simulation of soil water dynamics for sweet corn under tropical rainfed condition. *Applied Sciences* 10(4), 1219.
- Jadoon, K.Z., Weihermüller, L., Scharnagl, B., Kowalsky, M.B., Bechtold, M., Hubbard, S.S., Vereecken, H., Lambot, S., 2012. Estimation of soil hydraulic parameters in the field by integrated hydrogeophysical inversion of time-lapse ground-penetrating radar data. *Vadose Zone Journal* 11(4), vzt2011-0177.
- Kishné, A.S., Yimam, Y.T., Morgan, C.L., Dornblaser, B.C., 2017. Evaluation and improvement of the default soil hydraulic parameters for the Noah Land Surface Model. *Geoderma* 285, 247-259.

- Klotzsche, A., Jonard, F., Looms, M.C., van der Kruk, J., Huisman, J.A., 2018. Measuring soil water content with ground penetrating radar: A decade of progress. *Vadose Zone Journal* 17(1), 1-9.
- Kosugi, K.I., Hopmans, J.W., Dane, J.H., 2002. Parametric Models. In: Dane, J.H., Topp, C.G. (Eds.), *Methods of Soil Analysis: Part 4 Physical Methods*, 5. Soil Science Society of America, Madison, pp. 739-757.
- Kowalsky, M.B., Finsterle, S., Peterson, J., Hubbard, S., Rubin, Y., Majer, E., Ward, A., Gee, G., 2005. Estimation of field-scale soil hydraulic and dielectric parameters through joint inversion of GPR and hydrological data. *Water Resources Research* 41(11), W11424.
- Lassabatère, L., Angulo-Jaramillo, R., Soria Ugalde, J.M., Cuenca, R., Braud, I., Haverkamp, R., 2006. Beerkan estimation of soil transfer parameters through infiltration experiments—BEST. *Soil Science Society of America Journal* 70(2), 521-532.
- Lassabatère, L., Di Prima, S., Bouarafa, S., Iovino, M., Bagarello, V., Angulo-Jaramillo, R., 2019. BEST-2K method for characterizing dual-permeability unsaturated soils with ponded and tension infiltrometers. *Vadose Zone Journal* 18(1), 1-20.
- Léger, E., Saintenoy, A., Coquet, Y., 2014. Hydrodynamic parameters of a sandy soil determined by ground-penetrating radar inside a single ring infiltrometer. *Water Resources Research* 50(7), 5459-5474.
- Lu, J., Zhang, Q., Werner, A.D., Li, Y., Jiang, S., Tan, Z., 2020. Root-induced changes of soil hydraulic properties—A review. *Journal of Hydrology* 589, 125203.
- Mangel, A.R., Moysey, S.M.J., Ryan, J.C., Tarbutton, J.A., 2012. Multi-offset ground-penetrating radar imaging of a lab-scale infiltration test. *Hydrology and Earth System Sciences* 16(11), 4009-4022.

- Minasny, B., McBratney, A.B., 2007. Estimating the water retention shape parameter from sand and clay content. *Soil Science Society of America Journal* 71(4), 1105-1110.
- Moysey, S.M., 2010. Hydrologic trajectories in transient ground-penetrating-radar reflection data. *Geophysics* 75(4), WA211-WA219.
- Mualem, Y., 1976. A new model for predicting the hydraulic conductivity of unsaturated porous media. *Water Resources Research* 12(3), 513-522.
- Nash, J.E., Sutcliffe, J.V., 1970. River flow forecasting through conceptual models part I—A discussion of principles. *Journal of Hydrology* 10(3), 282-290.
- Pathirana, S., Lambot, S., Krishnapillai, M., Smeaton, C., Cheema, M., Galagedara, L., 2024. Potential of ground-penetrating radar to calibrate electromagnetic induction for shallow soil water content estimation. *Journal of Hydrology* 633, 130957.
- Pinheiro, E.A.R., van Lier, Q.D.J., Inforsato, L., Šimůnek, J., 2019. Measuring full-range soil hydraulic properties for the prediction of crop water availability using gamma-ray attenuation and inverse modeling. *Agricultural Water Management* 216, 294-305.
- Radcliffe, D.E., Šimůnek, J., 2018. *Soil Physics with HYDRUS: Modeling and Applications*. CRC Press, Boca Raton.
- Ramos, T.B., Liu, M., Paredes, P., Shi, H., Feng, Z., Lei, H., Pereira, L.S., 2023. Salts dynamics in maize irrigation in the Hetao plateau using static water table lysimeters and HYDRUS-1D with a focus on autumn leaching irrigation. *Agricultural Water Management* 283, 108306.
- Reynolds, W.D., Carter, M., Gregorich, E., 2008. Saturated hydraulic properties: Well permeameter. In: Carter, M.R., Gregorich, E.G. (Eds.), *Soil Sampling and Methods of Analysis*, CRC Press, Boca Raton, pp. 1025-1042.

- Rezaei, M., Saey, T., Seuntjens, P., Joris, I., Boëne, W., Van Meirvenne, M., Cornelis, W., 2016. Predicting saturated hydraulic conductivity in a sandy grassland using proximally sensed apparent electrical conductivity. *Journal of Applied Geophysics* 126, 35-41.
- Richards, L.A., 1941. A pressure-membrane extraction apparatus for soil solution. *Soil Science* 51(5), 377-386.
- Sanborn, P., Lamontagne, L., Hendershot, W., 2011. Podzolic soils of Canada: Genesis, distribution, and classification. *Canadian Journal of Soil Science* 91(5), 843-880.
- Schaap, M.G., Leij, F.J., van Genuchten, M.T., 2001. Rosetta: A computer program for estimating soil hydraulic parameters with hierarchical pedotransfer functions. *Journal of Hydrology* 251(3-4), 163-176.
- Schaap, M.G., van Genuchten, M.T., 2006. A modified Mualem–van Genuchten formulation for improved description of the hydraulic conductivity near saturation. *Vadose Zone Journal* 5(1), 27-34.
- Schindler, U., Durner, W., von Unold, G., Müller, L., 2010. Evaporation method for measuring unsaturated hydraulic properties of soils: Extending the measurement range. *Soil Science Society of America Journal* 74(4), 1071-1083.
- Šimůnek, J., van Genuchten, M.T., Šejna, M., 2009. The HYDRUS-1D software package for simulating the one-dimensional movement of water, heat, and multiple solutes in variably-saturated media. *University of California-Riverside Research Reports*, 3, 1-270.
- Šimůnek, J., van Genuchten, M.T., Šejna, M., 2008. Development and applications of the HYDRUS and STANMOD software packages and related codes. *Vadose Zone Journal* 7(2), 587-600.

- Šimůnek, J., van Genuchten, M.T., Šejna, M., 2016. Recent developments and applications of the HYDRUS computer software packages. *Vadose Zone Journal* 15(7), vzj2016-04.
- Soil Classification Working Group, 1998. *The Canadian System of Soil Classification*, 3rd ed. Agriculture and Agri-Food Canada, Ottawa.
- Steelman, C.M., Endres, A.L., 2011. Comparison of petrophysical relationships for soil moisture estimation using GPR ground waves. *Vadose Zone Journal* 10(1), 270-285.
- Topp, G.C., Davis, J.L., Annan, A.P., 1980. Electromagnetic determination of soil water content: Measurements in coaxial transmission lines. *Water Resources Research* 16(3), 574-582.
- van Genuchten, M.T., 1980. A closed-form equation for predicting the hydraulic conductivity of unsaturated soils. *Soil Science Society of America Journal* 44(5), 892-898.
- Verbist, K.M.J., Cornelis, W.M., Torfs, S., Gabriels, D., 2013. Comparing methods to determine hydraulic conductivities on stony soils. *Soil Science Society of America Journal* 77(1), 25-42.
- Vereecken, H., Huisman, J.A., Pachepsky, Y., Montzka, C., van der Kruk, J., Bogaen, H., Weihermüller, L., Herbst, M., Martinez, G., Vanderborght, J., 2014. On the spatio-temporal dynamics of soil moisture at the field scale. *Journal of Hydrology* 516, 76-96.
- Vogel, T., van Genuchten, M.T., Cislérova, M., 2000. Effect of the shape of the soil hydraulic functions near saturation on variably-saturated flow predictions. *Advances in Water Resources* 24(2), 133-144.
- Weihermüller, L., Huisman, J.A., Lambot, S., Herbst, M., Vereecken, H., 2007. Mapping the spatial variation of soil water content at the field scale with different ground penetrating radar techniques. *Journal of Hydrology* 340(3-4), 205-216.

- Wijewardana, Y.G.N.S., Galagedara, L.W., 2010. Estimation of spatio-temporal variability of soil water content in agricultural fields with ground penetrating radar. *Journal of Hydrology* 391(1-2), 24-33.
- Yu, Y., Huisman, J.A., Klotzsche, A., Vereecken, H., Weihermüller, L., 2022. Coupled full-waveform inversion of horizontal borehole ground penetrating radar data to estimate soil hydraulic parameters: A synthetic study. *Journal of Hydrology* 610, 127817.
- Zajícová, K., Chuman, T., 2019. Application of ground penetrating radar methods in soil studies: A review. *Geoderma* 343, 116-129.
- Zhang, M., Feng, X., Bano, M., Xing, H., Wang, T., Liang, W., Zhou, H., Dong, Z., An, Y., Zhang, Y., 2022. Review of ground penetrating radar applications for water dynamics studies in unsaturated zone. *Remote Sensing* 14(23), 5993.
- Zou, C., Zhang, S., Jiang, X., Chen, F., 2023. Monitoring and characterization of water infiltration in soil unsaturated zone through an integrated geophysical approach. *Catena* 230, 107243.

CHAPTER FIVE

5.1. General Discussion and Conclusions

This research proposes an innovative approach for estimating SHPs in podzolic soils by combining hydrological models with SWC variations derived from time-lapse GPR-DGW measurements during Beerkan infiltration experiments. For this purpose, two main objectives were set:

1. Evaluate the potential of estimating soil water content (SWC) variation using GPR-DGW and predicting field-saturated hydraulic conductivity (K_{fs}) by integrating the estimated SWC variation into the GA model.
2. Investigate the potential of obtaining Mualem-van Genuchten (M-vG) parameters and simulating soil water dynamics in podzolic soils using the Hydrus-1D model and GPR-DGW data.

Each objective was explored in two studies, detailed in Chapters 3 (Study One) and 4 (Study Two) of this thesis.

The first objective had two parts. The first part explored the potential of GPR-DGW to capture SWC variation during a limited-duration infiltration experiment conducted in the field. On this, the study concluded that GPR-DGW can effectively provide reliable information on SWC variation during a limited-duration infiltration process, like the Beerkan infiltration experiment, and these variations are consistent and comparable at different locations on the field. The second part of Study One focused on estimating field saturated hydraulic conductivity (K_{fs}) by using the SWC variation estimated from GPR time-lapse data in the GA model and assessing the accuracy of the estimates. Findings from this study revealed that plausible K_{fs} estimates can be obtained by applying SWC changes from GPR in the GA model. Further, the K_{fs} obtained were comparable in

magnitude to those obtained from applying SWC changes from installed soil moisture probes (SMPs) to the same model, theoretical values for the same soil type, and the BEST methods (Intercept and Steady). Overall, the study concludes that since this approach provided estimates that fall within the expected range for the soil type, its utilization for large-scale mapping of SHPs non-destructively is feasible and can be considered in relation to estimates from the same approach.

Similarly, the second objective consists of two parts. The first part was to obtain M-vG parameters from the Hydrus-1D model through the inverse modeling of SWC variation from GPR-DGW, utilizing experiments conducted under field and laboratory conditions. Findings from this part revealed that reliable M-vG parameters can be obtained by integrating SWC-variation from GPR-DGW in the Hydrus-1D inverse modeling. The inverted hydraulic parameters obtained were close to the Rosetta neural network prediction for soil type and estimates from conventional methods. The second part of the chapter included the validation and evaluation of the potential Hydrus-1D model for simulating soil water movement based on the time lapse GPR-DGW data. The findings of this study revealed a higher correlation between measured and simulated variation in SWC. Two noteworthy observations emerged: first, the maximum SWC variations observed under the laboratory conditions were consistently higher than those observed and simulated in the field. Second, there was a better agreement between measured and simulated SWC variations in the laboratory, indicated by lower root mean square errors and higher Nash-Sutcliffe efficiency values. These observations are likely due to reduced wetting coverage distance and indicate reduced macropores and more uniform flow obtainable under laboratory conditions. Overall, this study concluded that GPR-DGW information can be integrated with Hydrus-1D for site-specific calibration of the M-vG parameters and to improve simulation dynamics.

5.2. Limitations of this Study

This research utilizes the Beerkan method to evaluate the effectiveness and consistency of GPR-DGW under short-term duration, equal-volume infiltration experiments. This procedure involves minor disturbances, such as the insertion of a ring to a depth of 1 cm. Although minimal, such disturbances can still affect the infiltration process and, consequently, the SHPs.

The Beerkan method measures infiltration and SHPs on a small scale, which may not accurately represent field-scale or watershed-scale processes. Furthermore, the dependence of the method on simplified assumptions, such as homogenous soil profile and negligible lateral flow, introduces some uncertainties to its reliability under field conditions.

Further, although it could be argued that the higher cost of acquiring and using GPR for SHP estimation, compared to a simple method like the Beerkan method, is a limitation of this approach, such an argument would be overlooking the long-term advantages of the GPR approach. With GPR, there is a potential for fast and non-invasive mapping of SHPs on a watershed scale, especially when off-ground GPR techniques are combined with larger hydrological models like the Soil and Water Assessment Tool.

Overall, the findings from these studies demonstrate a significant and promising step toward utilizing time-lapse GPR direct ground wave information for large-scale and non-invasive estimation of (SHPs), which can be useful in reliable soil water management, especially for regions with unfavorable soil conditions like Newfoundland and Labrador. Nonetheless, there are still opportunities for further improvement and advancement of this work.

5.3. Recommendations

Based on the findings and limitations of this study, the following recommendations are suggested:

1. Further studies should be conducted to explore the effectiveness of this approach under different infiltration experiments, particularly those that can lead to increased wetting distance and sampling volume covered by GPR and prevent any form of disturbance.
2. This study was conducted in sandy podzolic soil. Further studies exploring this approach under different soil types and conditions are needed.
3. Since this study found an improvement under laboratory conditions, an investigation exploring this approach under improved soil conditions (i.e., sites with amendments compared with control) can be useful in evaluating its relevance to soil management.
4. This study focuses on the use of GPR-DGW. Further studies can explore this approach using different GPR data processing techniques, such as Full-waveform inversion (FWI), to enhance the accuracy of SHP estimations.
5. The use of 2 or 3-D simulation models, such as Hydrus 2D/3D, in future studies could improve the simulation of the soil water dynamics and enable visualizations of flow paths.
6. A continuous iteration of similar approaches under laboratory and field conditions is strongly suggested for improvement under uniform and non-uniform conditions.
7. Future research endeavors could explore combining GPR information and other geophysical techniques to derive parameters other than SWC variations for utilization in hydrological models for SHP estimations.

References and Bibliography

- Akinsunmade, A., 2021. GPR imaging of traffic compaction effects on soil structures. *Acta Geophysica* 69(2), 643–653. <https://doi.org/10.1007/s11600-020-00530-0>.
- Alagna, V., Bagarello, V., Di Prima, S., Guaitoli, F., Iovino, M., Keesstra, S., Cerdà, A., 2019. Using Beerkan experiments to estimate hydraulic conductivity of a crusted loamy soil in a Mediterranean vineyard. *Journal of Hydrology and Hydromechanics* 67(2), 191–200. <https://doi.org/10.2478/johh-2018-0023>.
- Albalasmeh, A., Mohawesh, O., Gharaibeh, M., Deb, S., Slaughter, L., El Hanandeh, A., 2022. Artificial neural network optimization to predict saturated hydraulic conductivity in arid and semi-arid regions. *CATENA* 217, 106459. <https://doi.org/10.1016/j.catena.2022.106459>.
- Ali, M.H., Islam, A.K.M.R., Zaman, M.H., 2014. Improving soil hydraulic properties for better agricultural water management and crop production – A review. *International Journal of Engineering and Technical Research* 2, 30–34.
- Allred, B., 2008. *Handbook of agricultural geophysics (Books in soils, plants, and the environment)*. CRC Press, Boca Raton.
- Allred, B.J., Freeland, R.S., Farahani, H.J., Collins, M.E., 2010. Agricultural geophysics: Past, present, and future. *Symposium on the Application of Geophysics to Engineering and Environmental Problems* 23, 190–202. <https://doi.org/10.4133/1.3445432>.
- Allroggen, N., Tronicke, J., 2015. Analysis of time-lapse GPR data to visualize preferential flow paths. *8th International Workshop on Advanced Ground Penetrating Radar (IWAGPR)*, 1–3. <https://doi.org/10.1109/IWAGPR.2015.7292627>.

- Angulo-Jaramillo, R., Bagarello, V., Di Prima, S., Gosset, A., Iovino, M., Lassabatere, L., 2019. Beerkan Estimation of Soil Transfer parameters (BEST) across soils and scales. *Journal of Hydrology* 576, 239–261. <https://doi.org/10.1016/j.jhydrol.2019.06.007>.
- Badewa, E., Unc, A., Cheema, M., Kavanagh, V., Galagedara, L., 2018. Soil moisture mapping using multi-frequency and multi-coil electromagnetic induction sensors on managed podzols. *Agronomy* 8(10), Article 10. <https://doi.org/10.3390/agronomy8100224>.
- Bagarello, V., Di Prima, S., Iovino, M., 2014. Comparing alternative algorithms to analyze the beerkan infiltration experiment. *Soil Science Society of America Journal* 78(3), 724–736. <https://doi.org/10.2136/sssaj2013.06.0231>.
- Baiamonte, G., 2019. SCS curve number and Green-Ampt infiltration models. *Journal of Hydrologic Engineering* 24(10), 04019034. [https://doi.org/10.1061/\(ASCE\)HE.1943-5584.0001838](https://doi.org/10.1061/(ASCE)HE.1943-5584.0001838).
- Binley, A., Winship, P., Middleton, R., Pokar, M., West, J., 2001. High-resolution characterization of vadose zone dynamics using cross-borehole radar. *Water Resources Research* 37(11), 2639–2652. <https://doi.org/10.1029/2000WR000089>.
- Binley, A., Beven, K., 2003. Vadose zone flow model uncertainty as conditioned on geophysical data. *Groundwater* 41(2), 119-127.
- Binley, A., Hubbard, S.S., Huisman, J.A., Revil, A., Robinson, D.A., Singha, K., Slater, L.D., 2015. The emergence of hydrogeophysics for improved understanding of subsurface processes over multiple scales. *Water Resources Research* 51(6), 3837–3866. <https://doi.org/10.1002/2015WR017016>.

- Birchak, J.R., Gardner, C.G., Hipp, J.E., Victor, J.M., 1974. High dielectric constant microwave probes for sensing soil moisture. *Proceedings of the Institute of Electrical and Electronics Engineers* 62(1), 93-98.
- Bitella, G., Rossi, R., Loperte, A., Satriani, A., Lapenna, V., Perniola, M., Amato, M., 2015. Geophysical techniques for plant, soil, and root research related to sustainability. In: *The sustainability of agro-food and natural resource systems in the Mediterranean Basin*, Springer International Publishing, pp. 353-372.
- Brooks, R.H., Corey, C.T., 1964. Hydraulic properties of porous media. *Hydrology Paper 3*. Colorado State University, Fort Collins.
- Burdine, N., 1953. Relative permeability calculations from pore size distribution data. *Journal of Petroleum Technology* 5(03), 71-78.
- Busch, S., Weihermüller, L., Huisman, J.A., Steelman, C.M., Endres, A.L., Vereecken, H., van der Kruk, J., 2013. Coupled hydrogeophysical inversion of time-lapse surface GPR data to estimate hydraulic properties of a layered subsurface. *Water Resources Research* 49(12), 8480–8494. <https://doi.org/10.1002/2013WR013992>.
- Busch, S., van der Kruk, J., Vereecken, H., 2014. Improved characterization of fine-texture soils using on-ground GPR full-waveform inversion. *IEEE Transactions on Geoscience and Remote Sensing* 52(7), 3947–3958. <https://doi.org/10.1109/TGRS.2013.2278297>.
- Cao, Q., Song, X., Wu, H., Gao, L., Liu, F., Yang, S., Zhang, G., 2020. Mapping the response of volumetric soil water content to an intense rainfall event at the field scale using GPR. *Journal of Hydrology* 583, 124605. <https://doi.org/10.1016/j.jhydrol.2020.124605>.

- Castellini, M., Di Prima, S., Moret-Fernández, D., Lassabatere, L., 2021. Rapid and accurate measurement methods for determining soil hydraulic properties: A review. *Journal of Hydrology and Hydromechanics* 69(2), 121–139. <https://doi.org/10.2478/johh-2021-0002>.
- Chanzy, A., Tarussov, A., Bonn, F., Judge, A., 1996. Soil water content determination using a digital ground-penetrating radar. *Soil Science Society of America Journal* 60(5), 1318–1326. <https://doi.org/10.2136/sssaj1996.03615995006000050005x>.
- Chow, V.T., Maidment, D.R., Mays, L.W., 1988. *Applied Hydrology*. McGraw-Hill Series in Water Resources and Environmental Engineering.
- Corwin, D.L., Lesch, S.M., 2003. Application of soil electrical conductivity to precision agriculture: Theory, principles, and guidelines. *Agronomy Journal* 95(3), 455–471. <https://doi.org/10.2134/agronj2003.4550>.
- Cui, F., Bao, J., Cao, Z., Li, L., Zheng, Q., 2020. Soil hydraulic parameters estimation using ground penetrating radar data via ensemble smoother with multiple data assimilation. *Journal of Hydrology* 583, 124552. <https://doi.org/10.1016/j.jhydrol.2020.124552>.
- Curtis, J.O., 2001. Moisture effects on the dielectric properties of soils. *IEEE Transactions on Geoscience and Remote Sensing* 39(1), 125-128.
- Dagenbach, A., Buchner, J.S., Klenk, P., Roth, K., 2013. Identifying a parameterisation of the soil water retention curve from on-ground GPR measurements. *Hydrology and Earth System Sciences* 17(2), 611–618. <https://doi.org/10.5194/hess-17-611-2013>.
- Dahunsi, J., Pathirana, S., Cheema, M., Krishnapillai, M., Galagedara, L., 2023. Advances in Ground Penetrating Radar application for estimating soil hydraulic properties: A mini-review. *Canadian Biosystems Engineering/Le génie des biosystèmes au Canada* 65, 1.17–1.27. <https://doi.org/10.7451/CBE.2023.65.1.17>.

- Dane, J.H., Topp, C.G. (Eds.), 2020. *Methods of Soil Analysis, Part 4: Physical Methods*, Vol. 20. John Wiley & Sons, New York.
- de Andrade Bonetti, J., Anghinoni, I., de Moraes, M.T., Fink, J.R., 2017. Resilience of soils with different texture, mineralogy and organic matter under long-term conservation systems. *Soil and Tillage Research* 174, 104–112. <https://doi.org/10.1016/j.still.2017.06.008>.
- Di Prima, S., Giannini, V., Ribeiro Roder, L., Giadrossich, F., Lassabatere, L., Stewart, R.D., Abou Najm, M.R., Longo, V., Campus, S., Winiarski, T., Angulo-Jaramillo, R., Del Campo, A., Capello, G., Biddoccu, M., Roggero, P.P., Pirastru, M., 2022. Coupling time-lapse ground penetrating radar surveys and infiltration experiments to characterize two types of non-uniform flow. *Science of The Total Environment* 806, 150410. <https://doi.org/10.1016/j.scitotenv.2021.150410>.
- Di Prima, S., Winiarski, T., Angulo-Jaramillo, R., Stewart, R.D., Castellini, M., Abou Najm, M.R., Ventrella, D., Pirastru, M., Giadrossich, F., Capello, G., Biddoccu, M., Lassabatere, L., 2020. Detecting infiltrated water and preferential flow pathways through time-lapse ground-penetrating radar surveys. *Science of The Total Environment* 726, 138511. <https://doi.org/10.1016/j.scitotenv.2020.138511>.
- Dojack, L., 2012. *Ground penetrating radar theory, data collection, processing, and interpretation: A guide for archaeologists*. University of British Columbia. <https://doi.org/10.14288/1.0086065>.
- Doolittle, J.A., Brevik, E.C., 2014. The use of electromagnetic induction techniques in soils studies. *Geoderma* 223, 33–45. <https://doi.org/10.1016/j.geoderma.2014.01.027>.
- Dragonetti, G., Farzamian, M., Coppola, A., Basile, A., Monteiro Santos, F., 2022. In-situ estimation of soil hydraulic and hydrodispersive properties by inversion of Electromagnetic

Induction measurements and soil hydrological modeling. *Hydrology and Earth System Sciences Discussions* 1-38

Fattahi Nafchi, R., Valiyari-Eskandari, M., Raeisi Vanani, H., Ostad-Ali-Askari, K., Bahrami, A., 2023. Evaluation of wetting front detector to estimate the dimensions of wetting front in the drip irrigation. *Journal of Engineering and Applied Science* 70(1), 126 <https://doi.org/10.1186/s44147-023-00295-5>.

Feki, M., Ravazzani, G., Barontini, S., Ceppi, A., Mancini, M., 2020. A comparative assessment of the estimates of the saturated hydraulic conductivity of two anthropogenic soils and their impact on hydrological model simulations. *Soil and Water Research* 15(3), 135–147. <https://doi.org/10.17221/33/2019-SWR>.

Fernández-Gálvez, J., Pollacco, J.A.P., Lassabatere, L., Angulo-Jaramillo, R., Carrick, S., 2019. A general Beerkan Estimation of Soil Transfer parameters method predicting hydraulic parameters of any unimodal water retention and hydraulic conductivity curves: Application to the Kosugi soil hydraulic model without using particle size distribution data. *Advances in Water Resources* 129, 118–130. <https://doi.org/10.1016/j.advwatres.2019.05.005>.

Fu, Z., Hu, W., Beare, M., Thomas, S., Carrick, S., Dando, J., Langer, S., Müller, K., Baird, D., Lilburne, L., 2021. Land use effects on soil hydraulic properties and the contribution of soil organic carbon. *Journal of Hydrology* 602, 126741. <https://doi.org/10.1016/j.jhydrol.2021.126741>.

Galagedara, L.W., Parkin, G.W., Redman, J.D., 2003a. An analysis of the ground-penetrating radar direct ground wave method for soil water content measurement. *Hydrological Processes* 17(18), 3615–3628. <https://doi.org/10.1002/hyp.1351>.

- Galagedara, L.W., Parkin, G.W., Redman, J.D., Endres, A.L., 2003b. Assessment of soil moisture content measured by borehole GPR and TDR under transient irrigation and drainage. *Journal of Environmental and Engineering Geophysics* 8(2), 77–86. <https://doi.org/10.4133/JEEG8.2.77>.
- Galagedara, L.W., Parkin, G.W., Redman, J.D., von Bertoldi, P., Endres, A.L., 2005. Field studies of the GPR ground wave method for estimating soil water content during irrigation and drainage. *Journal of Hydrology* 301(1), 182–197. <https://doi.org/10.1016/j.jhydrol.2004.06.031>.
- Galagedara, L.W., Redman, J.D., Parkin, G.W., Annan, A.P., Endres, A.L., 2005b. Numerical modeling of GPR to determine the direct ground wave sampling depth. *Vadose Zone Journal* 4(4), 1096–1106.
- Ghosh, B., Pekkat, S., 2019. A critical evaluation of the variability induced by different mathematical equations on hydraulic conductivity determination using disc infiltrometer. *Acta Geophysica* 67, 863–877. <https://doi.org/10.1007/s11600-019-00266-6>.
- Green, W. H., Ampt, G. A., 1911. Studies on soil physics. *The Journal of Agricultural Sciences*, 4(1), 1-24. <https://doi.org/10.1017/S0021859600001441>.
- Gribb, M.M., Forkutsa, I., Hansen, A., Chandler, D.G., McNamara, J.P., 2009. The effect of various soil hydraulic property estimates on soil moisture simulations. *Vadose Zone Journal* 8(2), 321–331. <https://doi.org/10.2136/vzj2008.0088>.
- Grote, K., Crist, T., Nickel, C., 2010a. Experimental estimation of the GPR groundwave sampling depth. *Water Resources Research* 46(10). <https://doi.org/10.1029/2009WR008403>.

- Grote, K., Anger, C., Kelly, B., Hubbard, S., Rubin, Y., 2010b. Characterization of soil water content variability and soil texture using GPR groundwave techniques. *Journal of Environmental & Engineering Geophysics* 15(3), 93-110.
- Hamidov, A., Helming, K., Bellocchi, G., Bojar, W., Dalgaard, T., Ghaley, B.B., Hoffmann, C., Holman, I., Holzkämper, A., Krzeminska, D., Kværnø, S.H., Lehtonen, H., Niedrist, G., Øygarden, L., Reidsma, P., Roggero, P.P., Rusu, T., Santos, C., Seddaiu, G., Schönhart, M., 2018. Impacts of climate change adaptation options on soil functions: A review of European case studies. *Land Degradation & Development* 29(8), 2378–2389. <https://doi.org/10.1002/ldr.3006>.
- Hartmann, A., Weiler, M., Blume, T., 2020. The impact of landscape evolution on soil physics: Evolution of soil physical and hydraulic properties along two chronosequences of proglacial moraines. *Earth System Science Data* 12(4), 3189–3204. <https://doi.org/10.5194/essd-12-3189-2020>.
- Haverkamp, R., Ross, P.J., Smettem, K.R.J., Parlange, J.Y., 1994. Three-dimensional analysis of infiltration from the disc infiltrometer: 2. Physically based infiltration equation. *Water Resources Research* 30(11), 2931-2935.
- Hillel, D., 2003. *Introduction to Environmental Soil Physics*. Elsevier, Amsterdam.
- Huang, L., Shao, M., 2019. Advances and perspectives on soil water research in China's Loess Plateau. *Earth-Science Reviews* 199, 102962. <https://doi.org/10.1016/j.earscirev.2019.102962>.
- Hubbard, S.S., Rubin, Y., 2005. Introduction to hydrogeophysics. In: Rubin, Y., Hubbard, S.S. (Eds.), *Hydrogeophysics*, Springer Netherlands, pp. 3–21. https://doi.org/10.1007/1-4020-3102-5_1.

- Huisman, J.A., Sperl, C., Bouten, W., Verstraten, J.M., 2001. Soil water content measurements at different scales: accuracy of time domain reflectometry and ground-penetrating radar. *Journal of Hydrology* 245(1-4), 48-58.
- Huisman, J.A., Snepvangers, J.J.J.C., Bouten, W., Heuvelink, G.B.M., 2002. Mapping spatial variation in surface soil water content: Comparison of ground-penetrating radar and time domain reflectometry. *Journal of Hydrology* 269(3), 194–207. [https://doi.org/10.1016/S0022-1694\(02\)00239-1](https://doi.org/10.1016/S0022-1694(02)00239-1).
- Huisman, J.A., Hubbard, S.S., Redman, J.D., Annan, A.P., 2003. Measuring soil water content with ground penetrating radar: A review. *Vadose Zone Journal* 2(4), 476–491. <https://doi.org/10.2136/vzj2003.4760>.
- Indoria, A.K., Sharma, K.L., Reddy, K.S., 2020. Hydraulic properties of soil under warming climate. In: *Climate change and soil interactions*, Elsevier, pp. 473–508. <https://doi.org/10.1016/B978-0-12-818032-7.00018-7>.
- Iqbal, M., Kamal, M.R., Che Man, H., Wayayok, A., 2020. HYDRUS-1D simulation of soil water dynamics for sweet corn under tropical rainfed condition. *Applied Sciences* 10(4), 1219.
- Jadoon, K.Z., Weihermüller, L., Scharnagl, B., Kowalsky, M.B., Bechtold, M., Hubbard, S.S., Vereecken, H., Lambot, S., 2012. Estimation of soil hydraulic parameters in the field by integrated hydrogeophysical inversion of time-lapse ground-penetrating radar data. *Vadose Zone Journal* 11(4), vzj2011.0177. <https://doi.org/10.2136/vzj2011.0177>.
- Jajarmizadeh, M., Harun, S., Salarpour, M., 2012. A review on theoretical consideration and types of models in hydrology. *Journal of Environmental Science and Technology* 5(5), 249–261.
- Jol, H.M., 2008. *Ground penetrating radar theory and applications*. Elsevier, Amsterdam.

- Kishné, A.S., Yimam, Y.T., Morgan, C.L., Dornblaser, B.C., 2017. Evaluation and improvement of the default soil hydraulic parameters for the Noah Land Surface Model. *Geoderma* 285, 247-259.
- Klenk, P., Jaumann, S., Roth, K., 2015. Quantitative high-resolution observations of soil water dynamics in a complicated architecture using time-lapse ground-penetrating radar. *Hydrology and Earth System Sciences* 19(3), 1125–1139. <https://doi.org/10.5194/hess-19-1125-2015>.
- Klotzsche, A., Jonard, F., Looms, M.C., van der Kruk, J., Huisman, J.A., 2018. Measuring soil water content with ground penetrating radar: A decade of progress. *Vadose Zone Journal* 17(1), 1–9. <https://doi.org/10.2136/vzj2018.03.0052>.
- Klotzsche, A., Lärm, L., Vanderborght, J., Cai, G., Morandage, S., Zörner, M., Vereecken, H., van der Kruk, J., 2019a. Monitoring soil water content using time-lapse horizontal borehole GPR data at the field-plot scale. *Vadose Zone Journal* 18(1), 190044. <https://doi.org/10.2136/vzj2019.05.0044>.
- Klotzsche, A., Vereecken, H., van der Kruk, J., 2019b. Review of crosshole ground-penetrating radar full-waveform inversion of experimental data: Recent developments, challenges, and pitfalls. *Geophysics* 84(6), H13–H28. <https://doi.org/10.1190/geo2018-0597.1>.
- Kosugi, K.I., Hopmans, J.W., Dane, J.H., 2002. Parametric Models. In: Dane, J.H., Topp, C.G. (Eds.), *Methods of Soil Analysis: Part 4 Physical Methods*, 5. Soil Science Society of America, Madison, pp. 739-757.
- Kowalsky, M.B., Finsterle, S., Peterson, J., Hubbard, S., Rubin, Y., Majer, E., Ward, A., Gee, G., 2005. Estimation of field-scale soil hydraulic and dielectric parameters through joint

- inversion of GPR and hydrological data. *Water Resources Research* 41(11).
<https://doi.org/10.1029/2005WR004237>.
- Kuroda, S., Jang, H., Kim, H.J., 2009. Time-lapse borehole radar monitoring of an infiltration experiment in the vadose zone. *Journal of Applied Geophysics* 67(4), 361–366.
<https://doi.org/10.1016/j.jappgeo.2008.07.005>.
- Lai, W.W.L., Kou, S.C., Poon, C.S., 2012. Unsaturated zone characterization in soil through transient wetting and drying using GPR joint time–frequency analysis and grayscale images. *Journal of Hydrology* 452–453, 1–13.
<https://doi.org/10.1016/j.jhydrol.2012.03.044>.
- Lambot, S., Antoine, M., Vanclooster, M., Slob, E.C., 2006a. Effect of soil roughness on the inversion of off-ground monostatic GPR signal for non-invasive quantification of soil properties. *Water Resources Research* 42(3). <https://doi.org/10.1029/2005WR004416>.
- Lambot, S., Slob, E.C., Vanclooster, M., Vereecken, H., 2006b. Closed loop GPR data inversion for soil hydraulic and electric property determination. *Geophysical Research Letters* 33(21). <https://doi.org/10.1029/2006GL027906>.
- Lambot, S., Slob, E., Rhebergen, J., Lopera, O., Jadoon, K.Z., Vereecken, H., 2009. Remote estimation of the hydraulic properties of a sand using full-waveform integrated hydrogeophysical inversion of time-lapse, off-ground GPR data. *Vadose Zone Journal* 8(3), 743–754. <https://doi.org/10.2136/vzj2008.0058>.
- Lambot, S., Slob, E., Minet, J., Jadoon, K.Z., Vanclooster, M., Vereecken, H., 2010. Full-waveform modeling and inversion of ground-penetrating radar data for non-invasive characterization of soil hydrogeophysical properties. In: Rossel, R.A.V., McBratney, A.B., Minasny, B.

- (Eds.), Proximal soil sensing, Springer Netherlands, pp. 299–311.
https://doi.org/10.1007/978-90-481-8859-8_25.
- Lambot, S., André, F., 2014. Full-wave modeling of near-field radar data for planar layered media reconstruction. *IEEE Transactions on Geoscience and Remote Sensing* 52(5), 2295–2303.
<https://doi.org/10.1109/TGRS.2013.2259243>.
- Lassabatère, L., Angulo-Jaramillo, R., Soria Ugalde, J.M., Cuenca, R., Braud, I., Haverkamp, R., 2006. Beerkan estimation of soil transfer parameters through infiltration experiments—BEST. *Soil Science Society of America Journal* 70(2), 521–532.
<https://doi.org/10.2136/sssaj2005.0026>.
- Lassabatère, L., Di Prima, S., Bouarafa, S., Iovino, M., Bagarello, V., Angulo-Jaramillo, R., 2019. BEST-2K method for characterizing dual-permeability unsaturated soils with ponded and tension infiltrometers. *Vadose Zone Journal* 18(1), 1-20.
- Lee, D.M., Elrick, D.E., Reynolds, W.D., Clothier, B.E., 1985. A comparison of three field methods for measuring saturated hydraulic conductivity. *Canadian Journal of Soil Science* 65(3), 563–573. <https://doi.org/10.4141/cjss85-060>.
- Lee, S., Chu, M.L., Schmidt, A.R., 2020. Effective green-ampt parameters for two-layered soils. *Journal of Hydrologic Engineering* 25(4), 04020004.
[https://doi.org/10.1061/\(ASCE\)HE.1943-5584.0001897](https://doi.org/10.1061/(ASCE)HE.1943-5584.0001897).
- Léger, E., Saintenoy, A., Coquet, Y., 2014. Hydrodynamic parameters of a sandy soil determined by ground-penetrating radar inside a single ring infiltrometer. *Water Resources Research* 50(7), 5459–5474. <https://doi.org/10.1002/2013WR014226>.
- Léger, E., Saintenoy, A., Tcholka, P., Coquet, Y., 2016. Hydrodynamic parameters of a sandy soil determined by ground-penetrating radar monitoring of porchet infiltrations. *IEEE Journal*

- of Selected Topics in Applied Earth Observations and Remote Sensing 9(1), 188–200.
<https://doi.org/10.1109/JSTARS.2015.2464231>.
- Léger, E., Saintenoy, A., Coquet, Y., Tucholka, P., Zeyen, H., 2020. Evaluating hydrodynamic parameters accounting for water retention hysteresis in a large sand column using surface GPR. *Journal of Applied Geophysics* 182, 104176.
<https://doi.org/10.1016/j.jappgeo.2020.104176>.
- Leuther, F., Schlüter, S., 2021. Impact of freeze–thaw cycles on soil structure and soil hydraulic properties. *SOIL* 7(1), 179–191. <https://doi.org/10.5194/soil-7-179-2021>.
- Li, H., Liao, X., Zhu, H., Wei, X., Shao, M., 2019. Soil physical and hydraulic properties under different land uses in the black soil region of Northeast China. *Canadian Journal of Soil Science* 99(4), 406–419. <https://doi.org/10.1139/cjss-2019-0039>.
- Li, S., Cui, P., Cheng, P., Wu, L., 2022. Modified green–ampt model considering vegetation root effect and redistribution characteristics for slope stability analysis. *Water Resources Management* 36(7), 2395–2410. <https://doi.org/10.1007/s11269-022-03149-6>.
- Liu, X., Dong, X., Leskovar, D.I., 2016. Ground penetrating radar for underground sensing in agriculture: A review. *International Agrophysics* 30(4), 533–543.
<https://doi.org/10.1515/intag-2016-0010>.
- Liu, X., Chen, J., Cui, X., Liu, Q., Cao, X., Chen, X., 2019. Measurement of soil water content using ground-penetrating radar: A review of current methods. *International Journal of Digital Earth* 12(1), 95–118. <https://doi.org/10.1080/17538947.2017.1412520>.
- Lombardi, F., Ortuani, B., Facchi, A., Lualdi, M., 2022. Assessing the perspectives of ground penetrating radar for precision farming. *Remote Sensing* 14(23), 6066.
<https://doi.org/10.3390/rs14236066>.

- Looms, M.C., Binley, A., Jensen, K.H., Nielsen, L., Hansen, T.M., 2008a. Identifying unsaturated hydraulic parameters using an integrated data fusion approach on cross-borehole geophysical data. *Vadose Zone Journal* 7(1), 238–248. <https://doi.org/10.2136/vzj2007.0087>.
- Looms, M.C., Jensen, K.H., Binley, A., Nielsen, L., 2008b. Monitoring unsaturated flow and transport using cross-borehole geophysical methods. *Vadose Zone Journal* 7(1), 227–237. <https://doi.org/10.2136/vzj2006.0129>.
- Lu, J., Zhang, Q., Werner, A.D., Li, Y., Jiang, S., Tan, Z., 2020. Root-induced changes of soil hydraulic properties—A review. *Journal of Hydrology* 589, 125203. <https://doi.org/10.1016/j.jhydrol.2020.125203>.
- Lunt, I.A., Hubbard, S.S., Rubin, Y., 2005. Soil moisture content estimation using ground-penetrating radar reflection data. *Journal of Hydrology* 307(1), 254–269. <https://doi.org/10.1016/j.jhydrol.2004.10.014>.
- Ma, D., Zhang, J., Horton, R., Wang, Q., Lai, J., 2017. Analytical method to determine soil hydraulic properties from vertical infiltration experiments. *Soil Science Society of America Journal* 81(6), 1303–1314. <https://doi.org/10.2136/sssaj2017.02.0061>.
- Ma, Y., Feng, S., Su, D., Gao, G., Huo, Z., 2010. Modeling water infiltration in a large layered soil column with a modified green–ampt model and HYDRUS-1D. *Computers and Electronics in Agriculture* 71, S40–S47. <https://doi.org/10.1016/j.compag.2009.07.006>.
- Mahmoudzadeh Ardekani, M.R., 2013. Off- and on-ground GPR techniques for field-scale soil moisture mapping. *Geoderma* 200–201, 55–66. <https://doi.org/10.1016/j.geoderma.2013.02.010>.

- Mangel, A.R., Linneman, D., Sprinkle, P., Jaysaval, P., Thomle, J., Strickland, C., 2022. Multifrequency electromagnetic geophysical tools for evaluating the hydrologic conditions and performance of evapotranspiration barriers. *Journal of Environmental Management* 303, 114123. <https://doi.org/10.1016/j.jenvman.2021.114123>.
- Mangel, A.R., Moysey, S.M.J., Ryan, J.C., Tarbuton, J.A., 2012. Multi-offset ground-penetrating radar imaging of a lab-scale infiltration test. *Hydrology and Earth System Sciences* 16(11), 4009–4022. <https://doi.org/10.5194/hess-16-4009-2012>.
- Meng, S., Yang, Y., 2019. Infiltration simulation with improved green-ampt model coupled with the wet zone partition function. *Journal of Hydrologic Engineering* 24(5), 04019014. [https://doi.org/10.1061/\(ASCE\)HE.1943-5584.0001782](https://doi.org/10.1061/(ASCE)HE.1943-5584.0001782).
- Minasny, B., McBratney, A.B., 2007. Estimating the water retention shape parameter from sand and clay content. *Soil Science Society of America Journal* 71(4), 1105-1110.
- Mohammadzadeh-Habili, J., Heidarpour, M., 2015. Application of the Green–Ampt model for infiltration into layered soils. *Journal of Hydrology* 527, 824–832. <https://doi.org/10.1016/j.jhydrol.2015.05.052>.
- Mohammadzadeh-Habili, J., Khalili, D., 2021. Development of the green-ampt infiltration rate model and relationship of the ga model parameters with soil hydraulic parameters. *Journal of Hydrologic Engineering* 26(11), 04021033. [https://doi.org/10.1061/\(ASCE\)HE.1943-5584.0002130](https://doi.org/10.1061/(ASCE)HE.1943-5584.0002130).
- Moysey, S.M., 2010. Hydrologic trajectories in transient ground-penetrating-radar reflection data. *Geophysics* 75(4), WA211–WA219. <https://doi.org/10.1190/1.3463416>.

- Mualem, Y., 1976. A new model for predicting the hydraulic conductivity of unsaturated porous media. *Water Resources Research* 12(3), 513–522.
<https://doi.org/10.1029/WR012i003p00513>.
- Nadler, A., Dasberg, S., Lapid, I., 1991. Time domain reflectometry measurements of water content and electrical conductivity of layered soil columns. *Soil Science Society of America Journal* 55(4), 938-943.
- Nash, J.E., Sutcliffe, J.V., 1970. River flow forecasting through conceptual models part I—A discussion of principles. *Journal of Hydrology* 10(3), 282-290.
- Picciafuoco, T., Morbidelli, R., Flammini, A., Saltalippi, C., Corradini, C., Strauss, P., Blöschl, G., 2019. A pedotransfer function for field-scale saturated hydraulic conductivity of a small watershed. *Vadose Zone Journal* 18(1), 1–15. <https://doi.org/10.2136/vzj2019.02.0018>.
- Pathirana, S., Lambot, S., Krishnapillai, M., Cheema, M., Smeaton, C., Galagedara, L., 2023. Ground-penetrating radar and electromagnetic induction: Challenges and opportunities in agriculture. *Remote Sensing* 15(11). <https://doi.org/10.3390/rs15112932>.
- Pathirana, S., Lambot, S., Krishnapillai, M., Smeaton, C., Cheema, M., Galagedara, L., 2024. Potential of ground-penetrating radar to calibrate electromagnetic induction for shallow soil water content estimation. *Journal of Hydrology* 633, 130957.
<https://doi.org/10.1016/j.jhydrol.2024.130957>.
- Pinheiro, E.A.R., van Lier, Q.D.J., Inforsato, L., Šimůnek, J., 2019. Measuring full-range soil hydraulic properties for the prediction of crop water availability using gamma-ray attenuation and inverse modeling. *Agricultural Water Management* 216, 294-305.
- Radcliffe, D.E., Šimůnek, J., 2018. *Soil Physics with HYDRUS: Modeling and Applications*. CRC Press, Boca Raton.

- Rahmati, M., Latorre, B., Lassabatere, L., Angulo-Jaramillo, R., Moret-Fernández, D., 2019. The relevance of Philip theory to Haverkamp quasi-exact implicit analytical formulation and its uses to predict soil hydraulic properties. *Journal of Hydrology* 570, 816–826. <https://doi.org/10.1016/j.jhydrol.2019.01.038>.
- Ramos, T.B., Liu, M., Paredes, P., Shi, H., Feng, Z., Lei, H., Pereira, L.S., 2023. Salts dynamics in maize irrigation in the Hetao plateau using static water table lysimeters and HYDRUS-1D with a focus on autumn leaching irrigation. *Agricultural Water Management* 283, 108306.
- Rawls, W.J., Brakensiek, D.L., Miller, N., 1983. Green-ampt infiltration parameters from soils data. *Journal of Hydraulic Engineering* 109(1), 62–70. [https://doi.org/10.1061/\(ASCE\)0733-9429\(1983\)109:1\(62\)](https://doi.org/10.1061/(ASCE)0733-9429(1983)109:1(62)).
- Reynolds, W.D., Elrick, D.E., 1986. A method for simultaneous in situ measurement in the vadose zone of field-saturated hydraulic conductivity, sorptivity and the conductivity-pressure head relationship. *Groundwater Monitoring & Remediation* 6(1), 84–95. <https://doi.org/10.1111/j.1745-6592.1986.tb01229.x>.
- Reynolds, W.D., Carter, M., Gregorich, E., 2008. Saturated hydraulic properties: Well permeameter. In: Carter, M.R., Gregorich, E.G. (Eds.), *Soil Sampling and Methods of Analysis*, CRC Press, Boca Raton, pp. 1025-1042.
- Rezaei, M., Saey, T., Seuntjens, P., Joris, I., Boënné, W., Van Meirvenne, M., Cornelis, W., 2016. Predicting saturated hydraulic conductivity in a sandy grassland using proximally sensed apparent electrical conductivity. *Journal of Applied Geophysics* 126, 35–41. <https://doi.org/10.1016/j.jappgeo.2016.01.010>.
- Richards, L.A., 1941. A pressure-membrane extraction apparatus for soil solution. *Soil Science* 51(5), 377-386.

- Rossi, M., Manoli, G., Pasetto, D., Deiana, R., Ferraris, S., Strobbia, C., Putti, M., Cassiani, G., 2015. Coupled inverse modeling of a controlled irrigation experiment using multiple hydrogeophysical data. *Advances in Water Resources* 82, 150–165. <https://doi.org/10.1016/j.advwatres.2015.03.008>.
- Roth, C.H., Malicki, M.A., Plagge, R., 1992. Empirical evaluation of the relationship between soil dielectric constant and volumetric water content as the basis for calibrating soil moisture measurements by TDR. *Journal of Soil Science* 43(1), 1–13. <https://doi.org/10.1111/j.1365-2389.1992.tb00115.x>.
- Rucker, D.F., Ferré, T.P.A., 2004. Parameter estimation for soil hydraulic properties using zero-offset borehole radar: Analytical method. *Soil Science Society of America Journal* 68(5), 1560–1567. <https://doi.org/10.2136/sssaj2004.1560>.
- Saintenoy, A., Schneider, S., Tucholka, P., 2008. Evaluating ground penetrating radar use for water infiltration monitoring. *Vadose Zone Journal* 7(1), 208–214. <https://doi.org/10.2136/vzj2007.0132>.
- Salako, A.O., Adepelumi, A.A., 2016. Evaluation of hydraulic conductivity of subsoil using electrical resistivity and ground penetrating radar data: Example from Southwestern Nigeria. *International Journal of Geo-Engineering* 7(1), 1–26. <https://doi.org/10.1186/s40703-016-0018-7>.
- Sanborn, P., Lamontagne, L., Hendershot, W., 2011. Podzolic soils of Canada: Genesis, distribution, and classification. *Canadian Journal of Soil Science* 91(5), 843–880. <https://doi.org/10.4141/cjss10025>.

- Saxton, K.E., Rawls, W.J., 2006. Soil water characteristic estimates by texture and organic matter for hydrologic solutions. *Soil Science Society of America Journal* 70(5), 1569–1578. <https://doi.org/10.2136/sssaj2005.0117>.
- Schaap, M.G., Leij, F.J., van Genuchten, M.T., 2001. Rosetta: A computer program for estimating soil hydraulic parameters with hierarchical pedotransfer functions. *Journal of Hydrology* 251(3-4), 163-176.
- Schaap, M.G., van Genuchten, M.T., 2006. A modified Mualem–van Genuchten formulation for improved description of the hydraulic conductivity near saturation. *Vadose Zone Journal* 5(1), 27–34. <https://doi.org/10.2136/vzj2005.0005>.
- Schindler, U., Durner, W., von Unold, G., Müller, L., 2010. Evaporation method for measuring unsaturated hydraulic properties of soils: Extending the measurement range. *Soil Science Society of America Journal* 74(4), 1071-1083.
- Scholer, M., Irving, J., Binley, A., Holliger, K., 2011. Estimating vadose zone hydraulic properties using ground penetrating radar: The impact of prior information. *Water Resources Research* 47(10). <https://doi.org/10.1029/2011WR010409>.
- Scholer, M., Irving, J., Looms, M.C., Nielsen, L., Holliger, K., 2012. Bayesian Markov-Chain-Monte-Carlo inversion of time-lapse crosshole GPR data to characterize the vadose zone at the Arrenaes Site, Denmark. *Vadose Zone Journal* 11(4), vzj2011.0153. <https://doi.org/10.2136/vzj2011.0153>.
- Serbin, G., Or, D., 2003. Near-surface soil water content measurements using horn antenna radar. *Vadose Zone Journal* 2(4), 500. <https://doi.org/10.2136/vzj2003.0500>.

- Serbin, G., Or, D., 2004. Ground-penetrating radar measurement of soil water content dynamics using a suspended horn antenna. *IEEE Transactions on Geoscience and Remote Sensing* 42(8), 1695–1705. <https://doi.org/10.1109/TGRS.2004.831693>.
- Singh, D., Mishra, A.K., Patra, S., Mariappan, S., Singh, N., Kar, S.K., 2023. Spatial variability of soil hydraulic and physical properties in erosive sloping agricultural fields. *Water Science and Engineering* 16(1), 57–66.
- Šimůnek, J., Huang, K., van Genuchten, M.T., 1998. The HYDRUS code for simulating the one-dimensional movement of water, heat, and multiple solutes in variably-saturated media. US Salinity Laboratory Research Report 144.
- Šimůnek, J., van Genuchten, M.T., Sejna, M., 2008. Development and applications of the HYDRUS and STANMOD software packages and related codes. *Vadose Zone Journal* 7(2), 587–600. <https://doi.org/10.2136/vzj2007.0077>.
- Šimůnek, J., van Genuchten, M.T., Šejna, M., 2009. The HYDRUS-1D software package for simulating the one-dimensional movement of water, heat, and multiple solutes in variably-saturated media. *University of California-Riverside Research Reports*, 3, 1-270.
- Šimůnek, J., van Genuchten, M.T., Šejna, M., 2016. Recent developments and applications of the HYDRUS computer software packages. *Vadose Zone Journal* 15(7), vzj2016-04.
- Slater, L., Comas, X., 2009. The contribution of ground penetrating radar to water resource research. In: *Ground penetrating radar: Theory and applications*, Elsevier, Amsterdam, pp. 203-246. <https://doi.org/10.1016/B978-0-444-53348-7.00007-7>.
- Smettem, K.R.J., Parlange, J.Y., Ross, P.J., Haverkamp, R., 1994. Three-dimensional analysis of infiltration from the disc infiltrometer: 1. A capillary-based theory. *Water Resources Research* 30(11), 2925-2929.

- Soil Classification Working Group, 1998. The Canadian System of Soil Classification, 3rd ed. Agriculture and Agri-Food Canada Publication, Ottawa.
- Steelman, C.M., Endres, A.L., 2011. Comparison of petrophysical relationships for soil moisture estimation using GPR ground waves. *Vadose Zone Journal* 10(1), 270–285. <https://doi.org/10.2136/vzj2010.0040>.
- Steelman, C.M., Endres, A.L., Jones, J.P., 2012. High-resolution ground-penetrating radar monitoring of soil moisture dynamics: Field results, interpretation, and comparison with unsaturated flow model. *Water Resources Research* 48(9). <https://doi.org/10.1029/2011WR011414>.
- Sünnemann, M., Beugnon, R., Breitzkreuz, C., Buscot, F., Cesarz, S., Jones, A., Lehmann, A., Lochner, A., Orgiazzi, A., Reitz, T., Rillig, M.C., Schädler, M., Smith, L.C., Zeuner, A., Guerra, C.A., Eisenhauer, N., 2023. Climate change and cropland management compromise soil integrity and multifunctionality. *Communications Earth & Environment* 4(1), 394. <https://doi.org/10.1038/s43247-023-01047-2>.
- Topp, G.C., Davis, J.L., Annan, A.P., 1980. Electromagnetic determination of soil water content: Measurements in coaxial transmission lines. *Water Resources Research* 16(3), 574–582. <https://doi.org/10.1029/WR016i003p00574>.
- Tronicke, J., Hamann, G., 2014. Vertical radar profiling: Combined analysis of travel times, amplitudes, and reflections. *Geophysics* 79(4), H23–H35. <https://doi.org/10.1190/geo2013-0428.1>.
- van Genuchten, M.T., 1980. A closed-form equation for predicting the hydraulic conductivity of unsaturated soils. *Soil Science Society of America Journal* 44(5), 892–898. <https://doi.org/10.2136/sssaj1980.03615995004400050002x>.

- Vereecken, H., Huisman, J.A., Pachepsky, Y., Montzka, C., van der Kruk, J., Bogaen, H., Weihermüller, L., Herbst, M., Martinez, G., Vanderborght, J., 2014. On the spatio-temporal dynamics of soil moisture at the field scale. *Journal of Hydrology* 516, 76-96.
- Verbist, K.M.J., Cornelis, W.M., Torfs, S., Gabriels, D., 2013. Comparing methods to determine hydraulic conductivities on stony soils. *Soil Science Society of America Journal* 77(1), 25–42. <https://doi.org/10.2136/sssaj2012.0025>.
- Vigo, Á. del, Zobelzu, S., Juana, L., 2021. Infiltration models and soil characterisation for hemispherical and disc sources based on Green-Ampt assumptions. *Journal of Hydrology* 595, 125966. <https://doi.org/10.1016/j.jhydrol.2021.125966>.
- Vogel, T., van Genuchten, M.T., Cislérova, M., 2000. Effect of the shape of the soil hydraulic functions near saturation on variably-saturated flow predictions. *Advances in Water Resources* 24(2), 133-144.
- Weihermüller, L., Huisman, J.A., Lambot, S., Herbst, M., Vereecken, H., 2007. Mapping the spatial variation of soil water content at the field scale with different ground penetrating radar techniques. *Journal of Hydrology* 340(3-4), 205-216.
- Weihnacht, B., Boerner, F., 2014. Measurement of retention functions with hysteresis using ground-penetrating radar. *Near Surface Geophysics* 12(4), 539–548. <https://doi.org/10.3997/1873-0604.2014001>.
- Weiler, K.W., Steenhuis, T.S., Boll, J., Kung, K.J.S., 1998. Comparison of ground penetrating radar and time-domain reflectometry as soil water sensors. *Soil Science Society of America Journal* 62(5), 1237–1239. <https://doi.org/10.2136/sssaj1998.03615995006200050008x>.

- Wijewardana, Y.G.N.S., Galagedara, L.W., 2010. Estimation of spatio-temporal variability of soil water content in agricultural fields with ground penetrating radar. *Journal of Hydrology* 391(1), 24–33. <https://doi.org/10.1016/j.jhydrol.2010.06.036>.
- Willems, P., 2000. Probabilistic modeling of the emission receiving surface waters. PhD Thesis, Faculty of Engineering, Katholieke Universiteit Leuven, Belgium.
- Yasir, S.F., Jani, J., Mukri, M., 2019. The estimation of hydraulic properties from geophysical measurement of subsoil depend on regression equation. *Modern Applied Science* 13(6), 1–12. <https://doi.org/10.5539/mas.v13n6p1>.
- Yang, X., Klotzsche, A., Meles, G., Vereecken, H., van der Kruk, J., 2013. Improvements in crosshole GPR full-waveform inversion and application on data measured at the Boise Hydrogeophysics Research Site. *Journal of Applied Geophysics* 99, 114–124. <https://doi.org/10.1016/j.jappgeo.2013.08.007>.
- Yilmaz, D., Lassabatere, L., Angulo-Jaramillo, R., Deneele, D., Legret, M., 2010. Hydrodynamic characterization of basic oxygen furnace slag through an adapted best method. *Vadose Zone Journal* 9(1), 107. <https://doi.org/10.2136/vzj2009.0039>.
- Yu, Y., Huisman, J.A., Klotzsche, A., Vereecken, H., Weihermüller, L., 2022. Coupled full-waveform inversion of horizontal borehole ground penetrating radar data to estimate soil hydraulic parameters: A synthetic study. *Journal of Hydrology* 610, 127817. <https://doi.org/10.1016/j.jhydrol.2022.127817>.
- Yu, Y., Klotzsche, A., Weihermüller, L., Huisman, J.A., Vanderborght, J., Vereecken, H., van der Kruk, J., 2020. Measuring vertical soil water content profiles by combining horizontal borehole and dispersive surface ground penetrating radar data. *Near Surface Geophysics* 18(3), 275–294.

- Yu, Y., Weihermüller, L., Klotzsche, A., Lärm, L., Vereecken, H., Huisman, J.A., 2021. Sequential and coupled inversion of horizontal borehole ground penetrating radar data to estimate soil hydraulic properties at the field scale. *Journal of Hydrology* 596, 126010. <https://doi.org/10.1016/j.jhydrol.2021.126010>.
- Zajícová, K., Chuman, T., 2019. Application of ground penetrating radar methods in soil studies: A review. *Geoderma* 343, 116-129.
- Zhang, M., Feng, X., Bano, M., Xing, H., Wang, T., Liang, W., Zhou, H., Dong, Z., An, Y., Zhang, Y., 2022. Review of ground penetrating radar applications for water dynamics studies in unsaturated zone. *Remote Sensing* 14(23), 5993. <https://doi.org/10.3390/rs14235993>.
- Zou, C., Zhang, S., Jiang, X., Chen, F., 2023. Monitoring and characterization of water infiltration in soil unsaturated zone through an integrated geophysical approach. *Catena* 230, 107243. <https://doi.org/10.1016/j.catena.2023.107243>.